National Library of Canada
Bibliothèque nationale du Canada

Canadian Theses Service
Service des thèses canadiennes

Ottawa, Canada
K1A 0N4

NOTICE

The quality of this microform is heavily dependent upon the quality of the original thesis submitted for microfilming. Every effort has been made to ensure the highest quality of reproduction possible.

If pages are missing, contact the university which granted the degree.

Some pages may have indistinct print especially if the original pages were typed with a poor typewriter ribbon or if the university sent us an inferior photocopy.

Reproduction in full or in part of this microform is governed by the Canadian Copyright Act, R.S.C. 1970, c. C-30, and subsequent amendments.

AVIS

La qualité de cette microforme dépend grandement de la qualité de la thèse soumise au microfilmage. Nous avons tout fait pour assurer une qualité supérieure de reproduction.

S'il manque des pages, veuillez communiquer avec l'université qui a conféré le grade.

La qualité d'impression de certaines pages peut laisser à désirer, surtout si les pages originales ont été dactylographiées à l'aide d'un ruban usé ou si l'université nous a fait parvenir une photocopie de qualité inférieure.

La reproduction, même partielle, de cette microforme est soumise à la Loi canadienne sur le droit d'auteur, SRC 1970, c. C-30, et ses amendements subséquents.

NL-339 (r. 88/04) c

Canada

UNIVERSITY OF ALBERTA

J-COMPENSATED MAGNETIZATION TRANSFER SEQUENCES

BY

ALLAN MARAÑON TORRES

A THESIS

SUBMITTED TO THE FACULTY OF GRADUATE STUDIES AND

RESEARCH IN PARTIAL FULFILLMENT OF THE REQUIREMENTS

FOR THE DEGREE OF DOCTOR OF PHILOSOPHY

DEPARTMENT OF CHEMISTRY

EDMONTON, ALBERTA

SPRING 1992

National Library of Canada
Bibliothèque nationale du Canada

Canadian Theses Service
Service des thèses canadiennes

Ottawa, Canada
K1A 0N4

The author has granted an irrevocable non-exclusive licence allowing the National Library of Canada to reproduce, loan, distribute or sell copies of his/her thesis by any means and in any form or format, making this thesis available to interested persons.

L'auteur a accordé une licence irrévocable et non exclusive permettant à la Bibliothèque nationale du Canada de reproduire, prêter, distribuer ou vendre des copies de sa thèse de quelque manière et sous quelque forme que ce soit pour mettre des exemplaires de cette thèse à la disposition des personnes intéressées.

The author retains ownership of the copyright in his/her thesis. Neither the thesis nor substantial extracts from it may be printed or otherwise reproduced without his/her permission.

L'auteur conserve la propriété du droit d'auteur qui protège sa thèse. Ni la thèse ni des extraits substantiels de celle-ci ne doivent être imprimés ou autrement reproduits sans son autorisation.

ISBN 0-315-73015-3

Canada

UNIVERSITY OF ALBERTA

RELEASE FORM

NAME OF AUTHOR: Allan Marañon Torres

TITLE OF THESIS: *J*-Compensated Magnetization Transfer Sequences

DEGREE: Doctor of Philosophy

YEAR THIS DEGREE GRANTED: 1992

Permission is hereby granted to the University of Alberta Library to reproduce single copies of this thesis and to lend or sell such copies for private, scholarly or scientific research purposes only.

The author reserves all other publication and other rights in association with the copyright in the thesis, and except as hereinbefore provided neither the thesis nor any substantial portion thereof may be printed or otherwise reproduced in any material form whatever without the author's prior written permission.

Allan Torres

Limjoco Street

San Fernando, Pampanga

Philippines

Date November 28, 1991

University of Alberta
Edmonton
Canada T6G 2G2

Department of Chemistry
Faculty of Science
E3-44 Chemistry Bldg., Tel. (403) 492-3254 Fax (403) 492-8231

1 page FAX

December 6, 1991

To: Martha Strassberger
Academic Press
Rights and Permissions
6277 Sea Harbor Drive
Orlando, Florida
U. S. A. 32887
FAX: (407) 352 – 8125

From: R. E. D. McClung
FAX: (403) 492 – 8231
Voice: (403) 492 – 5489

Re: Request for Permission to Include Copyright Material in Thesis

Dear Martha:

I have been referred to you by Liz Pope of the San Diego branch of Academic Press.

My graduate student, Allan Torres, is now submitting his dissertation to the Faculty of Graduate Studies at the University of Alberta in fulfillment of the requirements of the Ph. D. degree. Since all of the work in his thesis has been published or will be published in the Journal of Magnetic Resonance, the University requires permission from the copyright holder (Academic Press) so that the thesis may be stored on microfilm in the National Library of Canada. I am therefore requesting permission for the following articles:

1. "Compensated APT Pulse Sequences" by A. M. Torres, R. E. D. McClung, and T. T. Nakashima, J. Magn. Reson. **87**, 189-193 (1990).

2. "J-Compensated DEPT Sequences" by A. M. Torres and R. E. D. McClung, J. Magn. Reson. **92**, 45-63 (1991).

3. "Efficiency of Purging Sequences in the Long-Range Heteronuclear Shift Correlation Experiment" by A. M. Torres, T. T. Nakashima, and R. E. D. McClung, J. Magn. Reson. **96** (to be published Jan. 1992).

4. "Improvement of INADEQUATE using Compensated Delays and Pulses", by A. M. Torres, T. T. Nakashima, and R. E. D. McClung, J. Magn. Reson. **98** (to be published June 15, 1992).

to be microfilmed for deposition in the National Library of Canada.

I trust that this permission can be granted without delay so that Dr. Torres can submit his thesis as soon as possible. If possible, please FAX me the letter of permission at your earliest convenience. Please call me at (403) 492 – 5489 if you require further information

Sincerely yours

R. E. D. McClung, Professor of Chemistry

P. S. As Liz Pope suggested, a copy of this letter has been mailed today.

PLEASE TURN OVER

December 9, 1991

PERMISSION GRANTED, provided that 1) complete credit is given to the source, including the Academic Press copyright line; 2) the material to be used has appeared in our publication without credit or acknowledgement to another source and 3) if commercial publication should result, you must contact Academic Press again.

We realize that the National Library of Canada must have permission to sell copies of your thesis, and we agree to this. However, we must point out that we are not giving permission for separate sale of your article.

M. Strassberger

Martha Strassberger
Contracts, Rights and Permissions
ACADEMIC PRESS, INC.
Orlando, Florida 32887

THE UNIVERSITY OF ALBERTA

FACULTY OF GRADUATE STUDIES AND RESEARCH

The undersigned certify that they have read, and recommend to the Faculty of Graduate Studies and Research for acceptance, a thesis entitled

J-COMPENSATED MAGNETIZATION TRANSFER SEQUENCES

submitted by ALLAN MARAÑON TORRES in partial fulfillment of the requirements for the degree of DOCTOR OF PHILOSOPHY.

Supervisor Dr. R. E. D. McClung

Dr. J. S. Martin

Dr. J. Takats

Dr. G. Kotovych

Dr. D. G. Hughes

External Examiner Dr. W. F. Reynolds

Date November 28, 1991

To my family —

Irma, Werner, and Sean

Abstract

Various J-compensated magnetization transfer sequences which interconvert transverse in-phase and antiphase magnetizations are constructed from B_1 inhomogeneity-compensated pulses using direct product operator analogies between spin-spin coupling and rf pulses. The derived J-compensated sequences are incorporated into the pulse sequences of several multiple-pulse experiments and their efficiencies are tested by theoretical calculations and experimental investigations.

Practical J-compensated magnetization transfer sequences were patterned from the $90^\circ_0 180^\circ_{120}$ composite 90° pulse and the $90^\circ_0 180^\circ_{90} 90^\circ_0$ composite 180° pulse. Incorporation of heteronuclear J-compensated sequences into each of the three precession periods of DEPT shows that compensation of the first delay period results in a useful sequence, DEPTC1. The compensation of the second and third parts of DEPT does not lead to improved conversion efficiency. In APT-like experiments, the J-compensated sequence CAPT is found to provide useful improvements in both assigning and editing carbon spectra, while the sequence RAPT, which is based on the composite $180^\circ_0 360^\circ_{90} 360^\circ_{225}$ sequence, is shown to display the expected rectangular shaped inversion profile.

In the absence of large resonance offsets, J-compensated INADEQUATE, which includes an homonuclear J-compensated magnetization transfer sequence, is shown to have a signal profile which is broader than the INADEQUATE profile. Detailed study of the efficiency of various composite pulses in minimizing resonance offsets in the conventional and J-compensated INADEQUATE experiments showed that five-step symmetric phase-alternating composite pulses are most effective. The sequences C-INADEQUATE, which incorporates offset compensation with composite pulses, and JC-INADEQUATE, which includes both offset- and J-

compensations, are shown to have significantly higher sensitivity than conventional INADEQUATE.

The efficiency of a modified J-compensated sequence INEPT preparation sequence in removing directly bonded C–H correlations from long-range C–H shift correlation maps was tested and compared to those of other common purging sequences. A two-step J filter is shown to give better suppression than than this J-compensated sequence. The incorporation of the two-step J-filter into the long-range C–H shift correlation experiment with a BIRD sequence at the center of the refocusing period gives the BIRDTRAP sequence which is shown to yield artifact-free 2D maps with only a very few direct correlations of low intensity.

Acknowledgements

I wish to express my deepest gratitude to Dr. R. E. D. McClung for his untiring help during the entire course of this work. Dr. McClung provided me with valuable support, guidance, and assistance necessary to make this thesis possible.

I am very thankful to Dr. T. T. Nakasahima, who collaborated in most of the studies. I also thank to Dr. D. R. Muhandiram for his collaboration in Chapter 4 and for helpful discussions in Chapter 5. Special acknowledgements are due to the NMR service staff who were very helpful with regards to the instrumental aspects.

Mrs. Gerdy Aarts gave a lot moral support and help in preparing samples and in operating NMR spectrometers. My sincere thanks goes to her.

I thank the Department of Chemistry and the Natural Sciences and Engineering Research Council of Canada for the financial assistance.

Finally, I take this opportunity to acknowledge my parents for instilling into me the value of education.

Contents

Chapter Page

1 Introduction 1

References 11

2 *J*-Compensated DEPT Sequences 13

2.1 Introduction 13

2.2 Theory 15

J-Compensated conversion of I_y to $-I_y$ 17

J-Compensated conversion of I_y to $-2I_xS_z$ 19

Compensated conversion of $2I_xS_z$ to I_y 21

Construction of compensated DEPT sequences 24

Compensation of the first part of DEPT (DEPTC1) 27

Compensation of the second part of DEPT (DEPTC2) 30

Compensation of the third part of DEPT (DEPTC3) 31

2.3 Experimental 32

2.4 Results and Discussion 33

2.5 Conclusion 43

References 44

3 *J*-Compensated APT Sequences 46

References 52

4 Improvement of INADEQUATE Using Compensated Delays and Pulses **53**

4.1 Introduction 53

4.2 Theory 57

Construction of J-Compensated Inadequate Sequence 62

4.3 Experimental 64

4.4 Results and Discussion 66

Preliminary Testing of the J-compensated INADEQUATE on a Proton AX system 66

J-compensated INADEQUATE in Carbon-13 Spectroscopy 68

The Efficiency of the Symmetric Phase-alternating Composite 180° Pulses in the INADEQUATE sequence 69

C-INADEQUATE 76

JC-INADEQUATE 77

4.5 Conclusions 83

References 84

5 Efficiency of Purging Sequences in the Long-range Heteronuclear Shift Correlation Experiment **87**

5.1 Introduction 87

5.2 Experimental 89

5.3 Results and Discussion 91

Efficiency of Various Purging Sequences in Suppressing Directly Bonded Correlations 91

Efficiency of Various Purging Sequences in Eliminating Transverse Magnetizations of Directly Bonded Protons 97

Incorporation of BIRD and Two-Step J Filter Sequences to the Conventional Method: The BIRDTRAP Sequence 103

Comparison of BIRDTRAP and FLOCK 106

References 111

6 General Discussion and Conclusions **113**

References 123

Appendix **125**

A.1 Implementation of FLOCK on Bruker AM-300 and AM-400 Spectrometers 125

A.2 The FLOCK Sequence with the Modified Phase Cycle 135

References 144

List of Figures

Figure		Page
2.1	Pictorial Representations of Rotation and Bilinear Rotation Operators.	16
2.2	Product operator description of proton to carbon magnetization transfer in DEPT for CH, CH_2, and CH_3 spin systems	25
2.3	Pulse Sequences for DEPT and DEPTC1.	28
2.4	Modifications to DEPT for J-compensation.	29
2.5	Comparison of calculated and observed DEPT and DEPTC1 signal profiles for CH , CH_2, and CH_3 spin systems.	35
2.6	Comparison of DEPT and DEPTC1 spectra of 1:1 mole mixture of cholesterol and 3-methyl-1-pentyn-3-ol.	37
2.7	Comparison of DEPT and DEPTC2 Signal profiles for CH_2 and CH_3 spin systems.	39
2.8	Comparison of DEPT and DEPTC3 Signal profiles for CH_2 and CH_3 spin systems.	41
3.1	Pulse sequences for APT-like experiments.	48
3.2	Comparison of the observed and calculated signal intensities for APT-like pulse sequences.	50
4.1	Pulse sequences for regular and J-compensated INADEQUATE.	54

4.2 Comparison of the calculated and observed INADEQUATE and J-compensated INADEQUATE signal intensity profiles for the H-4 antiphase peak of 2,3-dibromothiophene. 67
4.3 Pulse sequences for regular and the modified INADEQUATE experiments. 72
4.4 The carbonyl antiphase doublet of ^{13}C-dilabeled acetaldehyde obtained with the regular, modified, C-INADEQUATE, and Levitt and Ernst compensated INADEQUATE sequences. 73
4.5 Selected regions from the ^{13}C natural abundance 1D spectra of 5-hexene-2-one obtained with INADEQUATE, C-INADEQUATE, and JC-INADEQUATE sequences. 79
4.6 Selected f_2 sections of the INADEQUATE and JC-INADEQUATE 2D spectra of crotonaldehyde. 82
5.1 Pulse sequence for the long-range heteronuclear shift correlation experiment and purge sequences (A – E). 90
5.2 f_1 slices from the long-range C–H correlation maps of **1** obtained with the conventional sequence and with purge sequences A – E. . 96
5.3 Effectiveness of purge sequences A – E in eliminating transverse magnetizations of directly bonded protons. 99
5.4 Calculated variation of the residual transverse magnetizations with $^1J_{CH}$ for purge sequences 100
5.5 Comparison of calculated and observed signals in 1D analogs of the purge sequences 102
5.6 Pulse sequences for the long-range heteronuclear shift experiment with a BIRD sequence in the middle Δ_2 and the BIRDTRAP sequence. 104

5.7 f_1 slices from the 2D map of **1** obtained with the regular long-range sequence, the long-range sequence with a BIRD sequence midway through Δ_2 and the BIRDTRAP sequence. 105

5.8 Long-range correlation spectra of **2** obtained with BIRDTRAP and FLOCK. 108

5.9 f_1 slices of the 2D maps in Fig. 5.8 corresponding to the protonated carbons of **2**. 109

A.1 Bruker DISNMR pulse program for standard FLOCK sequence. . . 126

A.2 Bruker DISNMR pulse program for modified FLOCK sequence . . . 127

A.3 Bruker DISNMR pulse program for "composite" FLOCK employing IPn commands to increment phases 129

A.4 f_1 slices from the 2D map of 2-pentanone obtained with "composite" FLOCK , "simple" FLOCK, and BIRDTRAP. 130

A.5 Bruker DISNMR pulse program for"simple" FLOCK employing revised phase cycle. 136

A.6 Bruker DISNMR pulse program for "composite" FLOCK employing revised phase cycle. 137

A.7 f_1 slices from the 2D map of 2-pentanone obtained using "simple" FLOCK with original and revised phase cycles. 138

List of Tables

Table		Page
2.1	β'-dependence of ^{13}C signal intensities in each part of conventional and J-compensated DEPT sequences	34
3.1	Signal Intensities in APT-like experiments	49
4.1	Calculated efficiencies of simple and composite 180° pulses in INADEQUATE experiments on $^{13}CH_3{}^{13}CHO$.	75

Acronyms

INEPT Insensitive Nucleus Enhancement by Polarization Transfer.

DEPT Distortionless Enhancement by Polarization Transfer.

APT Attached Proton Test.

INADEQUATE Incredible Natural Abundance Double Quantum Transfer Experiment.

BIRD Bilinear Rotational Decoupling Operator.

TANGO Testing for Adjacent Nuclei with a Gyration Operator.

CHAPTER 1

INTRODUCTION

Virtually all multiple-pulse NMR experiments devised in recent years incorporate precession periods during which spin-spin coupling interactions are operative. Examples include spin echo experiments such as spin-flip (1) and APT (2), and polarization transfer experiments like INEPT (3,4), DEPT (5), and INADEQUATE (6). The feature which is common to all of these experiments is the presence of one or more precession periods during which transverse in-phase and antiphase magnetizations are interconverted. The efficiency of the conversion depends on the matching of the duration of the precession period and the magnitude of the spin-spin coupling constant J.

In order to discuss the operations of pulse sequences, it is necessary to describe the magnetic properties of the spin system in terms of product operators (7) rather than by simple magnetization vector diagrams since vector diagrams are appropriate only for the simplest of pulse sequences. In the product operator nomenclature, the Cartesian components of carbon and proton magnetizations are represented by C_x,C_y,C_z and H_x,H_y,H_z respectively. The antiphase carbon magnetization, which is represented by a pair of vectors pointing in opposite directions along the x- or y-axis in a vector diagram, corresponds to the product operator $2C_xH_z$ or $2C_yH_z$. Other product operators which have no simple vector representions are the longitudinal spin-order, $2H_zC_z$, and the muliple-quantum coherences, $2C_xH_x$, $2C_xH_y$, $2C_yH_x$, $2C_yH_y$. The longitudinal spin order, which has the same product operator representation as the spin-spin coupling interaction, is associated with a non-equilibrium distribution of populations in which no transverse carbon or hydrogen magnetization exists. The multiple-quantum coherences, on the other

hand, are superpositions of zero- and double-quantum coherences which are invariant to spin-spin couplings, but precess at frequencies which are the difference and the sum of proton and carbon resonance frequencies.

In order to illustrate the importance of the precession period and its purpose in a pulse sequence, consider as an example the spin-flip experiment (1)

$$\begin{array}{lccccc} {}^{13}\mathrm{C} & 90^{\circ}_{0} & & 180^{\circ}_{90} & & \text{Acquire} \\ & & -\tau- & & -\tau- & \\ {}^{1}\mathrm{H} & & & 180^{\circ} & & \text{Decouple,} \end{array} \qquad [1\text{-}1]$$

which is used extensively in assigning and editing carbon spectra because carbon responses due to CH and CH_3 fragments appear as negative peaks while responses corresponding to CH_2 fragments and quartenary carbons are displayed as positive peaks. For brevity, only the CH spin case will be considered here. The $\tau - [180^{\circ}_{90}({}^{13}\mathrm{C}), 180^{\circ}({}^{1}\mathrm{H})] - \tau$ part of the sequence is conventionally referred to as a precession period of length 2τ during which carbon-hydrogen spin-spin coupling, but not chemical shift effects, are active. During this precession period, where the magnitude of τ is nominally set to $1/2J_{\mathrm{CH}}$, the spin-spin interaction between carbon and proton bilinearly rotates the transverse carbon magnetization C_y by an angle $\theta' = \pi$ so that it is inverted to $-C_y$. The bilinear rotation (propagator $2C_zH_z$) can be generally described by the transformation

$$C_y \xrightarrow{(\theta')\,2C_zH_z} C_y \cos\theta' - 2C_xH_z \sin\theta', \qquad [1\text{-}2]$$

where $\theta' = 2\pi J_{\mathrm{CH}}\tau$ and J_{CH} is the carbon-proton coupling constant. Any mismatch between the delay τ and $1/2J_{\mathrm{CH}}$ results in a deviation of θ' from π, so that some antiphase magnetization $2C_xH_z$ is created and the magnitude of $-C_y$ is less than maximal. Careful selection of the duration of the precession period is therefore necessary in order to achieve complete bilinear rotation of C_y to $-C_y$.

The choice of an appropriate value of τ for many multiple-pulse experiments

may be difficult (8). This is because molecules typically contain several CH fragments with a range of spin-spin coupling constants J_{CH}, so that even if a τ period matching $J_{CH}^{Average}$ is employed, the coherence conversion would still be imperfect for any CH fragment whose J_{CH} deviates significantly from $J_{CH}^{Average}$. As a result, a distribution of rotation angles θ' among the various fragments in the molecule is produced. This problem becomes serious when the values of J_{CH} are widely dispersed. In this case, a precession period of inappropriate duration could possibly give spectra that might lead to an entirely erroneous interpretation of the system being investigated. There is, therefore, a need to construct J-compensated experiments which are less sensitive to the choice of the value of τ and are therefore more effective over a wider range of J_{CH} than existing experiments.

The problem of inefficient bilinear rotation in multiple-pulse experiments is similar to the problem associated with the incomplete rotations produced by inhomogeneous radiofrequency pulses. To clearly illustrate this similarity, it is useful to compare the spin-spin transformation [1-2] to the action of an rf pulse on the magnetization of spin I initially aligned along the z-axis

$$I_z \xrightarrow{(\theta)\, I_y} I_z \cos\theta + I_x \sin\theta. \qquad [1\text{-}3]$$

where $\theta = \gamma B_1 t$, B_1 is the amplitude of the rf field, γ is the magnetogyric ratio of spin I, and t is the pulse duration. Spatial inhomogeneity of the rf field B_1 leads to a distribution of flip angles θ across the sample volume in the same manner that the presence of varied J_{IS} constants brings about a distribution of bilinear rotation angles θ' across the various nuclei in the molecule. This B_1 inhomogeneity problem is usually minimized by replacing the rf pulse with a suitable composite pulse (9-12) – a sequence of rf pulses whose flip angles and phases are carefully chosen so that it is much less sensitive to pulse imperfections than a regular simple

rf pulse.

Since their introduction (9), composite pulses have proved their usefulness in enhancing the efficiencies of many multiple-pulse experiments, by minimizing the effects of common pulse imperfections due to B_1 field inhomogeneity and resonance offset. The latter effect results when the frequency of the applied rf field is different from the resonance frequency of the spin, causing the orientation of the effective field to be tilted to some degree. Some composite pulses are specifically designed to eliminate either B_1 field inhomogeneity or resonance offsets effects, while others compensate for both effects. Since the B_1 inhomogeneity problem is closely related to the the bilinear rotation problem, the relevant composite pulses for this J-compensation study are, of course, those which have B_1 compensating properties. Such composite pulses may be used as patterns in constructing J-compensated experiments.

A popular composite pulse, which maybe useful in this regard, is the $90^\circ_0 180^\circ_{90} 90^\circ_0$ composite 180° sequence introduced by Levitt and Freeman (9). This sequence has been shown to be more effective than the simple 180° pulse in inverting spin-populations in the presence of B_1 field inhomogeneity and resonance offset effects. Levitt's $90^\circ_0 180^\circ_{120}$ sequence (11), on the other hand, is a short but effective 90° composite pulse which can be used as an excitation pulse in many multiple-pulse experiments. It has the desirable feature of bringing down magnetization aligned along the z-axis to the transverse plane with very small phase distortions, even in the presence of B_1 inhomogeneity and resonance offsets.

By recognizing certain analogies between the effects of rf pulses and precession periods in multiple-pulse sequences, several workers (13-17) have created J-compensated experiments based on B_1 inhomogeneity-compensated pulses. Perhaps, one of the earliest groups to apply this technique in devising J-compensated

sequences was Garbow, Weitekamp and Pines (13). In their description of the BIRD sequence,

$$\begin{array}{lccccc} {}^{13}\mathrm{C} & 90^\circ_0 & & 180^\circ_{90} & & 90^\circ_{180}, \\ & & -\tau- & & -\tau- & \\ {}^{1}\mathrm{H} & & & 180^\circ & & \end{array} \qquad [1\text{-}4]$$

which selectively inverts protons directly attached to ^{13}C while leaving $^{12}CH_n$ protons unaffected, Garbow and co-workers (13) used the $90^\circ_0 180^\circ_{90} 90^\circ_0$ composite inversion pulse as a basis for the creation of the J-compensated BIRD sequence

$$\begin{array}{lccccccccccc} {}^{13}\mathrm{C} & 90^\circ_0 & & 180^\circ_{90} & & 90^\circ_{270} & & 180^\circ_{90} & & 90^\circ_{90} & & 180^\circ_{90} & & 90^\circ_{180}. \\ & & -\frac{\tau}{2}- & & -\frac{\tau}{2}- & & -\tau- & & -\tau- & & -\frac{\tau}{2}- & & -\frac{\tau}{2}- & \\ {}^{1}\mathrm{H} & & & 180^\circ & & & & 180^\circ & & & & 180^\circ & & \end{array} \qquad [1\text{-}5]$$

This compensated sequence is expected to be less sensitive to variations in J than the regular BIRD sequence [1-4].

Wimperis and Bodenhausen (14) developed J-compensated INEPT sequences which transfer proton magnetization to carbon more effectively over a wider range of coupling constants than the regular refocused-INEPT experiment. In constructing the compensated INEPT sequences, they found it convenient to break down the regular refocused INEPT sequence

$$\begin{array}{lccccccc} {}^{13}\mathrm{C} & & 180^\circ & & 90^\circ_{90} & & 180^\circ_{90} & \mathrm{Acquire} \\ & -\frac{\tau}{2}- & & -\frac{\tau}{2}- & & -\frac{\tau'}{2}- & & -\frac{\tau'}{2}- \\ {}^{1}\mathrm{H} & 90^\circ_0 & 180^\circ_{90} & & 90^\circ_{90} & & 180^\circ & \mathrm{Decouple} \end{array} \qquad [1\text{-}6]$$

into two components: the preparation part

$$\begin{array}{lccccc} {}^{13}\mathrm{C} & & & 180^\circ & & \\ & & -\frac{\tau}{2}- & & -\frac{\tau}{2}- & \\ {}^{1}\mathrm{H} & 90^\circ_0 & & 180^\circ_{90} & & 90^\circ_{90} \end{array} \qquad [1\text{-}7]$$

which converts longitudinal proton magnetization H_z to longitudinal spin-order $2H_zC_z$ and the reconversion part

$$\begin{array}{lccccc} {}^{13}\mathrm{C} & 90^\circ_{90} & & 180^\circ_{90} & & \mathrm{Acquire} \\ & & -\frac{\tau'}{2}- & & -\frac{\tau'}{2}- & \\ {}^{1}\mathrm{H} & & & 180^\circ & & \mathrm{Decouple} \end{array} \qquad [1\text{-}8]$$

which transforms $2H_zC_z$ to observable carbon magnetization C_y. By exploiting the analogous transformation properties of the set of rf operators $\{I_x, I_y, I_z\}$ and the set of spin-spin coupling operators $\{2I_xS_z, 2I_yS_z, I_z\}$, Wimperis and Bodenhausen were able to derive a the broadband-INEPT preparation sequence

$$\begin{array}{lccccccccc} {}^{13}\mathrm{C} & & & & 180^\circ & & & & 180^\circ & \\ & & -\frac{\tau}{2}- & & & -\frac{\tau}{2}- & & -\tau- & & -\tau- \\ {}^{1}\mathrm{H} & 90^\circ_0 & & 180^\circ_{90} & & 120^\circ_{90} & & 180^\circ_{90} & & 30^\circ_{90} \end{array} \qquad [1\text{-}9]$$

and a broadband-INEPT reconversion sequence

$$\begin{array}{lccccccccc} {}^{13}\mathrm{C} & 30^\circ_{90} & & 180^\circ_{90} & & 120^\circ_{90} & & 180^\circ_{90} & & \text{Acquire} \\ & & -\tau'- & & -\tau'- & & -\frac{\tau'}{2}- & & -\frac{\tau'}{2}- & \\ {}^{1}\mathrm{H} & & & 180^\circ & & & & 180^\circ & & \text{Decouple} \end{array} \qquad [1\text{-}10]$$

which are J-compensated versions of sequences [1-7] and [1-8] respectively. These compensated sequences, which were both based on Levitt's $90^\circ_0 180^\circ_{120}$ composite 90° pulse, may be used together or independently in order to achieve the desired J-compensation. The advantages of the compensated sequences [1-9] and [1-10] over the regular sequences [1-7] and [1-8] were shown readily by product operator calculations of their efficiencies and the theoretical predictions were confirmed by experimental results. For CH, CH_2 and CH_3, the theoretical efficiency of the compensated preparation sequence [1-9] in producing longitudinal spin order was shown to be

$$f_{\text{compensated}}(\beta') = -(9\sin\beta' + \sin 3\beta')/8, \qquad [1\text{-}11]$$

where $\beta' = \pi J_{\mathrm{CH}}\tau$, compared to

$$f_{\text{uncompensated}}(\beta') = -\sin\beta'. \qquad [1\text{-}12]$$

for the regular preparation sequence [1-7]. Plots of these β'-dependent efficiencies definitely show that for $\beta' \neq 90^\circ$, the broadband-INEPT preparation sequence [1-9] produces longitudinal spin order of greater magnitude than the uncompensated sequence [1-7] does, and this ultimately leads to enhanced carbon signals.

Similar beneficial results were obtained when the refocusing efficiencies of broad-band-INEPT reconversion sequence [1-10] for the three CH_n spin systems were investigated. It is known that choosing the appropriate value for refocusing delay period τ' in refocused-INEPT is very difficult since the magnitude of the in-phase carbon magnetization created at the end of the period τ' depends not only to the values of J_{CH}, but also to the type of CH_n fragment. Even in the case where J_{CH} values are identical in a given molecule which contains three different CH_n fragments, it is not possible to find a value of τ' that would simultaneously refocus carbon magnetizations for all three spin systems. The rephasing delays employed are usually compromise values: $\tau' = 1/(2J_{\text{nominal}})$ when only CH is present and $\tau' = 1/(3J_{\text{nominal}})$ when CH, CH_2 and CH_3 are present (4). Under these two nominal conditions, the compensated sequence [1-10] refocuses carbon magnetizations better than the conventional reconversion sequence [1-8].

In a related study, Sørensen and co-workers (15,16) have developed compensated sequences for refocusing heteronuclear antiphase magnetization with enhanced sensitivity. The refocusing sequences derived include sequences which are effective for a wide range of J and those that simultaneously refocus antiphase magnetizations for various spin-spin systems. It was also shown that different compensated refocusing sequences may be designed for editing and for assigning multiplicities.

The utility of J-compensated sequences is not limited only to heteronuclear spin systems, but can be extended to homonuclear spin systems as well. Barbara, Tycko, and Weitekamp (17) have recognized that there is a formal analogy between rf pulses in the presence of B_1 inhomogeneity and the general double-quantum excitation sequence in a homonuclear spin system, regardless of the type of coupling. In their studies, they described procedures for constructing compensated double-quantum excitation sequences for a wide range of spin-spin, dipolar or quadrupolar

coupling constants based on any B_1-compensated pulse.

The analogies presented in all of the above studies relate the whole pulse sequence or some part thereof, which contains the J-dependent precession periods, to the behavior of rf pulses. The J-compensated sequences thus derived are tailored specifically to the experiment being considered and are not easily adaptable to the compensation of other pulse sequences. In this thesis, we present formal operator analogies which directly relate the operators involved in spin-spin coupling to the operators involved in rf pulses. Attention is focused here on the transformation of coherences in a more general way so that the J-compensated magnetization transfer sequences derived are of general utility and can be incorporated easily into the pulse sequences of any experiment which involves coherence transfer via spin-spin interaction. For example, a J-compensated sequence which transform magnetization I_y into antiphase magnetization $-2I_xS_z$ can be readily incorporated into the INEPT or DEPT sequences, or any 2D experiments which require magnetization transfer between protons and carbon.

Chapter 2 describes in detail the procedure for the construction of heteronuclear J-compensated magnetization transfer sequences from B_1 inhomogeneity-compensated pulses. Pictorial representations are used extensively in this chapter to clearly illustrate the formal analogies between the operators involved in rf pulses and in heteronuclear spin-spin coupling. Three J-compensated magnetization transfer sequences are incorporated into the DEPT (5) sequence, and their performance evaluated by experiments and by product operator calculations.

In Chapter 3, J-compensation of the spin-flip experiment (1) is considered. Two compensated versions of this heteronuclear spin-echo experiment are presented, one based on Levitt's popular $90^\circ_0 180^\circ_{90} 90^\circ_0$ composite inversion pulse (9) and the other on Wimperis' rectangular $180^\circ_0 180^\circ_{90} 90^\circ_{225}$ composite inversion pulse (18). The

merits of these compensated experiments are evaluated by comparing their signal intensity profiles for CH, CH_2, and CH_3 spin systems, to the signal profiles obtained in regular spin-flip experiments.

In Chapter 4, the operator correspondence is extended to homonuclear spin-systems. The J-compensated magnetization transfer sequence devised is incorporated into the INADEQUATE sequence and its efficiency is tested for applications in both proton and carbon spectroscopy. Different types of composite pulses are also investigated in order to make INADEQUATE experiments in carbon spectroscopy, where large resonance offset effects may be encountered, more efficient.

Besides their usefulness in enhancing signals, J-compensated sequences may be utilized to suppress responses from directly bonded CH_n fragments in 2D C–H shift correlation maps obtained in experiments which are designed for observation of long-range C–H couplings. The responses from protons directly attached to carbon are unwanted in these experiment since they needlessly complicate the 2D spectra. Purging sequences are usually inserted at the front end of these experiments in order to eliminate the undesirable direct responses. In describing the CH_n-edited HOHAHA relay experiment, Muhandiram *et. al* (19) showed that the broadband-INEPT preparation sequence [1-9] can be effectively used as a purging sequence, since this compensated sequence converts the in-phase magnetization of protons directly attached to carbon into longitudinal two-spin coherence so that it does not give observable magnetization during acquisition. The transverse magnetizations of protons remote to carbon, meanwhile, are essentially unaffected during the sequence since the long-range J_{CH} coupling constants are relatively small. It was found in their study (19) that J-compensated sequence [1-9] was more effective than two purging methods, a delay period of duration $1/(2^1 J_{CH})$, with ^1H and ^{13}C 180° pulses at the center, and the BIRD sequence (13), in removing directly bonded

correlations in HOHAHA relay maps. It is worthwhile therefore to investigate the performance of compensated sequence [1-9] and other J-compensated sequences, as purging elements in other long-range C–H shift correlation experiments. Chapter 5 presents a study of the efficiencies of several purging sequences for application in the two-dimensional C–H shift correlation experiment optimized for long-range magnetization transfer (20). Purging sequences investigated include a modified version of the broadband-INEPT preparation sequence [1-9], the TANGO sequence developed by Wimperis and Freeman (21), and the low-pass J-filters introduced by Kogler and co-workers (22). The most effective purging sequence is incorporated into a long-range C–H correlation experiment with a BIRD sequence at the center of the refocusing period, and its performance is compared to those of the purgeless sequence (23) and the FLOCK sequence devised by Reynolds and co-workers (24).

References

1. G. Bodenhausen, R. Freeman, R. Niedermeyer, and D. L. Turner, *J. Magn. Reson.* **24**, 291 (1976)

2. S. L. Patt and J. N. Shoolery, *J. Magn. Reson.* **46**, 535 (1982).

3. G. A. Morris and R. Freeman, *J. Am. Chem. Soc.* **101**, 760 (1979).

4. D. P. Burum and R. R. Ernst, *J. Magn. Reson.* **39**, 163 (1980).

5. D. T. Pegg, D. M. Doddrell, and M. R. Bendall, *J. Chem. Phys.* **77**, 2745 (1982).

6. A. Bax, R. Freeman, and S. P. Kempsell, *J. Am. Chem. Soc.* **102**, 4849 (1980).

7. O. W. Sørensen, G. W. Eich, M. H. Levitt, G. Bodenhausen, and R. R. Ernst, *Prog. NMR Spectrosc.* **16**, 163 (1983).

8. K. V. Schenker and W. von Philippsborn, *J. Magn. Reson.* **61**, 294 (1985).

9. M. H. Levitt and R. Freeman, *J. Magn. Reson.* **33**, 473 (1979).

10. M. H. Levitt and R. Freeman, *J. Magn. Reson.* **38**, 453 (1980).

11. M. H. Levitt, *J. Magn. Reson.* **48**, 234 (1982).

12. M. H. Levitt, *Prog. NMR Spectrosc.* **18**, 61 (1986).

13. J. R. Garbow, D. P. Weitekamp, and A. Pines, *Chem. Phys. Lett.* **93**, 504 (1982).

14. S. Wimperis and G. Bodenhausen, *J. Magn. Reson.* **69**, 264 (1986).

15. O. W. Sørensen, J. C. Madsen, N. C. Nielsen, H. Bildsoe, and H. J. Jakobsen, *J. Magn. Reson.* **77**, 170 (1988).

16. N. C. Nielsen, H. Bildsoe, H. J. Jakobsen, and O. W. Sørensen, *J. Magn. Reson.* **85**, 359 (1989).

17. T. M. Barbara, R. Tycko and D. P. Weitekamp, *J. Magn. Reson.* **62**, 54 (1985).

18. S. Wimperis, *J. Magn. Reson.* **83**, 509 (1989).

19. D. R. Muhandiram, T. T. Nakashima and R. E. D. McClung, *J. Magn. Reson.* **87**, 56 (1990).

20. W. F. Reynolds, R. G. Enriquez, L. I. Escobar, and X. Lozoya, *Can. J. Chem.* **62**, 2421 (1984); C. Wynants, K. Hallenga, G. van Binst, A. Michel, and J. Zanen, *J. Magn. Reson.* **57**, 93 (1984); M. J. Quast, E. L. Ezell, G. E. Martin, M. L. Lee, M. L. Tedjamulia, J. G. Stuart, and R. N. Castle, *J. Heterocyc. Chem.* **21**, 1453 (1985).

21. S. Wimperis and R. Freeman, *J. Magn. Reson.* **58**, 348 (1984).

22. H. Kogler, O. W. Sørensen, G. Bodenhausen and R. R. Ernst, *J. Magn. Reson.* **55**, 157 (1983).

23. C. Bauer, R. Freeman, and S. Wimperis, *J. Magn. Reson.* **58**, 526 (1984).

24. W. F. Reynolds, S. McLean, M. Perpick-Dumont, and R. G. Enriquez, *Magn. Reson. Chem.* **27**, 162 (1989).

CHAPTER 2

J-COMPENSATED DEPT SEQUENCES*

2.1 Introduction

DEPT (1) and INEPT (2, 3) are indispensable techniques for enhancing the sensitivity of low gyromagnetic ratio nuclei and for assigning the multiplicities of the carbon centers in a molecular skeleton. These heteronuclear polarization transfer experiments, like other multiple pulse experiments, contain precession periods of fixed duration in order to transfer proton polarization to carbon. During each fixed delay, spin-spin interactions between the I and S nuclei produce bilinear rotation of the I- and/or S-coherences. For example, the transverse proton magnetization, I_y, is transformed into proton magnetization which is antiphase with respect to carbon, $2I_xS_z$, by proton-carbon coupling during the first precession periods of the refocused-INEPT and DEPT sequences. This antiphase proton magnetization is transformed into carbon magnetization by rf pulses and precession periods in later stages of these sequences. The duration of each delay period in the polarization transfer sequences must be selected carefully in order to maximize the final carbon magnetization obtained.

The effectiveness of polarization transfer in INEPT or DEPT is strongly influenced by the magnitude of the spin-spin interaction during the precession periods. For a given molecular system containing several IS fragments with different spin-spin coupling constants, J_{IS}, the proper choice of the duration of a fixed delay, τ, which is inversely related to J_{IS}, may be difficult if the range of J_{IS} is large

*A version of this chapter has been published. A. M. Torres and R. E. D. McClung, *J. Magn. Reson.* **92**, 45 (1991). Copyright © 1991 by Academic Press, Inc.

(4). Imperfections in the $(\pi/2)$ bilinear rotations which interconvert in-phase and antiphase coherences cannot be avoided in such cases, and maximum polarization transfer cannot be attained for all IS fragments simultaneously because τ is chosen using a nominal (average) value of J_{IS}.

This problem of incomplete coherence conversion by spin-spin coupling is similar to the problems associated with the inhomogeneity of radio frequency pulses. Spatial inhomogeneity of the rf field produces a distribution of flip angles across the sample volume and can be minimized by replacing the rf pulse by an appropriate composite pulse (a sequence of phase-shifted radio frequency pulses) (5). Levitt and Freeman (6), for example, have shown that the composite pulse, $(\pi/2)_0-(\pi)_{90}-(\pi/2)_0$, is much less sensitive to B_1 inhomogeneity than a single $(\pi)_0$ pulse. Similarly, Levitt (7) has demonstrated that the composite pulse, $(\pi/2)_0-(\pi)_{120}$, is much more efficient than a single $(\pi/2)_0$ pulse in converting longitudinal to transverse magnetization in the presence of rf field inhomogeneity and resonance offsets.

Using the parallelism between rf pulses and spin-spin coupling, one can devise J-compensated coherence transfer sequences that are less sensitive to variations in J_{IS} based on composite pulses. Exploiting the formal analogy between the transformation properties of the operators $\{I_x, I_y, I_z\}$ and $\{2I_xS_z, 2I_yS_z, I_z\}$, Wimperis and Bodenhausen (8) have used Levitt's $(\pi/2)_0-(\pi)_{120}$ composite $(\pi/2)$ pulse to devise J-compensated INEPT sequences which are less sensitive to variations in J_{IS}. More recently, Sorensen *et al.* (9, 10) have presented J-compensated sequences, designated INEPT-CR, which refocus antiphase magnetization with enhanced sensitivity. These include sequences which are broadband over a range of coupling constants and sequences which provide optimum simultaneous refocusing of antiphase magnetization for different spin systems.

In this chapter, we present derivations of J-compensated magnetization transfer sequences from appropriate composite pulses, using analogies between the mutual transformation properties of sets of operators in the manner introduced by Wimperis and Bodenhausen (8), and describe the construction of J-compensated APT (11) and DEPT (1) sequences. For conciseness, the properties of the J-compensated APT sequences which are derived will be described fully in Chapter 3, so that the discussion here is directed only at the details of the construction of the compensated sequences and their application to the improvement of DEPT. The DEPT sequence (1) contains three fixed delays during which spin-spin coupling interchanges in-phase and antiphase coherences. We describe below the results of attempts to improve the efficiency of the interchanges in each of these periods. The efficiencies of these J-compensated DEPT sequences are compared with that of conventional DEPT using experimental and calculated results.

2.2 Theory

In attempting to construct J-compensated APT and DEPT sequences based on composite pulses, we found it necessary to make the operator analogies introduced by Wimperis and Bodenhausen (8) more explicit. Instead of concentrating on the conversion of longitudinal magnetization (I_z) to longitudinal two spin order ($2I_zS_z$), we consider the conversion of in-phase (I_y) to antiphase magnetization ($2I_xS_z$) under spin-spin coupling in a two spin 1/2 heteronuclear IS spin system. The analogous mutual transformation properties of the operators $\{I_x, I_y, I_z\}$ and $\{-2I_xS_z, 2I_zS_z, I_y\}$ are shown pictorially in Fig. 2.1a and 2.1b. The action of an rf pulse along the y-axis for period t rotates the magnetization initially aligned along the z-axis in the xz-plane by an angle $\beta = \gamma B_1 t$ and, in turn, creates magnetization

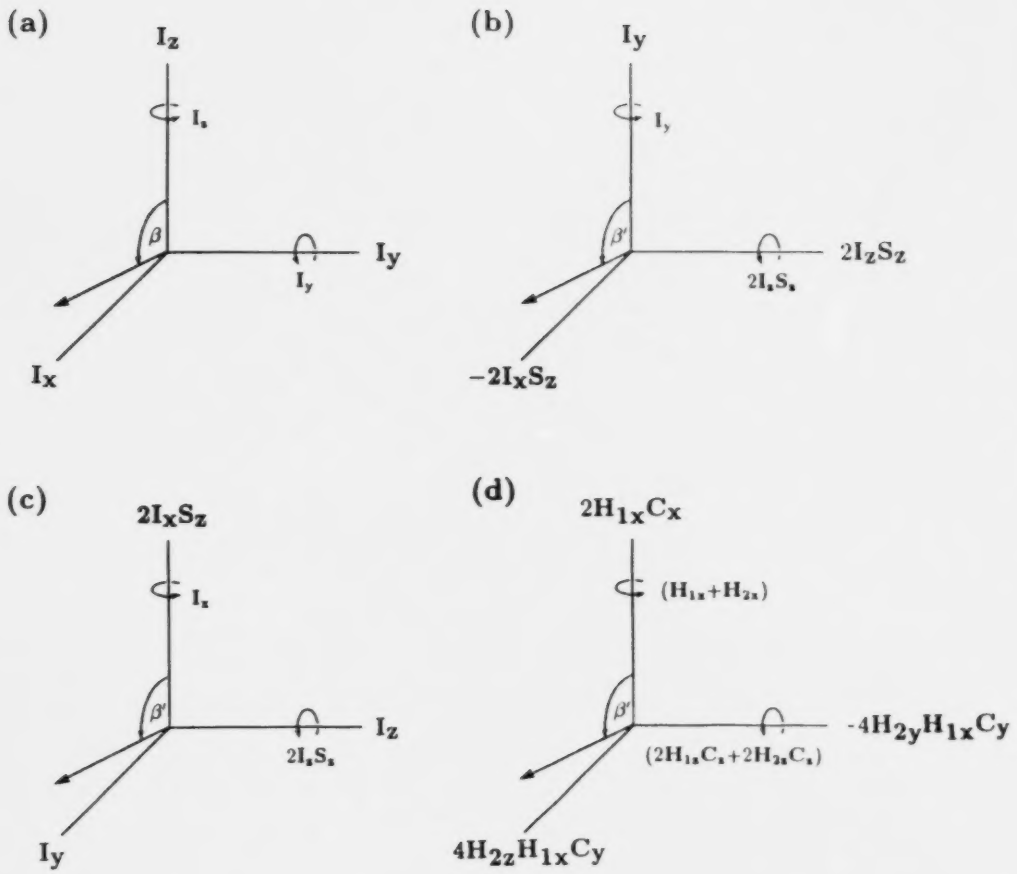

Figure 2.1: Pictorial Representations of Rotation and Bilinear Rotation Operators. The rotation arrows indicate the operators which are used in propagators associated with "rotations" about each axis, and the axis labels represent the product operator components which are interconnected by these "rotations". (a) Cartesian angular momentum operators involved in composite pulse sequences, (b) operators involved in the bilinear rotation of I_y and $2I_xS_z$, (c) operators involved in the composite bilinear rotation of $2I_xS_z$ into I_y, (d) operators involved in the construction of J-compensated conversion of $2H_{1x}C_x$ to $4H_{2z}H_{1x}C_y$.

along the x-axis

$$I_z \xrightarrow{(\beta)\, I_y} I_z \cos\beta + I_x \sin\beta. \qquad [2\text{-}1]$$

In an exactly analogous fashion, spin-spin coupling between nuclei I and S (operator $2I_zS_z$) for a period τ causes the transverse magnetization, I_y , to be rotated by angle $\beta' = \pi J_{IS}\tau$, producing I magnetization which is antiphase with respect to S, $-2I_xS_z$,

$$I_y \xrightarrow{(\beta')\, 2I_zS_z} I_y \cos\beta' - 2I_xS_z \sin\beta'. \qquad [2\text{-}2]$$

In short, the analogy implies the following correspondence: $I_x \leftrightarrow -2I_xS_z$, $I_y \leftrightarrow 2I_zS_z$, $I_z \leftrightarrow I_y$, $\beta \leftrightarrow \beta'$, and t $\leftrightarrow \tau$. In the following sections, we present derivations of compensated transfer sequences using this analogy between the actions of rf pulses and spin-spin coupling.

J-Compensated conversion of I_y to $-I_y$

The action of the composite inversion sequence $(\pi/2)_{90}-(\pi)_{180}-(\pi/2)_{90}$ on spin I magnetization aligned along the z-axis can be written as

$$I_z \xrightarrow{(\beta)\, I_y} \xrightarrow{(2\beta)\, I_x} \xrightarrow{(\beta)\, I_y} -I_z \qquad [2\text{-}3]$$

where β is nominally equal to $\pi/2$. Since a pulse along the x-axis is just a phase-shifted y-pulse, it is convenient to use the propagator equivalence

$$\xrightarrow{(\beta)\, I_x} \equiv \xrightarrow{(-\pi/2)\, I_z} \xrightarrow{(\beta)\, I_y} \xrightarrow{(\pi/2)\, I_z} \qquad [2\text{-}4]$$

to rewrite Eq. [2-3] as

$$I_z \xrightarrow{(\beta)\, I_y} \xrightarrow{(-\pi/2)\, I_z} \xrightarrow{(2\beta)\, I_y} \xrightarrow{(\pi/2)\, I_z} \xrightarrow{(\beta)\, I_y} -I_z, \qquad [2\text{-}5]$$

so that it contains only propagators involving I_y and I_z. A composite conversion of I_y to $-I_y$ via spin-spin coupling can be obtained from the composite transformation

in Eq. [2-5] by making the replacements $I_z \rightarrow I_y$, $I_y \rightarrow 2I_zS_z$, and $\beta \rightarrow \beta'$, as indicated above and in Fig. 2.1a and 2.1b. One obtains

$$I_y \xrightarrow{(\beta')2I_zS_z} \xrightarrow{(-\pi/2)I_y} \xrightarrow{(2\beta')2I_zS_z} \xrightarrow{(\pi/2)I_y} \xrightarrow{(\beta')2I_zS_z} -I_y. \quad [2\text{-}6]$$

This transformation of I_y to $-I_y$ is expected to be more effective, for a broader range of β', than the uncompensated

$$I_y \xrightarrow{(2\beta')2I_zS_z} -I_y \quad [2\text{-}7]$$

transformation employed in the spin-flip (12) and APT (11) experiments. In Chapter 3, we will show that the transformation in Eq. [2-6] can be implemented in a Compensated Attached Proton Test (CAPT) sequence

$$\begin{array}{ll} ^{13}\mathrm{C} & 90^\circ_0\text{-}\frac{\tau}{2} - 180^\circ_{90}\text{-}\frac{\tau}{2} - 90^\circ_{270}\text{-}\tau - 180^\circ_{90}\text{-}\tau\text{-}90^\circ_{90}\text{-}\frac{\tau}{2} - 180^\circ_{90}\text{-}\frac{\tau}{2}. \\ ^{1}\mathrm{H} & \qquad\qquad 180 \qquad\qquad\qquad\quad 180 \qquad\qquad\quad 180 \end{array} \quad [2\text{-}8]$$

which is expected to be less sensitive to variations in J_{CH} than the APT sequence (11). In sequence [2-8], the initial 90° pulse creates transverse I magnetization, and the 180° pulses at the center of each precession period refocus chemical shifts. The 180° carbon and proton pulses are shown explicitly at the center of each precession period in sequence [2-8], but will be omitted from all sequences discussed below for brevity.

Other composite inversion sequences which may be considered as bases for the construction of transformations for the compensated inversion of I_y via spin-spin coupling are the pulse sequence, $(\pi/2)_0\text{-}(4\pi)_{120}\text{-}(\pi/2)_0$ introduced by Levitt (7), and the rectangular inversion sequence, $(\pi)_0\text{-}(2\pi)_{90}\text{-}(2\pi)_{225}$, devised by Wimperis (13). Using the 90° phase-shifted versions of these sequences $[(\pi/2)_{90}\text{-}(\pi)_{210}\text{-}(\pi/2)_{90}$ and $(\pi)_{90}\text{-}(2\pi)_{180}\text{-}(2\pi)_{315}]$ and making the operator replacements indicated above, one can construct the corresponding compensated I_y to $-I_y$ sequences

$$\mathrm{I} \quad \tau - 120^\circ_{270} - 4\tau - 120^\circ_{90} - \tau \quad [2\text{-}9]$$

and

$$\mathrm{I} \quad \tau - 90^{\circ}_{270} - 2\tau - 135_{270} - 2\tau - 225_{90}. \qquad [2\text{-}10]$$

It can be shown, theoretically, that sequence [2-9] has a slightly broader profile than CAPT. Sequence [2-10] will be referred to in Chapter 3 as the Rectangular Attached Proton Test (RAPT) and is expected to display rectangular-shaped inversion profile with respect to J_{IS} especially for the CH spin system. However, due to the long times between excitation and detection in these sequences, they are less suitable for samples with short relaxation times.

J-Compensated conversion of I_y to $-2I_xS_z$

The composite pulse which we consider in developing broadband versions of DEPT, just as Wimperis and Bodenhausen (8) did in their work on INEPT, is Levitt's $(\pi/2)_0-(\pi)_{120}$ composite sequence (7). This sequence, compensated for both B_1 inhomogeneity and resonance offsets, brings down z-magnetization to a point in the xy-plane with very small phase distortion. For convenience, a $(\pi/6)$ rotation about the z-axis may be added to the end of this sequence so that the final magnetization lies along the x-axis, and the composite pulse sequence can be written

$$I_z \xrightarrow{(\beta)I_x} \xrightarrow{\{(2\beta)I_x\}_{120^0\ shift}} \xrightarrow{(\pi/6)\,I_z} I_x. \qquad [2\text{-}11]$$

An alternate version of this sequence

$$I_z \xrightarrow{(\beta)I_y} \xrightarrow{\{(2\beta)I_y\}_{120^0\ shift}} \xrightarrow{(-\pi/3)\,I_z} I_x, \qquad [2\text{-}12]$$

which uses rotations about y- and z-axes, is more convenient for our purposes. It can be shown (14) that

$$\xrightarrow{\{(2\beta)I_y\}_{120^0\ shift}} \equiv \xrightarrow{(-2\pi/3)\,I_z} \xrightarrow{(2\beta)\,I_y} \xrightarrow{(2\pi/3)\,I_z}, \qquad [2\text{-}13]$$

so that the transformation in Eq. [2-12] becomes

$$I_z \xrightarrow{(\beta)\,I_y} \xrightarrow{(-2\pi/3)\,I_z} \xrightarrow{(2\beta)\,I_y} \xrightarrow{(2\pi/3)\,I_z} \xrightarrow{(-\pi/3)\,I_z} I_x, \qquad [2\text{-}14]$$

or simply

$$I_z \xrightarrow{(\beta)\,I_y} \xrightarrow{(-2\pi/3)\,I_z} \xrightarrow{(2\beta)\,I_y} \xrightarrow{(\pi/3)\,I_z} I_x \qquad [2\text{-}15]$$

after adding the two adjacent rotations. By making the operator replacements shown in Fig. 2.1a and 2.1b, one can convert this composite pulse transformation into the compensated transformation

$$I_y \xrightarrow{(\beta')\,2I_zS_z} \xrightarrow{(-2\pi/3)\,I_y} \xrightarrow{(2\beta')\,2I_zS_z} \xrightarrow{(\pi/3)\,I_y} -2I_xS_z \qquad [2\text{-}16]$$

of I_y to $-2I_xS_z$.

The corresponding compensated pulse sequence,

$$\mathrm{I} \quad \tau - 120^\circ_{270} - 2\tau - 60^\circ_{90}, \qquad [2\text{-}17]$$

therefore converts in-phase to antiphase magnetization more effectively over a wider range of J_{IS} than a single τ period. A phase-shifted version of this sequence,

$$\mathrm{I} \quad \tau - 120^\circ_{90} - 2\tau - 60^\circ_{270}, \qquad [2\text{-}18]$$

produces the same transformation as [2-17], and the sequence

$$\mathrm{I} \quad \tau - 120^\circ_{270} - 2\tau - 120^\circ_{270} \qquad [2\text{-}19]$$

in which the pulses have identical lengths and phases is a compensated sequence for the conversion of I_y to $+2I_xS_z$.

The broadband preparation part of INEPT developed by Wimperis and Bodenhausen (8)

$$\mathrm{I} \quad 90^\circ_0 - \tau - 120^\circ_{90} - 2\tau - 30^\circ_{90} \qquad [2\text{-}20]$$

can be derived from the sequence [2-18] by inserting an initial 90°_0 pulse to convert I_z to $-I_y$, and appending a 90°_{90} pulse to convert $2I_xS_z$ to $-2I_zS_z$.

Compensated conversion of $2I_xS_z$ to I_y

As Wimperis and Bodenhausen (8) have pointed out, inverting the order and phases of all pulses and delays in a compensated sequence leads to compensated sequence which does the inverse conversion. A compensated sequence that converts antiphase to in-phase magnetization can therefore be obtained from the compensated sequence of Eq. [2-17]. The resulting sequence is

$$\mathrm{I} \quad 60^{\circ}_{270} - 2\tau - 120^{\circ}_{90} - \tau. \qquad [2\text{-}21]$$

Product operator calculations show that this sequence is indeed better than a single spin-spin coupling period τ in converting $2I_xS_z$ to $+I_y$. Sequences of this type are useful in experiments like refocused-INEPT (3) where the choice of refocusing delay, Δ, is critical.

A different compensated pulse sequence which transforms $2I_xS_z$ to I_y can be devised by making use of the analogous transformation properties of the operators $\{ I_x, I_y, I_z\}$ and $\{ I_y, 2I_zS_z, 2I_xS_z\}$. Levitt's composite pulse $(\pi/2)$, Eq. [2-12], provides the sequence

$$2I_xS_z \xrightarrow{(\beta')\,2I_zS_z} \xrightarrow{(-2\pi/3)\,2I_xS_z} \xrightarrow{(2\beta')\,2I_zS_z} \xrightarrow{(\pi/3)\,2I_xS_z} I_y. \qquad [2\text{-}22]$$

However, the propagators which involve $2I_xS_z$ and which represent phase shifts of the propagator $\xrightarrow{(2\beta')\ 2I_zS_z}$ will be imperfect due to the dispersion of J_{IS}. Detailed investigation of the propagator in Eq. [2-22] shows that the $\xrightarrow{(-2\pi/3)\ 2I_xS_z}$ element "stores" part of the $I_y \sin\beta'$ magnetization as longitudinal two-spin order, so that it will be invariant to the $\xrightarrow{(2\beta')\ 2I_zS_z}$ evolution, then the $\xrightarrow{(\pi/3)\ 2I_xS_z}$ revives this component. This "storing" of I_y magnetization during the $2\beta'$ evolution period can be achieved more conveniently and without imperfections by replacing the

propagators containing $2I_xS_z$ with propagators involving I_x:

$$2I_xS_z \xrightarrow{(\beta')\,2I_zS_z} \xrightarrow{(-2\pi/3)\,I_x} \xrightarrow{(2\beta')\,2I_zS_z} \xrightarrow{(\pi/3)\,I_x} I_y. \qquad [2\text{-}23]$$

With this propagator, some of the $I_y \sin\beta'$ produced in the β' evolution is "stored" as longitudinal magnetization I_z during the $2\beta'$ evolution period, and is recovered by the $(\pi/3)I_x$ pulse. The extended analogy between the sets of operator $\{ I_x, I_y, I_z\}$ and $\{ I_y, 2I_zS_z, 2I_xS_z\}$ is represented pictorially in Fig. 2.1a and 2.1c.

The compensated pulse sequence based on the transformation of $2I_xS_z$ to I_y in Eq. [2-23] is

$$\mathrm{I} \quad \tau - 120^\circ_{180} - 2\tau - 60^\circ_0. \qquad [2\text{-}24]$$

It is important to note that the inverse of this sequence,

$$\mathrm{I} \quad 60^\circ_{180} - 2\tau - 120^\circ_0 - \tau, \qquad [2\text{-}25]$$

like the pulse sequence of Eq. [2-17], transforms I_y to $-2I_xS_z$.

It is instructive to look at the mechanics of the two compensated sequences [2-17] and [2-25] which convert in-phase I_y to antiphase $-2I_xS_z$ magnetization. In the following discussion, the magnitudes of the various components of the density operator will be described by the leading terms in their Taylor expansions in the imperfection parameter

$$\delta = \pi \mathrm{J}_{IS}\tau - \pi/2. \qquad [2\text{-}26]$$

In this way, the compensation effects can be readily understood.

In the compensated sequence [2-17], the initial magnetization I_y produces a large antiphase magnetization component, $2I_xS_z$, of magnitude $-1 + \delta^2/2$, and a smaller I_y component, $-\delta$, during the τ evolution period. The $(2\pi/3)_{270}$ pulse on the I spin leaves the small I_y component unchanged, but halves the magnitude of

the $2I_xS_z$ component, inverts its phase, and "stores" the rest as longitudinal two-spin order, $2I_zS_z$. During the 2τ evolution period, the small I_y component results in an I_y component of magnitude $+\delta$ and a $2I_xS_z$ component of magnitude $-2\delta^2$, while the "half size" $2I_xS_z$ component leads to an I_y component of magnitude $-\delta$ and a $2I_xS_z$ component of magnitude $(-1+5\delta^2)/2$. Thus, to second order in δ, the I_y component vanishes at this point. The $(\pi/3)_{90}$ pulse on spin I rotates the $2I_xS_z$ and $2I_zS_z$ components so that, to second order in δ, the desired $2I_xS_z$ component has a magnitude of -1 and a small $2I_zS_z$ of magnitude $\sqrt{3}\,\delta^2/2$ remains.

In the alternative sequence [2-25], the initial magnetization I_y is halved in magnitude by the $(\pi/3)_{180}$ pulse on the I nuclei, and the remainder is "stored" as longitudinal magnetization I_z. During the 2τ evolution period, spin-spin coupling converts the "half-size" I_y component into an I_y component of magnitude $-1/2+\delta$, and a $2I_xS_z$ component of magnitude δ. The $(2\pi/3)_0$ pulse on spin I leaves the $2I_xS_z$ component unchanged, and rotates the I_y and I_z components to produce an I_y component of magnitude $1-\delta^2/2$ and an I_z component of magnitude $\sqrt{3}\delta^2/2$. Spin-spin coupling during the final τ period converts the dominant I_y component into a $2I_xS_z$ component of magnitude $-1+\delta^2$ and a small I_y component of magnitude $-\delta$, while the small $2I_xS_z$ component evolves to produce an I_y component of magnitude $+\delta$ and a $2I_xS_z$ of magnitude $-\delta^2$. To second order in δ, the $2I_xS_z$ component has magnitude of -1, the I_y component vanishes, and a small I_z component of magnitude $\sqrt{3}\delta^2/2$ remains.

Both compensated conversion sequences transform I_y to $-2I_xS_z$ exactly to second order in δ. The first produces a very small second order $2I_zS_z$ component, while the second gives an I_z component of the same magnitude. It is clear that the two conversion sequences should be equally efficient in converting I_y to $-2I_xS_z$. The important features of each are the "storing" of magnetization during the 2τ

evolution period so that only the "half-size" magnetization experiences the "double imperfection" which is essentially canceled by the imperfections produced by the evolution of the total magnetization in the single length τ period.

Construction of compensated DEPT sequences

DEPT (Distortionless Enhancement Polarization Transfer) (1) is a widely used pulse sequence derived from refocused-INEPT (3). In contrast to refocused-INEPT (3), DEPT gives signals from CH, CH_2, and CH_3 fragments which are simultaneously in-phase at the start of the acquisition so that $^{13}C\{^1H\}$ spectra are easily obtained (15). Although the DEPT sequence is longer time-wise than that for refocused-INEPT, it has fewer refocusing pulses so that it is less sensitive to pulse imperfections. In spectral editing applications, DEPT is superior to refocused-INEPT since it employs spectra obtained with read pulses of different flip angles rather than spectra obtained from experiments with spin-spin coupling periods of different lengths. This makes DEPT somewhat less sensitive to variations in spin-spin coupling constants than INEPT.

In order to incorporate the compensated magnetization transfer sequences derived above into the DEPT sequence, it is important to look at the signal pathways for CH, CH_2, and CH_3 in detail. Figure 2.2 shows the signal intensity pathways by tracing the transformation of proton to carbon magnetization for each spin system. For convenience, the DEPT sequence is divided into three parts, each of which contains a τ delay period, and chemical shift effects are ignored. Figure 2.2 also presents the β' and the θ dependence of each of the terms in the density operator for each spin system as it progresses through the DEPT sequence. For simplicity, we have labeled the spin operators as C, H_1, H_2, and H_3, and we shall focus our attention on the carbon signal which is derived from the H_{1z} term in the initial

$$\mathrm{CH}\quad H_{1z} \xrightarrow{\mathcal{H}_1\tau} 2H_{1x}C_z\,s \xrightarrow{\mathcal{H}_2\tau} 2H_{1x}C_x\,s \xrightarrow{\mathcal{H}_3\tau} C_y\,s^2\,S_\theta$$

$$\mathrm{CH_2}\quad H_{1z} \xrightarrow{\mathcal{H}_1\tau} 2H_{1x}C_z\,s \xrightarrow{\mathcal{H}_2\tau} \begin{array}{l} 4H_{2z}H_{1x}C_y\,s^2 \\ +\,2H_{1x}C_x\,sc \end{array} \xrightarrow{\mathcal{H}_3\tau} \begin{array}{l} C_y\,s^4\,(S_{2\theta}/2) \\ +\,C_y\,s^2c^2\,(S_\theta) \end{array}$$

$$\mathrm{CH_3}\quad H_{1z} \xrightarrow{\mathcal{H}_1\tau} 2H_{1x}C_z\,s \xrightarrow{\mathcal{H}_2\tau} \begin{array}{l} -\,8H_{3z}H_{2z}H_{1x}C_x\,s^3 \\ +\,2H_{1x}C_x\,sc^2 \\ +\,4H_{2z}H_{1x}C_y\,s^2c \\ +\,4H_{3z}H_{1x}C_y\,s^2c \end{array} \xrightarrow{\mathcal{H}_3\tau} \begin{array}{l} C_y\,s^6\,[(S_{3\theta}+S_\theta)/4] \\ +\,C_y\,s^2c^4\,(S_\theta) \\ +\,C_y\,s^4c^2\,(S_{2\theta}/2) \\ +\,C_y\,s^4c^2\,(S_{2\theta}/2) \end{array}$$

Figure 2.2: Product operator description of proton to carbon magnetization transfer in DEPT for CH, CH_2, and CH_3 spin systems. The following abbreviations are used: $\xrightarrow{\mathcal{H}_1\tau}=\xrightarrow{(\pi/2)\,H_x}\xrightarrow{(\beta')\,2H_zC_z}$, $\xrightarrow{\mathcal{H}_2\tau}=\xrightarrow{(\pi/2)\,C_y}\xrightarrow{(\beta')\,2H_zC_z}$, $\xrightarrow{\mathcal{H}_3\tau}=\xrightarrow{(\theta)\,H_y}\xrightarrow{(\pi)\,C_y}\xrightarrow{(\beta')\,2H_zC_z}$, $s = \sin\beta'$, $c = \cos\beta'$, $S_\theta = \sin\theta$, $S_{2\theta} = \sin 2\theta$, and $S_{3\theta} = \sin 3\theta$

density operator. For the CH_2 spin system, the terms H_{1z} and H_{2z} in the initial density operator produce equivalent contributions to the final signal, and the terms H_{1z}, H_{2z} and H_{3z} give equivalent contributions to the signal for CH_3.

For all spin systems, H_{1z} is converted to transverse magnetization, $-H_{1y}$, by the initial proton pulse, this magnetization is converted to $2H_{1x}C_z$ during the first τ delay period and the $(\pi/2)_{90}$ carbon pulse converts this antiphase magnetization to multiple quantum coherence, $2H_{1x}C_x$. For the CH spin system, this coherence is unaffected by coupling during the second delay period, $2H_{1z}C_x$ is produced by the action of the $(\theta)_{90}$ proton pulse on $2H_{1x}C_x$, and this antiphase carbon magnetization, which has a maximum amplitude for $\theta = \pi/2$, is converted to C_y during the third delay period.

In the CH_2 spin system, the multiple quantum coherence, $2H_{1x}C_x$, is transformed by spin-spin coupling during the second delay period into multiple quantum coherence which is antiphase with respect to the second proton, $4H_{2z}H_{1x}C_y$. The $(\theta)_{90}$ proton pulse converts this into carbon magnetization antiphase with respect to both protons, $4H_{1z}H_{2z}C_y$, which has a maximum amplitude for $\theta = 45°$. There are two operator terms which contribute to the carbon signals from CH_2 fragments when the lengths of the last two delay periods are not equal to $1/(2J_{CH})$: $4H_{2z}H_{1z}C_y$, the principal term (P), and $2H_{1z}C_x$, the ancillary term (A). The ancillary term results in an observable carbon signal only when the delays in the second and third part of DEPT sequence are misset.

In the CH_3 spin system, four terms in the density operator: $8H_{3z}H_{2z}H_{1z}C_x$ (the principal term), $4H_{3z}H_{1z}C_y$, $4H_{2z}H_{1z}C_y$, and $2H_{1z}C_x$ (the ancillary terms) contribute to the observed signal when the delays in the second and third part of DEPT are misset. We will refer to the $8H_{3z}H_{2z}H_{1z}C_x$ term as P, the term $2H_{1z}C_x$ as A_1, and the sum of the terms $4H_{3z}H_{1z}C_y + 4H_{2z}H_{1z}C_y$ as A_2.

It is clear that proton chemical shifts are effective during the first and second delay periods in the DEPT sequence, and that carbon chemical shifts are operative during the second and third delay periods. In order to cancel these effects, a $(\pi)_0$ proton refocusing pulse is placed between the first and second delay periods, and a $(\pi)_{90}$ carbon pulse is inserted between the second and the third delay periods in the standard DEPT experiment (1) as shown in Fig. 2.3a. For the introduction of J-compensation into the delay periods in DEPT, it is more convenient to insert simultaneous proton and carbon refocusing pulses at the center of each delay period as shown in Fig. 2.4. The $(\pi)_{90}$ carbon pulse coincident with the $(\theta)_{90}$ proton pulse in the original DEPT sequence (Fig. 2.3a) is retained in this expanded version of DEPT because this $(\pi)_{90}$ carbon pulse, besides serving as a chemical shift refocusing pulse in regular DEPT, also serves as an inversion pulse to attain the right signal intensity profile.

Compensation of the first part of DEPT (DEPTC1)

As pointed out above, the first part of the DEPT sequence,

$$^1\mathrm{H} \quad 90^\circ_0 - \tau, \qquad [2\text{-}27]$$

is characterized by the conversion of H_{1z} to $2H_{1x}C_z$ for all spin systems. Using the sequences [2-17] and [2-25] above for the conversion of $-H_{1y}$ to $2H_{1x}C_z$, one can construct the composite pulse sequences

$$^1\mathrm{H} \quad 90^\circ_0 - \tau - 120^\circ_{270} - 2\tau - 60^\circ_{90} \qquad [2\text{-}28]$$

and

$$^1\mathrm{H} \quad 90^\circ_0 - 60^\circ_{180} - 2\tau - 120^\circ_0 - \tau \quad \equiv \quad 30^\circ_0 - 2\tau - 120^\circ_0 - \tau \qquad [2\text{-}29]$$

for the first part of the DEPT sequence. The complete DEPT sequence based on the compensated sequence [2-29] is shown in Fig. 2.3b, and the incorporation

(a) CONVENTIONAL DEPT

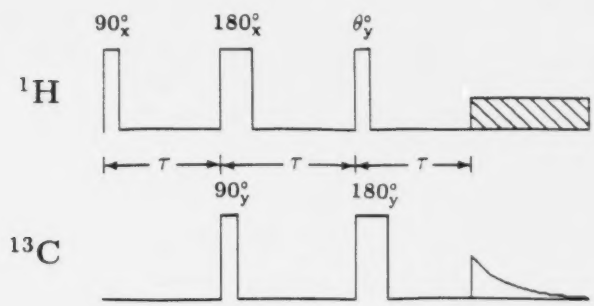

(b) DEPTC1

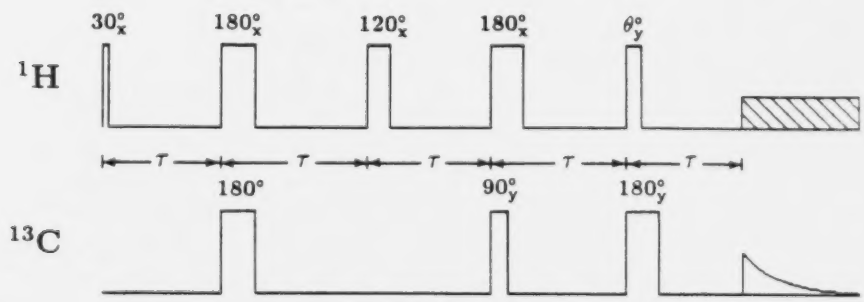

Figure 2.3: Pulse Sequences for (a) DEPT and (b) DEPTC1. $\tau = 1/2\,{}^1J_{CH}^{nom}$.

of sequence [2-28] into DEPT is shown in Fig. 2.4a. The sequences which incorporate [2-28] or [2-29] are referred to as DEPTC1 sequences since they have J-compensation in the first part of the DEPT sequence. It is clear from Fig. 2.3b and 2.4a that the incorporation of sequence [2-29] is preferable since it requires far fewer refocusing pulses. This is so because the compensated sequence [2-29], like the first part of the conventional DEPT sequence [2-27], ends with a precession period of length τ so that the $(\pi)_0$ proton and carbon refocusing pulses in normal DEPT may be retained, resulting to a much simpler version of DEPTC1. This

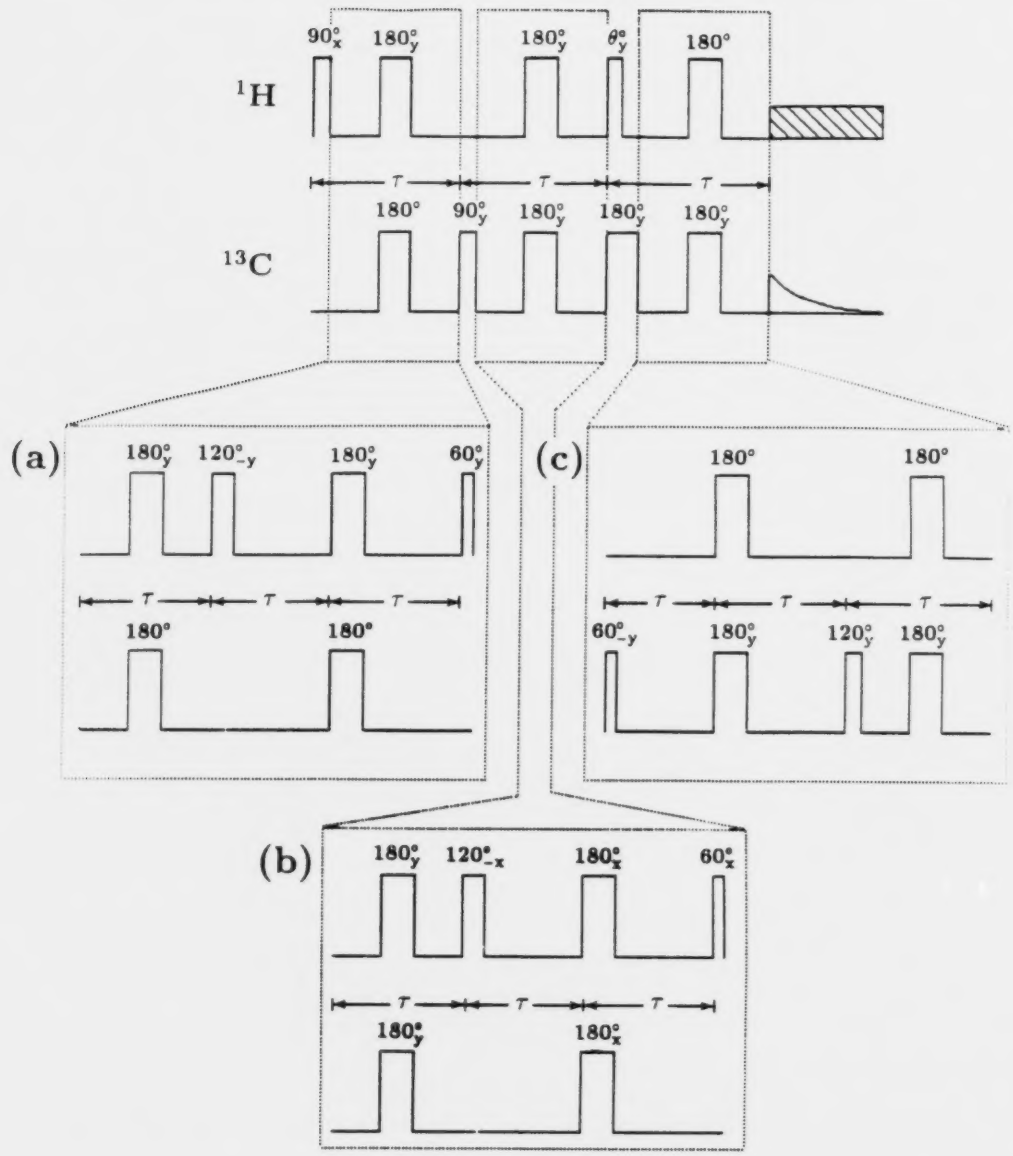

Figure 2.4: Modifications to DEPT for J-compensation. Top – DEPT sequence with explicit refocusing pulses in each delay period. (a) compensation of the first part, (b) compensation of the second part, (c) compensation of the third part. $\tau = 1/2\,{}^1J^{nom}_{CH}$.

simplification is not possible with [2-28] since it ends with a $(\pi/3)_{90}$ proton pulse. Hence, in the version of DEPTC1 based on sequence [2-28] (Fig. 2.4a), refocusing pulses must be inserted at the center of each delay period in order to eliminate chemical shift effects. Note that the $(\pi)_{90}$ carbon pulse coincident with the $(\theta)_{90}$ proton pulse in the original DEPT sequence (Fig. 2.3a) must be retained in both implementations of DEPTC1.

Compensation of the second part of DEPT (DEPTC2)

During the second delay period in DEPT, the density operator term $2H_{1x}C_x$ is invariant to spin-spin coupling for CH systems, but evolves for CH_2 and CH_3 systems to become $4H_{2z}H_{1x}C_x$ and $-8H_{3z}H_{2z}H_{1x}C_x$ respectively as shown in Fig. 2.2. These dominant terms together with some ancillary terms in the density operator involve more than two spins so that sequences [2-17] and [2-25], devised for a two-spin system, are not directly applicable. For the CH_2 spin system, we wish to construct a compensated sequence, which converts $2H_{1x}C_x$ to $4H_{2z}H_{1x}C_y$, leaving as small a $2H_{1x}C_x$ component as possible, from Levitt's compensated $(\pi/2)$ sequence [2-5]. The operator replacements $I_x \rightarrow 4H_{2z}H_{1x}C_y$, $I_y \rightarrow 2H_{1z}C_z + 2H_{2z}C_z$, and $I_z \rightarrow 2H_{1x}C_x$, which one might develop from a simple comparison of the effects of the $\xrightarrow{(\beta)\ I_y}$ and $\xrightarrow{(\beta')\ (2H_{1z}C_z + 2H_{2z}C_z)}$ propagators, do not yield a compensated conversion of $2H_{1x}C_x$ to $4H_{2z}H_{1x}C_y$. Instead, one must design the compensated conversion sequence with propagator elements which mimic the effects of the various propagators in sequences [2-17] and [2-25]. The sequence

$$^1\mathrm{H} \quad \tau - 120^\circ_{180} - 2\tau - 60^\circ_0. \qquad \text{[2-30]}$$

has the required elements. The $(2\pi/3)_{180}$ proton pulse "stores" part of the principal $4H_{2z}H_{1x}C_y$ component of the density operator produced by spin-spin coupling

during the first delay as a $4H_{2y}H_{1x}C_y$ component which is invariant to spin-spin coupling during the 2τ evolution period, just as the $(2\pi/3)_{270}$ pulse in the sequence [2-17] "stores" part of the principal $2I_xS_z$ component as $2I_zS_z$. The "half-size" $4H_{2z}H_{1x}C_y$ component and the ancillary $2H_{1x}C_x$ component evolve during the 2τ period so that the $2H_{1x}C_x$ component vanishes (to second order in δ) at the end of this period. The $(\pi/3)_0$ proton pulse rotates the $4H_{2y}H_{1x}C_y$ and $4H_{2z}H_{1x}C_y$ components into the desired $4H_{2z}H_{1x}C_y$ component. Similarly, for CH_3 spin system, the $(2\pi/3)_{180}$ proton pulse "stores" part of the principal $-8H_{3z}H_{2z}H_{1x}C_y$ component as $-8H_{3y}H_{2y}H_{1x}C_y$ and the $(\pi/3)_0$ proton pulse, after the second delay period, converts this magnetization back to the desired $-8H_{3z}H_{2z}H_{1x}C_y$. Note that, in Fig. 2.2, the β' dependence of $-8H_{3z}H_{2z}H_{1x}C_y$ in the CH_3 case is different from that of $4H_{2z}H_{1x}C_y$ in the CH_2 case so that the compensation effects of sequence [2-30] in these two spin systems will be somewhat different. The implementation of pulse sequence [2-30] to obtain a DEPT sequence with the second part J-compensated (DEPTC2) is shown in Fig. 2.4b.

Compensation of the third part of DEPT (DEPTC3)

The behavior of the CH, CH_2, and CH_3 spin systems during the third part of DEPT involves a number of different product operator terms (see Fig. 2.2) and ultimately produces carbon C_y magnetization. It is not easy, therefore, to devise a sequence that compensates the conversion of all these terms into observable carbon magnetization. By considering only the principal $2H_{1x}C_y$ term of the CH spin system, one can construct a DEPT sequence in which the third delay is compensated, DEPTC3, by incorporating either sequence [2-21] or [2-24] into the basic DEPT sequence. Figure 2.4c shows the compensated sequence based on sequence [2-21] (DEPTC3). In the implementation of the DEPTC3 sequence, the phases of the

$(\pi/3)_{270}$ and $(2\pi/3)_{90}$ carbon pulses must be alternated together in order to suppress signals originating from the residual $H_{1_y}\cos\beta'$ term from the first evolution period. It is expected that this sequence will applicable for the CH spin system, but not necessarily for the CH_2 and CH_3 spin systems, since the density operators for these systems contain terms (including their respective $2H_{1_z}C_x$ terms) which behave differently under spin-spin coupling during the third delay period.

2.3 Experimental

All experiments were performed on a Bruker AM-400 spectrometer. For verification of the DEPTC1 sequence (Fig. 2.3b), 90% (v/v) solutions of C_6H_6 in $CDCl_3$ (CH spin system, $^1J_{CH} = 160$ Hz), CH_2Cl_2 in C_6D_6 (CH_2 spin system, $^1J_{CH} = 178$ Hz), and CH_3OH in C_6D_6 (CH_3 spin system, $^1J_{CH} = 141$ Hz) were chosen for the three spin systems. All samples were slightly doped with chromium(III) acetylacetonate to achieve repetition times of 30-40 seconds. Four scans were accumulated for each experiment and proper incrementation of τ was done so that β' varied from 40° to 140° in 10° steps. The standard DEPT phase cycle (16) was adopted. The 30° and 120° pulses were not phase cycled since their phases are tied to that of the first proton pulse. The first 180° proton refocusing pulse must be along the same axis as the 30° proton pulse, while the phase of the first 180° carbon pulse was not varied.

The sample used for comparison of the relative efficiencies of DEPT and DEPTC1 was a 1:1 mole mixture of cholesterol (50mg) and 3-methyl-1-pentyn-3-ol (13mg) in $CDCl_3$ (0.35ml). In each experiment, 128 scans were recorded with a delay interval of 4 seconds between scans. Three different τ values corresponding to $\beta' = 55°$, 90°, and 125° (based on $^1J_{CH}^{Avg} = 129$ Hz for cholesterol) were used in the comparison.

2.4 Results and Discussion

The calculated β'-dependence of the ^{13}C signal intensities in each part of the conventional and compensated DEPT sequences are presented in Table 1. For convenience, only the carbon signal from the H_{1z} term for each spin system was considered. The overall β'-dependence of the ^{13}C intensity for a particular spin system subjected to a specified pulse sequence can be obtained by multiplying the appropriate factors for each of the three parts of the sequence. For example, for a conventional DEPT experiment on a CH_2 spin system, the total β'-dependence will be $\sin\beta' \sin\theta[\cos\theta \sin\beta'(1 - \cos 2\beta') + \cos\beta' \sin 2\beta']/2$ which is obtained after multiplying the factor $\sin\beta'$ for the first part by the sum of the products $\sin\beta' \times \sin\theta\cos\theta(1 - \cos 2\beta')/2$ and $\cos\beta' \times \sin\theta(\sin 2\beta')/2$, which describe the evolution of the principal (P) and ancillary (A) terms in the density operator during the second and third parts of the sequence. Similarly, for the DEPTC1 experiment (part one is J-compensated, parts two and three are uncompensated) on the CH spin system, the ^{13}C signal will be proportional $\sin\theta \sin\beta'(9\sin\beta' + \sin 3\beta')/8$ which is just the product of the factors $(9\sin\beta' + \sin 3\beta')/8$ for the first part, 1 for the second part, and $\sin\theta \sin\beta'$ for the third part as given in Table 1.

Figure 2.5 shows the calculated and the normalized experimental ^{13}C signal intensities as a function of β' for DEPT and DEPTC1 on the CH, CH_2 and CH_3 spin systems. The flip angles for the ^1H pulses were 90°, 45°, and 35° for the CH, CH_2 and CH_3 spin systems respectively, where the principal components of the respective density operators have maxima. The observed signal to noise ratios in the two sequences were essentially equivalent and the small variations observed can be attributed to relaxation effects. It is clear that the experimental results agree well with the calculated predictions. For all spin systems, DEPTC1 produces a

Table 2.1: β'-dependence of ^{13}C signal intensities in each part of conventional and J-compensated DEPT sequences[a].

System	First part		Second part	Third part
			Conventional DEPT	
CH	s		1	$S_\theta s$
CH_2	s	(P)	s	$S_\theta C_\theta(1-c_2)/2$
		(A)	c	$S_\theta(s_2)/2$
CH_3	s	(P)	$(1-c_2)/2$	$S_\theta C_\theta^2(3s-s_3)/4$
		(A_1)	$(1+c_2)/2$	$S_\theta(s+s_3)/4$
		(A_2)	$s_2/2$	$S_\theta C_\theta(c-c_3)/4$
			J-Compensated DEPT	
CH	$(9s+s_3)/8$		1	$S_\theta(9s+s_3)/8$
CH_2	$(9s+s_3)/8$	(P)	$(9s+s_3)/8$	$S_\theta C_\theta(4-3c_2-c_6)/8$
		(A)	$(3c+c_3)/4$	$S_\theta(9s_2+s_6)/16$
CH_3	$(9s+s_3)/8$	(P)	$(82-63c_2-18c_4-c_6)/128$	$S_\theta C_\theta^2(27s-6s_3-s_9)/32$
		(A_1)	$(10+15c_2+6c_4+c_6)/32$	$S_\theta(9s+10s_3+s_9)/32$
		(A_2)	$(21s_2+12s_4+s_6)/64$	$S_\theta C_\theta(3c-2c_3-c_9)/8$

[a]Abbreviations: $s = \sin\beta'$, $s_n = \sin n\beta'$, $c = \cos\beta'$, $c_n = \cos n\beta'$, $S_\theta = \sin\theta$, and $C_\theta = \cos\theta$.

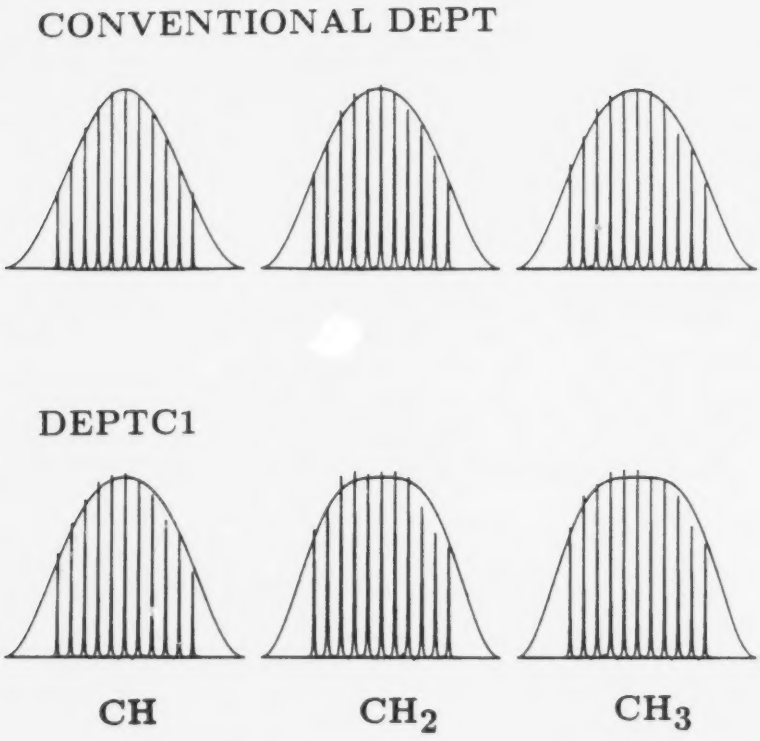

Figure 2.5: Comparison of calculated and observed DEPT and DEPTC1 signal profiles for CH (C_6H_6), CH_2 (CH_2Cl_2), and CH_3 (CH_3OH) spin systems. The flip angles of the ^1H θ pulses were 90°, 45°, and 35° respectively.

more broadband magnetization transfer profile than conventional DEPT due to the replacement of the simple $\sin\beta'$ dependence in the first part of the sequence by the compensated $(9\sin\beta' + \sin 3\beta')/8$ dependence. For the CH spin system, DEPTC1 gives near perfect magnetization transfer (> 90%) for $\beta' = 66° - 114°$ as compared to conventional DEPT which gives magnetization transfer greater than 90% over the narrower region $\beta' = 72° - 108°$. Moreover, in the region near $\beta' = 50°$ (and $\beta' = 130°$), this J-compensated DEPT sequence yields ^{13}C signals from CH system which are 20% larger than in conventional DEPT. The superiority of DEPTC1 is more pronounced for CH_2 and CH_3 spin systems. For CH_2 and CH_3

spin systems, greater than 90% polarization transfer is attained for β' in the range (56°, 124°), while the corresponding region using regular DEPT is (67°, 113°).

Regular DEPT and DEPTC1 spectra of a 1:1 mole mixture of cholesterol and 3-methyl-1-pentyn-3-ol at three different delay periods (β'_{nominal} = 55°, 90°, and 125° based on $^1J_{\text{CH nominal}}$ = 129Hz for cholesterol) are shown in Fig. 2.6. In every case $\theta = 45°$ so that the signals from all CH_n fragments are positive. It can be seen from the figure that the peak intensities from the various CH_n fragments in the two "misset" DEPTC1 spectra ($\beta' = 55°_{\text{nom}}$ and 125°) vary less from fragment to fragment than the corresponding peaks in the conventional DEPT spectra. Measurements of the relative intensities of the DEPTC1 spectra at β'_{nom} = 55°, 90°, and 125° indicate that the average ratio $I_{55°}/I_{90°}$ is 0.95 and the average $I_{125°}/I_{90°}$ is 0.79. The corresponding ratios for the conventional DEPT spectra are $I_{55°}/I_{90°} = 0.91$ and $I_{125°}/I_{90°} = 0.72$. This shows that DEPTC1 is less sensitive to variations in coupling constants and/or τ delay misset than conventional DEPT. In the spectra shown in Fig. 2.6 for both DEPT sequences, it can be noticed that the carbon peak for the methyne CH fragment of 3-methyl-1-pentyn-3-ol, in which $^1J_{\text{CH}}$ = 250Hz, appeared only in the misset spectra. Since the effective β' for this fragment is approximately $2\beta'_{\text{nom}}$, the proton experiences a 180° (not 90°) bilinear rotation during the first part of DEPT or DEPTC1 and does not produce carbon magnetization. It is therefore not surprising that DEPTC1 does not give an observable signal for this methyne fragment. One can also observe in the spectra of both DEPT sequences that the peaks at β'_{nom} = 55° are generally larger than the peaks at 125°. Proton and carbon relaxation effects account for this difference since the evolution times in these two cases (β'_{nom} = 55° and 125°) are quite different. In Fig. 2.6, the peaks in the DEPTC1 spectra are slightly smaller than those in the DEPT spectra. This loss of signal is undoubtedly due to pulse imperfections and proton relaxation

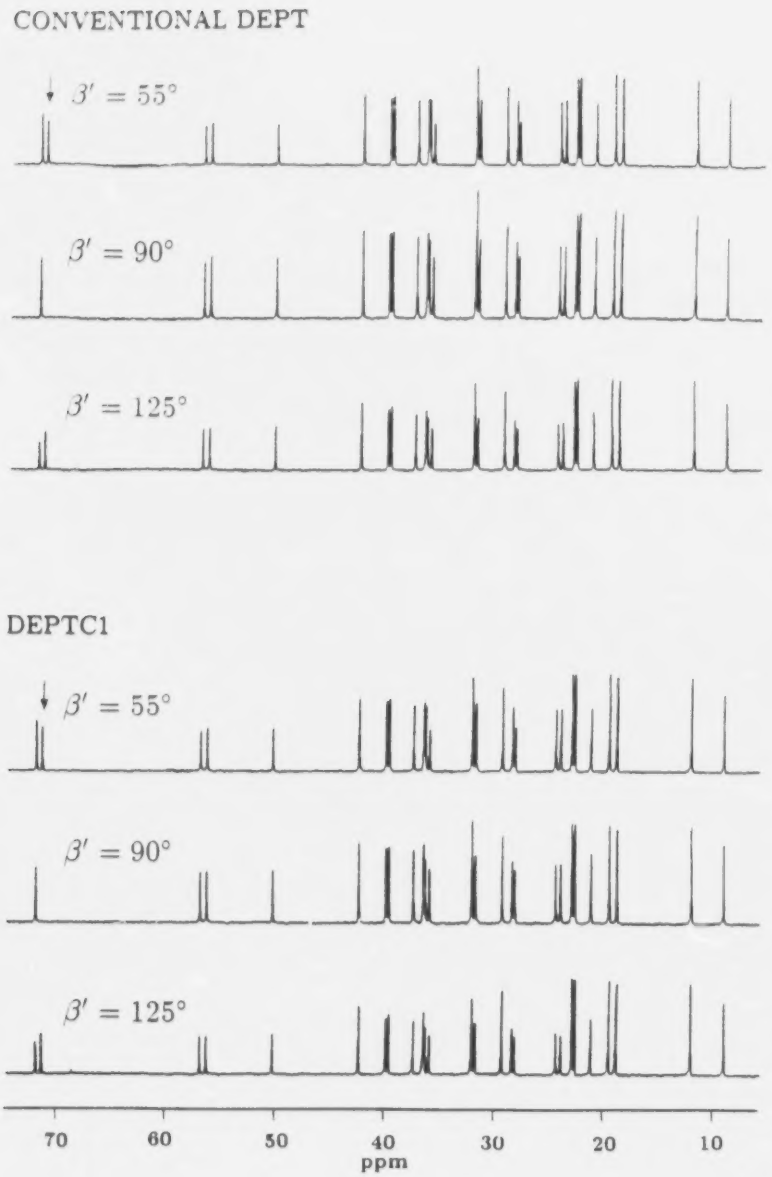

Figure 2.6: Comparison of DEPT and DEPTC1 spectra of 1:1 mole mixture of cholesterol and 3-methyl-1-pentyn-3-ol in $CDCl_3$ for delay periods of different lengths. The values of $\beta' = \pi {}^1J_{CH}\tau$ are based on ${}^1J_{CH}^{Avg} = 129\,Hz$. The arrow in each DEPT spectra indicates the methyne CH peak of 3-methyl-1-pentyn-3-ol.

during the extended first precession period in DEPTC1.

Figure 2.7 shows the calculated ^{13}C signal intensity profiles for conventional DEPT and DEPTC2. Since no compensation is expected for the CH spin system, only the profiles for CH_2 and CH_3 are presented. In addition to the overall signal, the principal (P) and the ancillary (A) components of the signal for CH_2 and CH_3 spin systems are also shown in Fig. 2.7 so that the effect of J-compensation on each component is clearly shown. For CH_2, DEPTC2 gives a broader P signal profile as expected. One can also observe that the A signal, which is a result of the delay misset in the second and third parts, is significantly smaller in DEPTC2 than in conventional DEPT, particularly in the region of $\beta' = 90°$. These results are expected since the P signal arises from the $4H_{2z}H_{1x}C_x$ term in the density operator, while the A signal comes from the $2H_{1x}C_x$ term. Compensation of the second part of DEPT, as in DEPTC2, makes the conversion of $2H_{1x}C_x$ to $4H_{2z}H_{1x}C_x$ more efficient leading a broader P signal profile and an A signal which is substantially reduced in magnitude near $\beta' = 90°$. As shown in Fig. 2.7, the addition of the P and A signals does not, unfortunately, give an overall signal profile for CH_2 which is broader than that for regular DEPT. One obtains 90% magnetization transfer for β' in the range $74° - 106°$ with DEPTC2, which is much narrower than the corresponding range $66° - 114°$ for DEPT.

A similar result is obtained for the CH_3 spin system. DEPTC2 produces a broader P signal profile, while the ancillary signals (A_1 and A_2) are significantly reduced in amplitude and shifted away from $\beta' = 90°$. The overall signal profile, which is obtained by adding the three signal components, is found to be narrower than the conventional DEPT profile. Based on the results for these two spin systems, one must conclude that J-compensation of the spin-spin coupling conversions in the second part of DEPT does not produce overall signal profiles that are broader

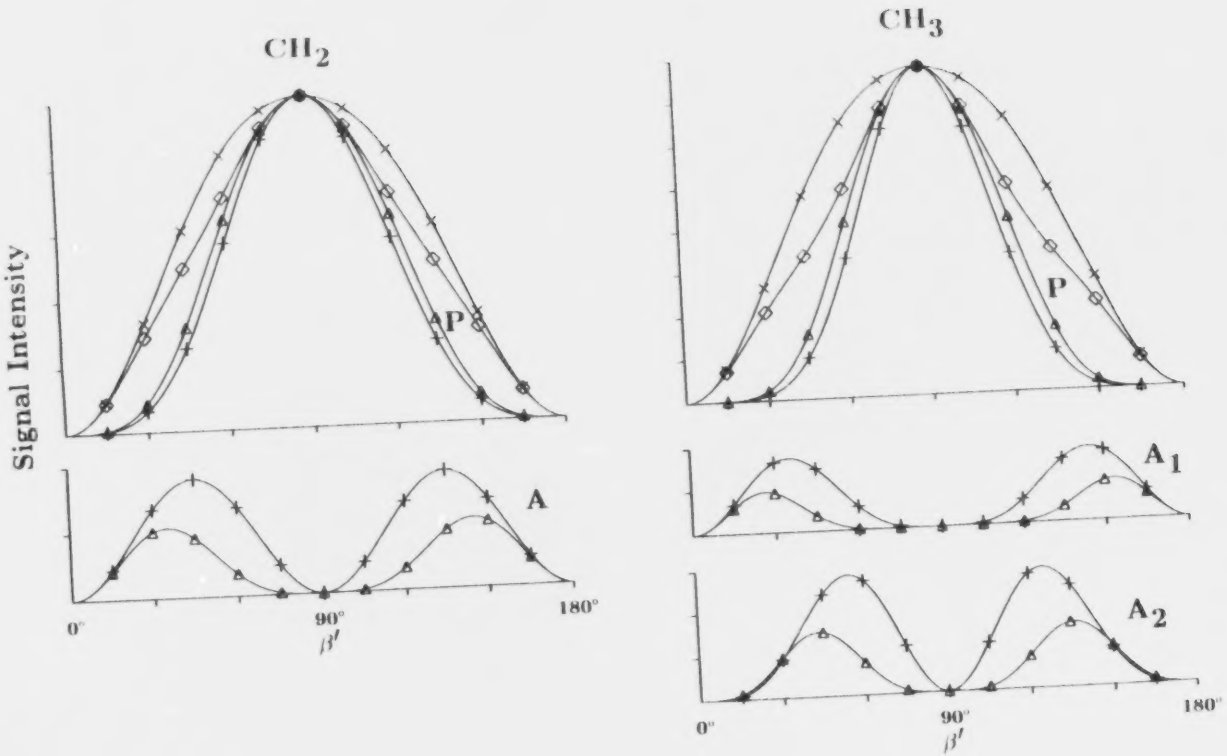

Figure 2.7: Comparison of DEPT and DEPTC2 Signal profiles for CH_2 and CH_3 spin systems. $\times - \times - \times$ – total DEPT signal, $\diamond - \diamond - \diamond$ – total DEPTC2 signal, $+ - + - +$ – component DEPT signal, $\triangle - \triangle - \triangle$ – component DEPTC2 signal. Total signal = P + A for CH_2, and $P + A_1 + A_2$ for CH_3. The flip angles of the ^1H θ pulses were 45° for CH_2 and 35° for CH_3.

than the overall signal profiles obtained in conventional DEPT.

The J-compensation of the third part of the DEPT sequence (DEPTC3), as shown in Fig. 2.4c, gives a broadband signal profile for the CH spin system which is identical to the signal profile obtained for CH in DEPTC1 (see Fig. 2.5). Detailed DEPTC3 signal profiles for the CH_2 and CH_3 spin systems are shown in Fig. 2.8 and reveal that J-compensation is achieved for the A signal in CH_2 and the A_1 signal in CH_3, which are associated with the $2H_{1z}C_x$ term in the density operator, and for the P signal in CH_3. Although the β' dependence of the signal coming from the $2H_{1z}C_x$ term in each spin system is different, the above observation is not surprising since the $(\pi/3)_{270}$ carbon pulse in DEPTC3 "stores" part of the $2H_{1z}C_x$ component for each spin system as $2H_{1z}C_z$ during the 2τ delay so that the compensating effect on the conversion of $2H_{1z}C_x$ to C_y will be more or less equivalent for each spin system. Similarly, DEPTC3 yields a broader profile for the P signal in CH_3 since part of the $-8H_{3z}H_{2z}H_{1z}C_x$ component is "stored" as $-8H_{3z}H_{2z}H_{1z}C_z$ by the $(\pi/3)_{270}$ carbon pulse.

The effect of DEPTC3 on signals originating from antiphase carbon magnetization aligned along the y-axis is not advantageous. For CH_2, DEPTC3 yields a P signal (coming from $4H_{2z}H_{1z}C_y$) that is less broadband than the corresponding DEPT profile. Actually, if the compensated sequence [2-24], instead of sequence [2-21], is used to make a third part compensated DEPT, only half of the expected P signal can be obtained. This can be explained by the fact that these two compensated sequences are not designed to compensate the transformation of $4H_{2z}H_{1z}C_y$ to C_y in CH_2. In sequence [2-24], the $(\pi/3)_{180}$ carbon pulse "stores" part of the C_y $\sin\beta'$ as C_z but the $(\pi/6)_0$ pulse after the 2τ evolution period does not recover all the "stored" longitudinal magnetization and as a result, only half of the maximum recoverable carbon magnetization is converted to C_y. Sequence [2-21] performs

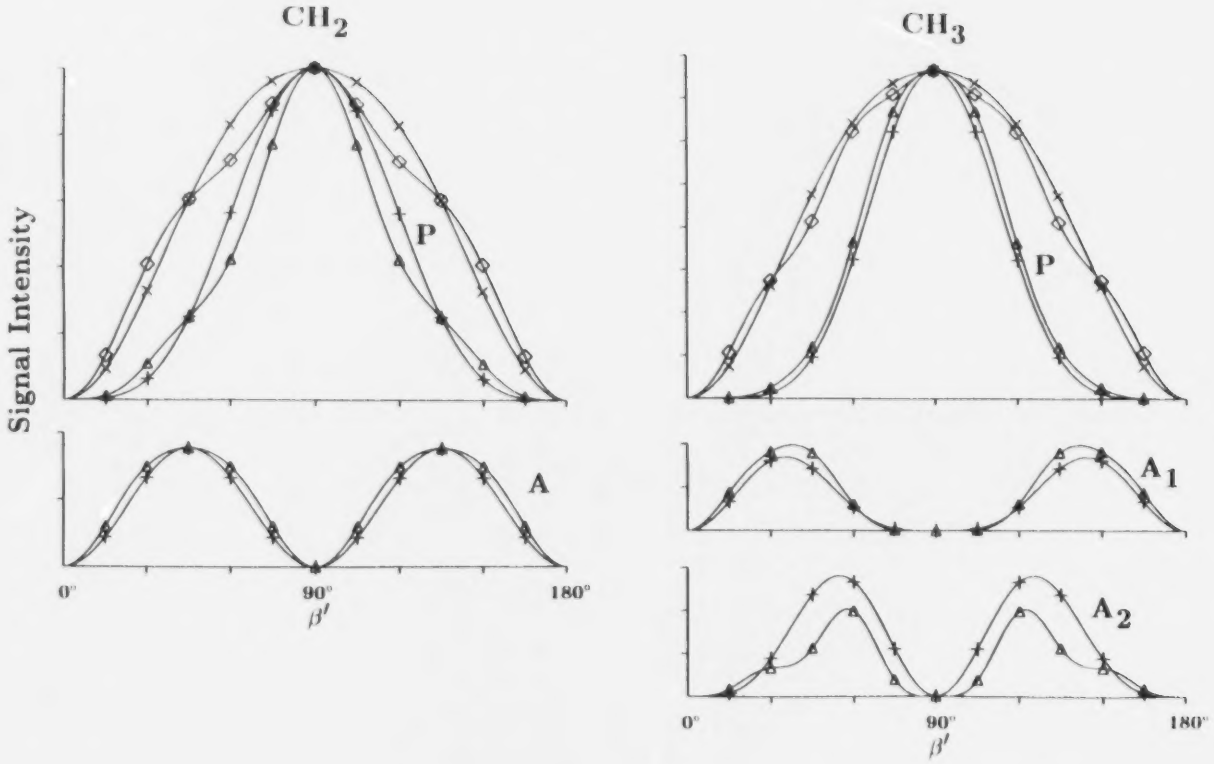

Figure 2.8: Comparison of DEPT and DEPTC3 Signal profiles for CH_2 and CH_3 spin systems. $\times - \times - \times$ - total DEPT signal, $\diamond - \diamond - \diamond$ - total DEPTC3 signal, $+ - + - +$ - component DEPT signal, $\triangle - \triangle - \triangle$ - component DEPTC3 signal. Total signal = P + A for CH_2, and $P + A_1 + A_2$ for CH_3. The flip angles of the ^1H θ pulses were 45° for CH_2 and 35° for CH_3.

better than sequence [2-24] because it involves a $(\pi/6)_{270}$ carbon pulse to which $4H_{2z}H_{1z}C_y$ is invariant and thus, no unnecessary "storing" of magnetization occurs. In addition, the $(\pi/3)_{90}$ carbon pulse only reduces the magnitudes of the "misset" $2H_{1z}C_x$ and $2H_{2z}C_x$ components produced by the spin-spin interconversion during the 2τ period while leaving the $4H_{2z}H_{1z}C_y$, which gives the C_y signal in the final τ period, unchanged. It is for these reasons that DEPTC3 is devised from sequence [2-21] rather than from sequence [2-24]. For CH_3, DEPTC3 shows a significant reduction in the signal intensity coming from the A_2 component.

Although compensation is achieved for signal components coming from antiphase carbon magnetizations aligned along the x-axis, the overall DEPTC3 signal profiles for CH_2 and CH_3 shown in Fig. 2.8 are not encouraging. For CH_2, while the regions $\beta' = 0° - 44°$ and $\beta' = 136° - 180°$ manifest a higher signal for DEPTC3 than for conventional DEPT, the DEPTC3 intensities in the important region near $\beta' = 90°$ are smaller than the DEPT intensities. The results shown in Fig. 2.8 also reveal that no beneficial overall compensation is attained for CH_3 spin systems.

In contrast to the broadband-INEPT reconversion sequence (8), DEPTC3 fails to produce overall signal profiles for CH_2 and CH_3 which are broader that the DEPT profiles. This is due to the presence of antiphase carbon magnetization components, in addition to $2H_{1z}C_x$, in the third part of DEPT which contribute to the observed ^{13}C signals for these spin systems. In the second part of refocused-INEPT, the only terms in the density operators which are converted to the C_y are $2H_{1z}C_x$, $2H_{2z}C_x$ and $2H_{3z}C_x$, so that the broadband-INEPT reconversion sequence devised for the CH spin system (8) gives signal profiles which are broader for CH, CH_2 and CH_3 spin systems. As shown above, similar effects are achieved in the conversion of $2H_{1z}C_x$ to C_y in DEPTC3, but the beneficial effects on the P signal profiles are overshadowed by the unfavorable effects on the conversions of the other

antiphase carbon magnetization terms in CH_2 and CH_3, and this leads to overall profiles which are less broad than the overall profiles obtained in conventional DEPT.

2.5 Conclusion

We have developed J-compensated sequences for the conversion of I_y to $-I_y$, I_y to $-2I_xS_z$, and $2I_xS_z$ to I_y for the two spin 1/2 IS spin system, and a compensated sequence for the conversion of $2H_{1x}C_x$ to $4H_{2z}H_{1x}C_y$ for the CH_2 spin system. Incorporation of the J-compensated conversion I_y to $-2I_xS_z$ into the first part of the DEPT sequence (1) gives a useful broadband DEPTC1 sequence. Unfortunately, attempts to make the second and third parts of DEPT less sensitive to the magnitudes of $^1J_{CH}$ by incorporating J-compensated sequences were unsuccessful. The J-compensated conversion sequences developed here should prove useful in the modification of the pulse sequences for heteronuclear correlation experiments (17) in order to enhance or suppress directly-bonded correlations.

References

1. D. T. Pegg, D. M. Doddrell, and M. R. Bendall, *J. Chem. Phys.* **77**, 2745 (1982).

2. G. A. Morris and R. Freeman, *J. Am. Chem. Soc.* **101**, 760 (1979).

3. D. P. Burum and R. R. Ernst, *J. Magn. Reson.* **39**, 163 (1980).

4. K. V. Schenker and W. von Philipsborn, *J. Magn. Reson.* **61**, 294 (1985).

5. R. Freeman, S. P. Kempsell, and M. H. Levitt, *J. Magn. Reson.* **38**, 453 (1980).

6. M. H. Levitt and R. Freeman, *J. Magn. Reson.* **33**, 473 (1979).

7. M. H. Levitt, *J. Magn. Reson.* **48**, 234 (1982).

8. S. Wimperis and G. Bodenhausen, *J. Magn. Reson.* **69**, 264 (1986).

9. O. W. Sørensen, J. C. Madsen, N. C. Nielsen, H. Bildsøe, and H. J. Jakobsen, *J. Magn. Reson.* **77**, 170 (1988).

10. N. C. Nielsen, H. Bildsøe, H. J. Jakobsen, and O. W. Sørensen, *J. Magn. Reson.* **85**, 359 (1989).

11. S. L. Patt and J. N. Shoolery, *J. Magn. Reson.* **46**, 535 (1982).

12. G. Bodenhausen, R. Freeman, R. Niedermeyer, and D. L. Turner, *J. Magn. Reson.* **24**, 291 (1976).

13. S. Wimperis, *J. Magn. Reson.* **83**, 509 (1989).

14. O. W. Sørensen, G. W. Eich, M. H. Levitt, G. Bodenhausen, and R. R. Ernst, *Progress NMR Spectrosc.* **16**, 163 (1983).

15. D. T. Pegg, D. M. Doddrell, and M. R. Bendall, *J. Magn. Reson.* **51**, 264 (1983).

16. K. V. Schenker and W. von Philipsborn, *J. Magn. Reson.* **66**, 219 (1986).

17. G. E. Martin and A. S. Zektzer, *Magn. Reson. Chem.* **26**, 631 (1988); W. F. Reynolds, S. McLean, M. Perpick-Dumont, and R. G. Enriquez, *Magn. Reson. Chem.* **27**, 162 (1989); D. R. Muhandiram, T. T. Nakashima, and R. E. D. McClung, *J. Magn. Reson.* **87**, 56 (1990).

CHAPTER 3

J-COMPENSATED APT SEQUENCES*

Heteronuclear *J*-modulated spin-echo experiments such as spin-flip (1) and APT (2), and polarization transfer experiments like INEPT (3) and DEPT (4) are used extensively in assigning and editing ^{13}C NMR spectra. In these experiments, the resonances for carbon with an even or odd number of attached protons are distinguishable. The amplitudes of these signals depend very strongly on the magnitudes of the $^{13}C-^{1}H$ spin-spin coupling constant, $^{1}J_{CH}$, and on the type of CH_n fragment. Hence, the proper choice of interpulse delay, τ, which is related to $^{1}J_{CH}$, is essential (5). Wimperis and Bodenhausen (6) have recently devised a compensated version of the INEPT experiment which transfers magnetization more effectively over a wider range of coupling constants. This "broadband" INEPT sequence was developed from Levitt's composite 90° pulse sequence (7) by exploiting the analogous operator mechanics of the operators $\{I_x,I_y,I_z\}$ and $\{2I_xS_z,\ 2I_yS_z,\ I_z\}$. Sørensen *et al.* (8) have introduced a different compensated version of INEPT (INEPT CR) in which enhanced sensitivity for CH and CH_3 groups is obtained.

In their description of the BIRD sequence, which inverts the magnetization from protons directly attached to ^{13}C but does not invert the magnetization of protons in $^{12}CH_n$ fragments, Garbow, Weitekamp, and Pines (9) described a compensated BIRD sequence which was less sensitive to variations in $^{1}J_{CH}$. Wimperis and Freeman (10) have also reported *J*-compensated inversion sequences for discriminating between direct and long-range C–H couplings. This earlier work (9,10) concentrated on the selective inversion of longitudinal magnetization of protons in

*A version of this chapter has been published. A. M. Torres, R. E. D. McClung, and T. T. Nakashima, *J. Magn. Reson.* **87**, 189 (1990). Copyright © 1990 by Academic Press, Inc.

$^{13}CH_n$ fragments. In this chapter, we focus on the behavior of transverse carbon magnetizations for ^{13}CH, $^{13}CH_2$, and $^{13}CH_3$ fragments during APT-like sequences. Two J-compensated spin-echo experiments related to the spin-flip experiment (1) are described and their relative merits evaluated.

The Compensated Attached Proton Test (CAPT) sequence is analogous to Levitt's $90^\circ_0 180^\circ_{90} 90^\circ_0$ composite inversion pulse sequence (7) and is shown in Fig. 3.1b. This sequence is very closely related to the J-compensated BIRD sequence (9). A Rectangular Attached Proton Test (RAPT) sequence, derived from Wimperis' $180^\circ_0 180^\circ_{90} 90^\circ_{225}$ rectangular inversion pulse sequence (11), is shown in Fig. 3.1c. The derivations of these two sequences from the corresponding composite pulses are presented in Chapter 2.

Product operator calculations (12) of the behavior of CH, CH_2, and CH_3 spin systems during the spin-flip, CAPT, and RAPT pulse sequences (Fig. 3.1) were carried out, and the calculated dependence of the ^{13}C signal intensities on the delay τ is given in Table 3.1.

Experimental comparisons of the three APT-like experiments were performed on Bruker AM-400 and WM-360 spectrometers. The samples selected for the three spin systems were 90% (v/v) solutions of C_6H_6 in $CDCl_3$ (CH), CH_2Cl_2 in C_6D_6 (CH_2), and CH_3OH in C_6D_6 (CH_3). All samples were doped with chromium (III) acetylacetonate to reduce experiment repetition times. Thirty-two scans were accumulated in each experiment with delays of 7–9 s between scans. The angle $\theta = \pi^1 J_{CH} \tau$ was varied from 80° to 280° in 20° increments by appropriate incrementation of τ in order to mimic variation in coupling constants. The experimental data shown in Fig. 3.2 are normalized to the calculated intensities. The observed signal-to-noise ratios in the three APT-like experiments were not substantially different, and relaxation effects accounted for the small variations observed.

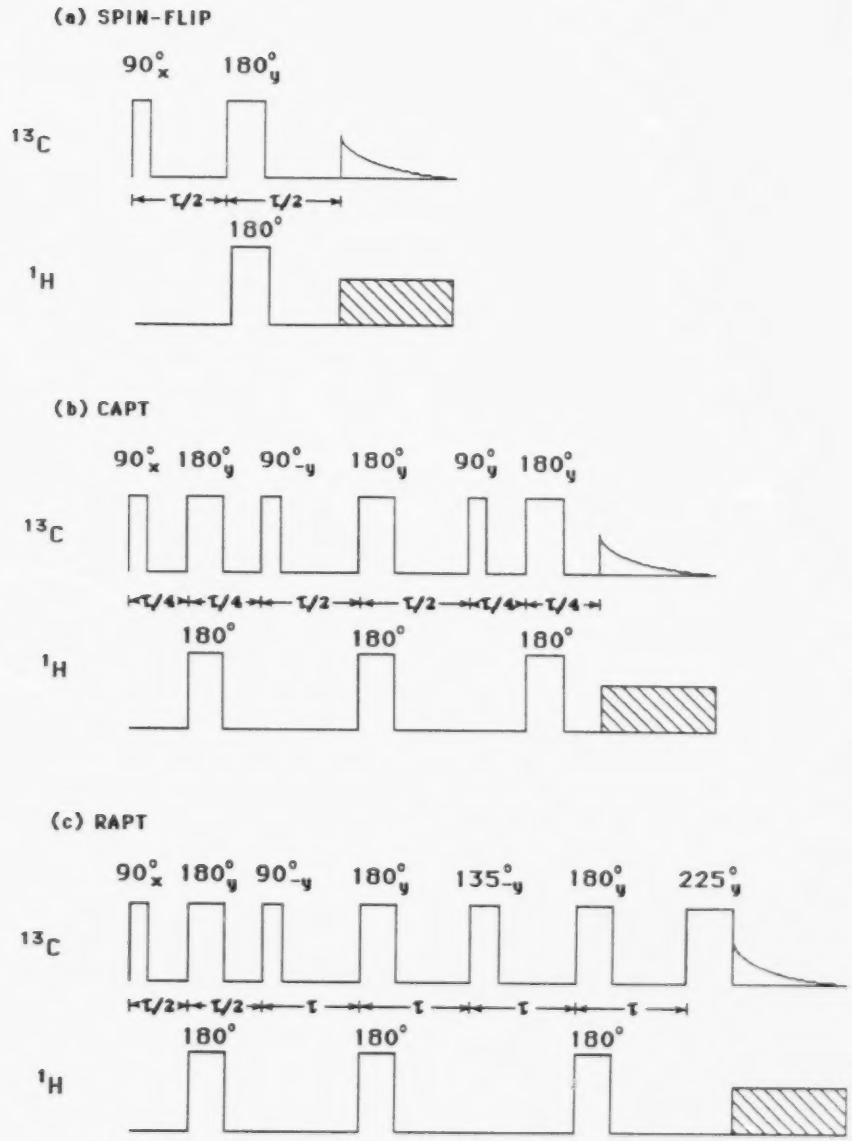

Figure 3.1: Pulse sequences for APT-like experiments. For optimum operation, $\tau = 1/{}^1J_{CH}$. The phases of the carbon π pulses in each sequence should be alternated independently and the phase of the initial $\pi/2$ pulse cycled in concert with the detector.

Table 3.1: Signal Intensities in APT-like experiments[a]

Spin System	Experiment		
	Spin-flip	CAPT	RAPT
CH	c	$(-1+4c+c_2)/4$	$1.207c-0.280c_3+0.073c_5$
CH_2	$(1+c_2)/2$	$(3+4c_2+c_4)/8$	$0.500+0.604c_2-0.140c_6$ $+0.037c_{10}$
CH_3	$(3c+c_3)/4$	$(-4+12c+3c_2$ $+4c_3+c_6)/16$	$0.889c+0.088c_3+0.054c_5$ $-0.046c_9+0.015c_{15}$

[a] $c=\cos\theta$, $c_n=\cos n\theta$, $\theta=\pi J_{CH}\tau$.

Figure 3.2 shows the experimental and calculated (Table 3.1) variations of the ^{13}C signal intensities with $\theta=\pi^1 J_{CH}\tau$ for the spin-flip, CAPT, and RAPT sequences. As expected, the inversion profiles obtained with CAPT and RAPT sequences for the CH spin system have broader regions of maximal inversion than one finds in the spin-flip experiments. The RAPT inversion profile for CH has an approximately rectangular shape as Wimperis has predicted (11). In all cases, the observed θ dependence agrees with that predicted by the product operator calculations. In discussing the results, it is convenient to use the ratio

$$R = {}^1J_{CH} \,/\, {}^1J_{CH_{nominal}}$$

to characterize the range of coupling constants, ${}^1J_{CH}$, for which particular features occur. ${}^1J_{CH_{nominal}}$ is the value of ${}^1J_{CH}$ used to select the value τ.

For the CH spin system, RAPT gives nearly perfect inversion (>90%) for $R=$ 0.66 to 1.34; CAPT gives >90% inversion for $R=0.69$ to 1.31; while spin-flip gives >90% inversion for the narrower region $R=0.86$ to 1.14. CAPT gives negative ^{13}C intensities for R on the interval (0.37, 1.63), while both RAPT and spin-flip give negative responses over the narrower region (0.5, 1.5).

The results for the CH_2 spin system show that RAPT gives the broadest maximum about $R=1$, with carbon intensities greater than 90% of the maximum

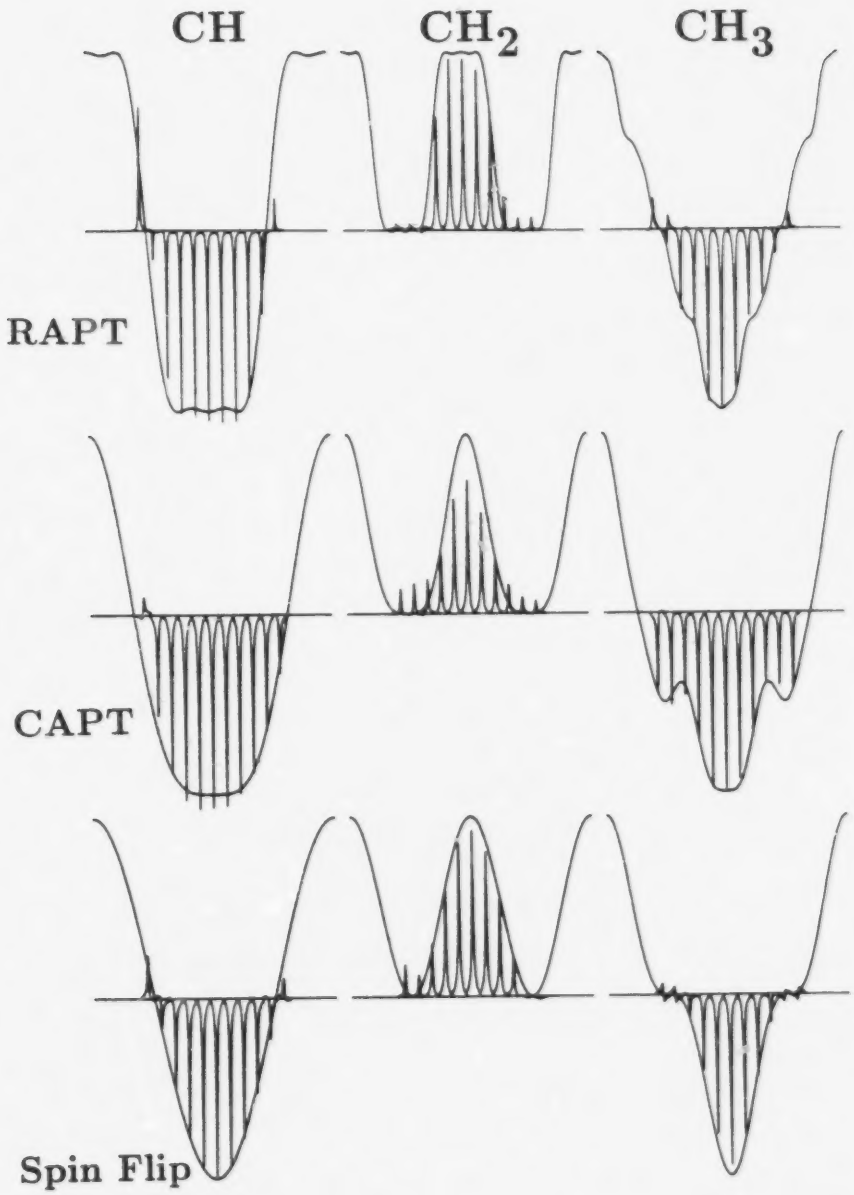

Figure 3.2: Comparison of the observed and calculated signal intensities for APT-like pulse sequences. In each case, the intensities are calculated for $\theta = \pi^1 J_{CH}\tau$ ranging from 0° to 360°, and observed spectra are shown for $\theta = 80°, 100°, \ldots, 280°$.

intensity for $R = 0.82$ to 1.18. The range is to be compared with the corresponding ones, (0.90, 1.10) and (0.93, 1.07) for spin-flip and CAPT, respectively. CAPT intensities are more sensitive to the value of $^1J_{CH}$ than either spin-flip or RAPT.

For CH_3 CAPT has the broadest region, $R = 0.85$ to 1.15, for >90% inversion. The corresponding regions for RAPT and spin-flip are (0.88, 1.12) and (0.92, 1.08), respectively. CAPT has a much larger range of R (0.28, 1.72) for which negative responses are observed than the range (0.50, 1.50) obtained in RAPT and spin-flip.

The much broader ranges of $^1J_{CH}$ for which inversion of CH and CH_3 carbon resonances is obtained make CAPT the best sequence for determining the number of attached protons. The narrower CAPT profile for CH_2 carbons does detract from the superiority of CAPT, but the performance of CAPT for CH and CH_3 systems makes up for this minor deficiency since the largest variations in $^1J_{CH}$ are expected for CH fragments. Comparisons of the spectra from spin-flip, CAPT and RAPT experiments on cholesterol demonstrate the overall superiority of CAPT. One may use CAPT for editing purposes in much the same way as APT has been used (13): one collects A – the normal $^{13}C\{^1H\}$ spectrum, CAPT spectra for $B - \theta = 180°$, $C - \theta = 75°$, and $D - \theta = 112°$; $A + B$ identifies CH_2 and quarternary carbons, $C - D$ identifies CH carbons, and $A - B$ gives both CH and CH_3 carbons. RAPT cannot be used easily for editing because the profile for the CH_3 spin system does not have a broad region of zero response like spin-flip does, nor does it have a local minimum in the region of $\theta = 90°$ as CAPT does.

References

1. G. Bodenhausen, R. Freeman, R. Niedermeyer, and D. L. Turner, *J. Magn. Reson.* **24**, 291 (1976).

2. S. L. Patt and J. N. Shoolery, *J. Magn. Reson.* **46**, 535 (1982).

3. G. A. Morris and R. Freeman, *J. Am. Chem. Soc.* **101**, 760 (1979).

4. D. T. Pegg, D. M. Doddrell, and M. R. Bendall, *J. Chem. Phys.* **77**, 2745 (1982).

5. K. V. Schenker and W. von Philippsborn, *J. Magn. Reson.* **61**, 294 (1985).

6. S. Wimperis and G. Bodenhausen, *J. Magn. Reson.* **69**, 264 (1986).

7. M. H. Levitt, *J. Magn. Reson.* **48**, 234 (1982).

8. O. W. Sørensen, J. C. Madsen, N. C. Nielsen, H. Bildsoe, and H. J. Jakobsen, *J. Magn. Reson.* **77**, 170 (1988).

9. J. R. Garbow, D. P. Weitekamp, and A. Pines, *Chem. Phys. Lett.* **93**, 504 (1982).

10. S. Wimperis and R. Freeman, *J. Magn. Reson.* **62**, 147 (1985).

11. S. Wimperis, *J. Magn. Reson.* **83**, 509 (1989).

12. T. T. Nakashima and R. E. D. McClung, *J. Magn. Reson.* **70**, 187 (1986).

13. D.W. Brown, T. T. Nakashima, and D. L. Rabenstein, *J. Magn. Reson.* **45**, 302 (1981).

CHAPTER 4

IMPROVEMENT OF INADEQUATE USING COMPENSATED DELAYS AND PULSES*

4.1 Introduction

Since its introduction (1), the INADEQUATE experiment (Fig. 4.1a) has proven its usefulness in establishing the carbon connectivities in complex organic molecules (2-4). This experiment provides relatively clean spectra because only signals that have passed through double-quantum coherence are detected, while responses from isolated spins are suppressed. Compared to other multiple-pulse techniques (5), INADEQUATE has been slow to gain popularity in carbon-13 spectroscopy mainly because of its inherently low sensitivity. One important factor which may contribute to the weak signals is the inefficiency of coherence conversion in each step of the pulse sequence. The first 90° pulse in the sequence converts the z–magnetizations $(I_{1z} + I_{2z})$ into transverse magnetization $-(I_{1y} + I_{2y})$. During the precession period, spin-spin coupling converts $-(I_{1y} + I_{2y})$ into antiphase magnetizations, $(2I_{1x}I_{2z} + 2I_{1z}I_{2x})$, which are then converted by the succeeding 90° pulse into the desired double quantum coherences. The efficiencies of the rf pulses and precession periods in effecting the desired transformations strongly affect the intensity of the observed signals and it is therefore desirable to make them as efficient as possible.

Rf field imperfections and resonance offset effects degrade the performance of rf pulses. Spatial inhomogeneity of the rf field causes a distribution of flip angles

*A version of this chapter has been accepted for publication. A.M. Torres, T.T Nakashima, R.E.D. McClung, and D.R. Muhandiram, 1992. *Journal of Magnetic Resonance*. Copyright © 1992 by Academic Press, Inc.

(a) Regular INADEQUATE

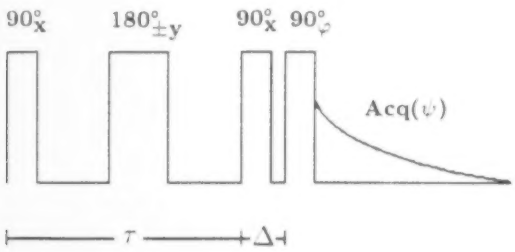

(b) J-Compensated INADEQUATE

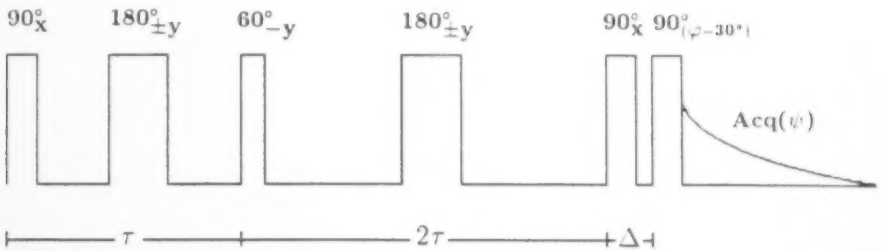

Figure 4.1: Pulse sequences for (a) regular and (b) J-compensated INADEQUATE. Resonance offset compensated C-INADEQUATE and JC-INADEQUATE sequences may be created from (a) and (b) respectively by replacing the 60°_α, 90°_α and 180°_α pulses with $12^\circ_\alpha 158^\circ_{-\alpha} 352^\circ_\alpha 158^\circ_{-\alpha} 12^\circ_\alpha$, $24^\circ_\alpha 152^\circ_{-\alpha} 346^\circ_\alpha 152^\circ_{-\alpha} 24^\circ_\alpha$, and $58^\circ_\alpha 140^\circ_{-\alpha} 344^\circ_\alpha 140^\circ_{-\alpha} 58^\circ_\alpha$ composite pulses respectively. Δ is set to $3\,\mu$s for 1D experiments and is incremented in 2D experiments, and τ is normally set to $1/2J$. The phases φ and ψ are cycled to select signals which pass through double quantum coherences.

across the sample volume so that some of the spins may not be excited to the desired coherence. Resonance offset effects, which are more prevalent in carbon spectroscopy than in proton spectroscopy, reduce the efficiency of an rf pulse by tilting the orientation of the effective field. The effects of these rf imperfections are usually minimized by using composite pulses – clusters of phase-shifted rf pulses (6-8).

Various kinds of composite pulses have been developed in order to improve the efficiency of the rf pulses in the INADEQUATE experiment. Wimperis and Bodenhausen (9) showed that compensation for rf field inhomogeneity in this experiment can be achieved by replacing the last two 90° pulses in the sequence with phase-distortionless $90^\circ_0 180^\circ_{105} 180^\circ_{315}$ composite pulses (10). After careful analysis of the double quantum sequence, Levitt and Ernst (11) developed a resonance offset compensated sequence based on the $90^\circ_0 180^\circ_{180} 270^\circ_0$ phase-alternating composite 180° pulse (12,13), which is tailored so that the phase shift errors induced by the compensated excitation pulse sequence are canceled by the phase shift errors produced by the composite read pulse. In another study, Levitt (8) showed how a resonance offset compensated double quantum sequence can be constructed using the $180^\circ_{180} 360^\circ_0 180^\circ_{180} 270^\circ_0 90^\circ_{90}$ composite 90° pulse, and the resulting sequence, which incorporates a five pulse composite sequence for each pulse in the regular sequence, was found to significantly enhance the sensitivities of the ^{13}C double-quantum peaks of crotonaldehyde.

One type of composite pulse which may be useful in minimizing resonance offset effects in the INADEQUATE experiment is the symmetric phase-alternating composite sequence introduced by Shaka and Pines (14). Unlike many composite pulses, these compensated pulses may be constructed for any desired flip angle, and approximate ideal rf pulses by providing uniform rotation or transformation

of any initial spin state over a large bandwidth, and can therefore be substituted directly in place of a single rf pulse. Since these composite pulses involve only 180° phase shifts, they can be easily implemented, even on older spectrometers.

Of primary interest in this investigation is the problem associated with inefficient coherence conversion by homonuclear spin-spin coupling during the precession period in the INADEQUATE experiment. There is often a mismatch between the length of the delay period τ used and the values of $1/2J$ for the various homonuclear spin-spin coupling constants J found in a given molecule, so that the in-phase magnetizations are not efficiently converted into antiphase magnetizations. Barbara and co-workers (15) have recognized a formal analogy between the double-quantum excitation sequence when a range of dipolar couplings are present, and the behavior of an inhomogeneous rf pulse. Using this analogy, they constructed a compensated double quantum excitation sequence for a homonuclear system containing two spin-$\frac{1}{2}$ nuclei patterned after the inhomogeneity compensated $270^{\circ}_{0}360^{\circ}_{169}180^{\circ}_{33}180^{\circ}_{178}$ composite pulse (10). Wimperis and Bodenhausen (16) later used a similar analogy, which was applied to heteronuclear spin systems, to create J-compensated INEPT sequences.

In this chapter, we develop an operator analogy which relates homonuclear spin-spin coupling and rf pulses in a manner similar to the analogies developed for the heteronuclear case (17,18), which was discussed in Chapter 2. This analogy affords the construction of J-compensated homonuclear spin-echo sequences from ΔB_1-compensated composite pulses, and a J-compensated INADEQUATE sequence is developed by incorporation of a J-compensated spin-echo element. Practical pulse sequences for the regular and J-compensated INADEQUATE experiments are developed by exploiting symmetric phase-alternating composite pulses (14).

4.2 Theory

The construction of J-compensated homonuclear spin-echo sequences from ΔB_1-compensated composite pulse sequences can be understood by recognizing the analogous transformation properties of the sets of product operators involved in rf pulses and in homonuclear spin-spin coupling. This analogy is less explicit than the analogy between the product operators for rf pulses and for heteronuclear spin-spin coupling developed earlier in Chapter 2 and cannot be illustrated using a simple pictorial representation. To elucidate the similarity, we first demonstrate the analogous properties of the set of operators $\{ I_z, I_x, I_y\}$ and the set $\{(I_{1y} + I_{2y}), 2I_{1z}I_{2z}, (2I_{1x}I_{2z} + 2I_{1z}I_{2x})\}$. An rf pulse applied along the x-axis for time t interconverts I_z and I_y, and leaves I_x invariant:

$$\begin{aligned} I_z &\xrightarrow{(\beta)\, I_x} I_z \cos\beta - I_y \sin\beta \\ I_y &\xrightarrow{(\beta)\, I_x} I_y \cos\beta - I_z \sin\beta \\ I_x &\xrightarrow{(\beta)\, I_x} I_x. \end{aligned} \qquad [4\text{-}1]$$

where $\beta = \gamma B_1 t$. In a similar fashion, homonuclear spin-spin coupling (product operator $2I_{1z}I_{2z}$) for a period τ interconverts the $(I_{1y} + I_{2y})$ and $(2I_{1x}I_{2z} + 2I_{1z}I_{2x})$ coherences of spins I_1 and I_2, but leaves the longitudinal spin order, $2I_{1z}I_{2z}$, unchanged:

$$\begin{aligned} (I_{1y} + I_{2y}) &\xrightarrow{(\beta')\,(2I_{1z}I_{2z})} (I_{1y} + I_{2y})\cos\beta' - (2I_{1x}I_{2z} + 2I_{1z}I_{2x})\sin\beta' \\ (2I_{1x}I_{2z} + 2I_{1z}I_{2x}) &\xrightarrow{(\beta')\,(2I_{1z}I_{2z})} (2I_{1x}I_{2z} + 2I_{1z}I_{2x})\cos\beta' - (I_{1y} + I_{2y})\sin\beta' \\ (2I_{1z}I_{2z}) &\xrightarrow{(\beta')\,(2I_{1z}I_{2z})} (2I_{1z}I_{2z}). \end{aligned} \qquad [4\text{-}2]$$

where $\beta' = \pi J_{12}\tau$ and J_{12} is the spin-spin coupling constant. The following correspondences are clearly noted: $I_z \leftrightarrow (I_{1y} + I_{2y})$, $I_y \leftrightarrow (2I_{1x}I_{2z} + 2I_{1z}I_{2x})$,

$I_x \leftrightarrow (2I_{1z}I_{2z})$, $\beta \leftrightarrow \beta'$, and $t \leftrightarrow \tau$.

The operator correspondences presented above illustrate a simple analogy when the rf pulse is applied exactly along the x-axis. Since composite pulse sequences are made up of phase-shifted rf pulses, it is more useful to see the general correspondences when the rf pulse is applied along an axis in the xy-plane at angle ϕ from the x-axis. The operator for such an rf pulse is defined as (19):

$$\xrightarrow{P(\beta,\phi)} \equiv \xrightarrow{-\phi(I_z)} \xrightarrow{\beta(I_x)} \xrightarrow{\phi(I_z)}. \qquad [4\text{-}3]$$

This general rf pulse transforms I_z, I_y ,and I_x in the following manner:

$$\begin{aligned}
I_z &\xrightarrow{P(\beta,\phi)} I_z\cos\beta - I_y\sin\beta\cos\phi + I_x\sin\beta\sin\phi \\
I_y &\xrightarrow{P(\beta,\phi)} I_y(\cos\beta\cos^2\phi + \sin^2\phi) + I_z\sin\beta\cos\phi + I_x\sin^2(\beta/2)\sin(2\phi) \\
I_x &\xrightarrow{P(\beta,\phi)} I_x(\cos\beta\sin^2\phi + \cos^2\phi) - I_z\sin\beta\sin\phi \\
&\quad + I_y\sin^2(\beta/2)\sin(2\phi) \qquad [4\text{-}4]
\end{aligned}$$

Using the analogy between rf pulse and homonuclear spin-spin coupling operators given above, one can construct from transformation [4-3] a spin-spin coupling propagator

$$\xrightarrow{\mathcal{P}(\beta',\phi')} \equiv \xrightarrow{-\phi'(I_{1y}+I_{2y})} \xrightarrow{\beta'(2I_{1z}I_{2z})} \xrightarrow{\phi'(I_{1y}+I_{2y})}. \qquad [4\text{-}5]$$

When applied to $(I_{1y} + I_{2y})$ magnetizations, this propagator creates $(2I_{1z}I_{2z} - 2I_{1x}I_{2x})$ coherences, in addition to the $(2I_{1x}I_{2z} + 2I_{1z}I_{2x})$ coherences:

$$\begin{aligned}
(I_{1y}+I_{2y}) &\xrightarrow{\mathcal{P}(\beta',\phi')} (I_{1y}+I_{2y})\cos\beta' - (2I_{1x}I_{2z}+2I_{1z}I_{2x})\sin\beta'\cos(2\phi') \\
&\quad + (2I_{1z}I_{2z} - 2I_{1x}I_{2x})\sin\beta'\sin(2\phi'). \qquad [4\text{-}6]
\end{aligned}$$

Comparing transformations [4-4] and [4-6], one observes that I_x magnetization, which corresponds to longitudinal spin-order, $2I_{1z}I_{2z}$, in the simple analogy developed from Eqs. [4-1] and [4-2] above, corresponds to $(2I_{1z}I_{2z} - 2I_{1x}I_{2x})$ in the

more general analogy. Furthermore, ϕ' in Eq. [4-6] must be set equal to $\phi/2$ so that the transformation of $(I_{1y} + I_{2y})$ under $\mathcal{P}(\beta', \phi')$ given in Eq. [4-6] has the same functional form as the transformation of I_z under $\mathrm{P}(\beta, \phi)$ in Eq. [4-4]. It is therefore more appropriate to look at the transformations of the set of operators $\{(I_{1y} + I_{2y}), (2I_{1x}I_{2z} + 2I_{1z}I_{2x}), (2I_{1z}I_{2z} - 2I_{1x}I_{2x})\}$ under $\mathcal{P}(\beta', \phi/2)$, the spin-spin coupling propagator phase-shifted by $\phi/2$:

$$
\begin{aligned}
(I_{1y} + I_{2y}) \xrightarrow{\mathcal{P}(\beta', \phi/2)} & (I_{1y} + I_{2y})\cos\beta' - (2I_{1x}I_{2z} + 2I_{1z}I_{2x})\sin\beta'\cos\phi \\
& + (2I_{1z}I_{2z} - 2I_{1x}I_{2x})\sin\beta'\sin\phi \\
(2I_{1x}I_{2z} + 2I_{1z}I_{2x}) \xrightarrow{\mathcal{P}(\beta', \phi/2)} & (2I_{1x}I_{2z} + 2I_{1z}I_{2x})(\cos\beta'\cos^2\phi + \sin^2\phi) \\
& + (I_{1y} + I_{2y})\sin\beta'\cos\phi \\
& + (2I_{1z}I_{2z} - 2I_{1x}I_{2x})\sin^2(\beta'/2)\sin(2\phi) \\
(2I_{1z}I_{2z} - 2I_{1x}I_{2x}) \xrightarrow{\mathcal{P}(\beta', \phi/2)} & (2I_{1z}I_{2z} - 2I_{1x}I_{2x})(\cos\beta'\sin^2\phi + \cos^2\phi) \\
& - (I_{1y} + I_{2y})\sin\beta'\sin\phi \\
& + (2I_{1x}I_{2z} + 2I_{1z}I_{2x})\sin^2(\beta'/2)\sin(2\phi) \qquad [4\text{-}7]
\end{aligned}
$$

Comparison of the transformations in [4-4] and [4-7] indicates the following general correspondences:

$$
\begin{aligned}
I_z &\longleftrightarrow (I_{1y} + I_{2y}) \\
I_x &\longleftrightarrow (2I_{1z}I_{2z} - 2I_{1x}I_{2x}) \\
I_y &\longleftrightarrow (2I_{1x}I_{2z} + 2I_{1z}I_{2x}) \\
\xrightarrow{P(\beta, \phi)} &\longleftrightarrow \xrightarrow{\mathcal{P}(\beta', \phi/2)}. \qquad [4\text{-}8]
\end{aligned}
$$

Having established the general analogy between rf pulses and spin-spin coupling in a homonuclear system, one can use any ΔB_1-compensated composite pulse sequence, $\xrightarrow{P(\beta_1, \phi_1)}\ \xrightarrow{P(\beta_2, \phi_2)}\ \ldots\ \xrightarrow{P(\beta_n, \phi_n)}$, which transforms I_z to $-I_y$ to

create a J-compensated homonuclear coherence transfer sequence, $\xrightarrow{\mathcal{P}(\beta_1', \phi_1/2)}$ $\xrightarrow{\mathcal{P}(\beta_2', \phi_2/2)}$ . . . $\xrightarrow{\mathcal{P}(\beta_n', \phi_n/2)}$, which converts $(I_{1y} + I_{2y})$ magnetization into $-(2I_{1x}I_{2z} + 2I_{1z}I_{2x})$ antiphase magnetization.

The product operator analogy presented here is similar to that used by Barbara and co-workers (15) to create general compensated sequences for double quantum excitation in solids via dipolar coupling. In fact, the correspondences in Eq.[4-8] may also be employed to create compensated double quantum excitation sequences. Our analogy is, however, more direct and can be used in compensating any sequence which requires transformation of homonuclear in-phase into antiphase magnetization.

In principle, any ΔB_1-compensated 90° pulse which transforms I_z to $-I_y$ can be used to create a J-compensated sequence which converts $(I_{1y} + I_{2y})$ to $-(2I_{1x}I_{2z} + 2I_{1z}I_{2x})$. However, long composite pulse sequences generate long J-compensated sequences with many pulses and delays so that significant loss of signal due to rf pulse imperfections and relaxation would be expected. Hence, the long J-compensated double-quantum excitation sequence devised by Barbara *et al.* (15) from the $270^\circ_0 360^\circ_{169} 180^\circ_{33} 180^\circ_{178}$ composite pulse sequence is unlikely to be useful for homonuclear systems in liquids. For this reason, we chose to base our J-compensated sequence on Levitt's $90^\circ_\alpha 180^\circ_{\alpha+2\pi/3}$ sequence (20) – a short but effective composite 90° pulse.

The conversion of I_z to $-I_y$ using a $90^\circ_\alpha 180^\circ_{\alpha+2\pi/3}$ composite sequence is achieved by setting $\alpha = -\pi/3$. This transformation can be written as

$$I_z \xrightarrow{P(\beta, -\pi/3)} \xrightarrow{P(2\beta, \pi/3)} -I_y, \qquad [4\text{-}9]$$

where β is nominally 90°. By replacing each rf operator with the corresponding spin-spin coupling operator given in Eq. [4-8], one obtains a J-compensated con-

version of $(I_{1y} + I_{2y})$ to $-(2I_{1x}I_{2z} + 2I_{1z}I_{2x})$:

$$(I_{1y} + I_{2y}) \xrightarrow{\mathcal{P}(\beta', -\pi/6)} \xrightarrow{\mathcal{P}(2\beta', \pi/6)} -(2I_{1x}I_{2z} + 2I_{1z}I_{2x}). \qquad [4\text{-}10]$$

In creating a practicable J-compensated pulse sequence, it is useful to write this compensated transformation more explicitly as

$$\begin{aligned}(I_{1y} + I_{2y}) \xrightarrow{(\pi/6)(I_{1y}+I_{2y})} \xrightarrow{(\beta')\,2I_{1z}I_{2z}} \\ \xrightarrow{(-\pi/6)(I_{1y}+I_{2y})} \xrightarrow{(-\pi/6)(I_{1y}+I_{2y})} \xrightarrow{(2\beta')\,2I_{1z}I_{1z}} \\ \xrightarrow{(\pi/6)(I_{1y}+I_{2y})} -(2I_{1x}I_{2z} + 2I_{1z}I_{2x}).\end{aligned} \qquad [4\text{-}11]$$

This transformation is readily simplified by eliminating the first rf pulse along the y-axis, since $(I_{1y} + I_{2y})$ is invariant to this pulse, and by combining the two adjacent rf pulses to obtain

$$\begin{aligned}(I_{1y} + I_{2y}) \xrightarrow{(\beta')\,2I_{1z}I_{2z}} \\ \xrightarrow{(-\pi/3)(I_{1y}+I_{2y})} \xrightarrow{(2\beta')\,2I_{1z}I_{1z}} \\ \xrightarrow{(\pi/6)(I_{1y}+I_{2y})} -(2I_{1x}I_{2z} + 2I_{1z}I_{2x}).\end{aligned} \qquad [4\text{-}12]$$

This simplified spin-spin coupling conversion corresponds to a compensated pulse sequence

$$\frac{\tau}{2} - 180^\circ_{\pm 90} - \frac{\tau}{2} - 60^\circ_{270} - \tau - 180^\circ_{\pm 90} - \tau - 30^\circ_{90}, \qquad [4\text{-}13]$$

where $\tau = 1/2J_{1,2}^{\text{nominal}}$, which is expected to be more effective than the uncompensated sequence

$$\frac{\tau}{2} - 180^\circ_{\pm 90} - \frac{\tau}{2} \qquad [4\text{-}14]$$

in transforming homonuclear in-phase magnetizations into antiphase magnetizations for a sample containing spin systems with a range of values of $J_{1,2}$. For clarity, the 180° refocusing pulse at the center of each precession period will not be displayed explicitly in the sequences discussed below.

Construction of J-Compensated Inadequate Sequence

In creating a J-compensated INADEQUATE sequence, it is important to look at the transformation of the magnetization in detail as it progresses through the regular sequence. For simplicity, only the one-dimensional INADEQUATE sequence (Fig. 4.1a), which can be written as

$$90^\circ_0 - \tau - 90^\circ_0 - \Delta - 90^\circ_\varphi - \mathrm{acq}(\psi) \qquad [4\text{-}15]$$

will be considered. The transformation of magnetizations for each step of the pulse sequence is

$$\begin{aligned}
(I_{1z} + I_{2z}) \quad &\xrightarrow{(\pi/2)\,(I_{1x} + I_{2x})} \quad -(I_{1y} + I_{2y}) \\
&\xrightarrow{(\pi/2)\,2I_{1z}I_{2z}} \quad (2I_{1x}I_{2z} + 2I_{1z}I_{2x}) \\
&\xrightarrow{(\pi/2)\,(I_{1x} + I_{2x})} \quad -(2I_{1x}I_{2y} + 2I_{1y}I_{2x}) \\
&\xrightarrow{\{(\pi/2)\,(I_{1x} + I_{2x})\}_\varphi} \quad -(2I_{1x}I_{2z} + 2I_{1z}I_{2x})\cos\varphi \\
&\qquad\qquad\qquad\qquad + (2I_{1z}I_{2y} + 2I_{1y}I_{2z})\sin\varphi
\end{aligned} \qquad [4\text{-}16]$$

The equilibrium magnetizations, $(I_{1z} + I_{2z})$, are converted by the first $(\pi/2)_x$ pulse into transverse magnetizations, $-(I_{1y} + I_{2y})$; these magnetizations are transformed by spin-spin coupling during the τ period into $(2I_{1x}I_{2z} + 2I_{1z}I_{2x})$; and then changed into double quantum coherences, $-(2I_{1x}I_{2y} + 2I_{1y}I_{2x})$, by the second $(\pi/2)_x$ pulse. The delay time Δ, which is kept to a minimum value of about $3\,\mu$s in the one-dimensional experiment, is required in order to allow time for setting the phase of the last 90° pulse which reconverts the double-quantum coherences into antiphase magnetizations. Selection of the antiphase signals which have passed through double-quantum coherences is achieved by cycling the phase of the last (read) pulse through $\varphi = 0^\circ, 90^\circ, 180^\circ, 270^\circ$ while cycling the receiver phase through $\psi = 0^\circ, 270^\circ, 180^\circ, 90^\circ$.

It is interesting to investigate the details of magnetization transfer in the INADEQUATE experiment. When the read pulse phase φ is 0° or 180°, there is no transfer of magnetization from one spin to the other so that the magnetization which began as I_{1y} is detected as $2I_{1x}I_{2z}$ and not as transferred $2I_{1z}I_{2y}$. The opposite is however true when the read pulse phase φ is 90° or 270°, where the antiphase signal detected originated as a y-magnetization of the other spin. Since φ is cycled through 0°, 90°, 180°, and 270°, half of the total detected antiphase signal assigned to a particular spin is due to magnetization transferred from the other spin.

It is also important to note the effect of rf pulse imperfections on the INADEQUATE experiment. After the delay period τ, the coherences which are involved in the succeeding transformations are two-spin $(2I_{1x}I_{2z} + 2I_{1z}I_{2x})$ and $-(2I_{1x}I_{2y} + 2I_{1y}I_{2x})$ coherences. Conversion of these two-spin coherences into the desired double quantum coherences, for example, $(2I_{1x}I_{2z} + 2I_{1z}I_{2x})$ into $-(2I_{1x}I_{2y} + 2I_{1y}I_{2x})$, requires rf pulses to be efficient in transforming both I_1 and I_2 spins. Since rf pulses are applied to the two-spins simultaneously, small errors in transforming I_1 and I_2 coherences may lead to significant reductions in antiphase signal intensities. This explains why the INADEQUATE experiment is more sensitive to rf pulse imperfections than many multiple-pulse experiments are.

It is clear that the τ delay period in the INADEQUATE sequence transforms in-phase into antiphase magnetization. One can therefore devise a J-compensated INADEQUATE sequence

$$90^\circ_0 - \tau - 60^\circ_{270} - 2\tau - 30^\circ_{90}90^\circ_0 - \Delta - 90^\circ_\varphi - \mathrm{acq}(\psi) \qquad [4\text{-}17]$$

by replacing the single τ period in the regular sequence [4-15] with the compensated sequence [4-13]. This new sequence will excite double quantum coherences over a wider range of J than the regular INADEQUATE experiment. For practical

implementation, the adjacent pulses in the J-compensated sequence [4-17] must be simplified and combined into a single pulse. This is done by using the equivalence $30^\circ_{90} \equiv 90^\circ_0 30^\circ_z 90^\circ_{180}$, where 30°_z is a 30° z-pulse, to obtain the revised sequence

$$90^\circ_0 - \tau - 60^\circ_{270} - 2\tau - 90^\circ_0 30^\circ_z 90^\circ_{180} 90^\circ_0 - \Delta - 90^\circ_\varphi - \mathrm{acq}(\psi) \qquad [4\text{-}18]$$

or, after adding adjacent pulses and interchanging the position of Δ and the 30°_z rotation, simply,

$$90^\circ_0 - \tau - 60^\circ_{270} - 2\tau - 90^\circ_0 - \Delta - 30^\circ_z 90^\circ_\varphi - \mathrm{acq}(\psi). \qquad [4\text{-}19]$$

The z-pulse can be deleted by noting the equivalence $90^\circ_{\varphi-30} \equiv 30^\circ_z 90^\circ_\varphi 30^\circ_{-z}$ to obtain an intermediate sequence

$$90^\circ_0 - \tau - 60^\circ_{270} - 2\tau - 90^\circ_0 - \Delta - 90^\circ_{\varphi-30} 30^\circ_z - \mathrm{acq}(\psi). \qquad [4\text{-}20]$$

The z-pulse in this sequence gives the proper phase shift to the detected antiphase signal, but is not important since phase correction can always be applied after Fourier transformation. Hence the z-pulse is dropped to give the final J-compensated INADEQUATE sequence

$$90^\circ_0 - \tau - 60^\circ_{270} - 2\tau - 90^\circ_0 - \Delta - 90^\circ_{\varphi-30} - \mathrm{acq}(\psi). \qquad [4\text{-}21]$$

The detailed pulse sequence for J-compensated INADEQUATE is given in Fig. 4.1b.

4.1 Experimental

The experiments were carried out on Bruker AM-400, AM-300, and AMX-500 spectrometers. The sample used in the proton experiments was a dilute solution of 2,3-dibromothiophene (an AX spin system) in $CDCl_3$. A small amount of 2,5-dibromothiophene (an X spin system) was added to this sample in order to make

sure that single quantum signals are effectively suppressed in the INADEQUATE spectra. For the carbon experiments, the samples used were 90% (v/v) solutions of 90% ^{13}C-dilabeled acetaldehyde in CD_2Cl_2, and natural abundance samples of 5-hexene-2-one in CD_2Cl_2 and crotonaldehyde in DMSO-d_6. All of the samples used in the carbon experiments were slightly doped with chromium(III) acetylacetonate in order to reduce the repetition times.

The proton experiments on 2,3-dibromothiophene were performed on the AM-400 spectrometer. For the regular INADEQUATE experiment, the 8 step phase cycle (1), where the phase of the 180° pulse was alternated after cycling the phases of the read pulse and receiver channel through a four step cycle, was adopted. In J-compensated INADEQUATE experiments, the phase of the additional 180° pulse was alternated after performing the above 8 step cycle, extending the cycle to 16 steps. The waiting period employed between scans was 35 s. No dummy scans were performed prior to acquisition and a total of 16 scans were collected per experiment.

Broadband proton decoupling was applied throughout all carbon experiments. For experimental comparison of various composite pulses, the AM-400 spectrometer was used, two dummy scans were employed, and only the minimum 16 scans, as required by the phase cycle (11,21), were collected. The waiting time between scans was 17 s which is equal to three times T_1 of the carbonyl carbon of the acetaldehyde sample.

In order to suppress the single quantum peaks more effectively, a more extensive phase cycling scheme was used for the natural abundance ^{13}C INADEQUATE experiments on 5-hexene-2-one and crotonaldehyde. In these experiments, the phases of all the pulses and receiver channels were incremented by 90° after performing the 8 step cycle (1). The overall phase incrementation was performed three times so

that, in all, 32 scans were required to complete the phase cycles of regular and C-INADEQUATE experiments, while 64 scans were required for JC-INADEQUATE.

For the 1D experiments on 5-hexene-2-one, the AM-300 spectrometer was used and a 7.2 s repetition time was employed. Four dummy scans were performed for every 128 scans recorded. A total of 3840 scans were gathered for each experiment.

For the 2D experiments on crotonaldehyde carried out on the AMX-500 spectrometer, 128 scans were accumulated for each t_1 increment. The total measuring time for each experiment was 30 hours. The spectral widths were 10 kHz for f_1 and 25 kHz for f_2. The 2D data sets, which consisted of 116 × 16K data matrices, were zero filled to 256 × 16K and processed with 2 Hz line-broadening in f_2. No window function was used in f_1. The 2D INADEQUATE spectra are displayed in magnitude mode.

4.4 Results and Discussion

Preliminary Testing of the J-compensated INADEQUATE on a Proton AX system

To test the effectiveness of the new J-compensated INADEQUATE sequence, we chose to perform preliminary experiments on the much more sensitive proton nucleus using a dilute sample of 2,3-dibromothiophene (an AX spin system). This choice minimized both resonance offset effects, which are usually present in carbon spectroscopy, and the effects of fast relaxation encountered in large molecules. The experimental and calculated variations of the H-4 peak intensities of 2,3-dibromothiophene with $\beta' = \pi J\tau$ ($J = 5.7$ Hz) in the regular and J-compensated INADEQUATE experiments are shown in Fig. 4.2. The variations in the H-5 peak intensity are not shown since they are identical to those found for the H-4 peak. The peak intensities in the two sequences for $\beta' = 90°$ are not significantly different

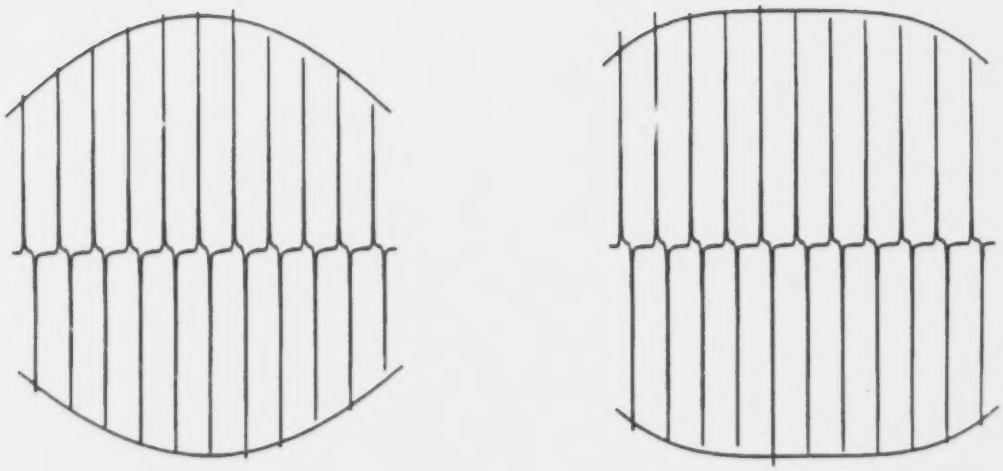

Regular
INADEQUATE

J-Compensated
INADEQUATE

Figure 4.2: Comparison of the calculated and observed INADEQUATE and J-compensated INADEQUATE signal intensity profiles for the H-4 antiphase peak of 2,3-dibromothiophene. The observed antiphase peaks correspond to $\beta' = 40°$, $50° \ldots 140°$. The calculated peaks are normalized to the observed signals.

and the small variations observed can be attributed to relaxation and rf imperfections. For convenience, the calculated intensities $\sin\beta'$, for the normal experiment, and $(9\sin\beta' + \sin 3\beta')/8$, for the compensated method, are normalized to fit the experimental results.

There is good agreement between the experimental and calculated intensities. For regions near $\beta' = 40°$ (and $\beta' = 140°$), the compensated sequence gives signals which are 30% larger than those obtained with the regular sequence. These results show that the J-compensated INADEQUATE sequence, which incorporates the compensated spin-echo sequence [4-13], is less sensitive to the choice of τ and is

more effective in exciting double-quantum coherences over a wider range of J values than the conventional sequence does.

The compensated sequence [4-13] may also be incorporated into other homonuclear experiments, making them less sensitive to variations in J. We have devised a J-compensated zero quantum sequence by replacing the period τ of the zero quantum pulse sequence introduced by Müller (22) with sequence [4-13]. Experiments on 2,3-dibromothiophene, in which τ was deliberately misset so that $\beta' = 40°$, showed that the zero-quantum signals produced by the J-compensated sequence are about 30% larger than those generated by the regular sequence.

Although very effective on the 2,3-dibromothiophene sample, the J-compensated INADEQUATE sequence (or the J-compensated zero-quantum sequence) is not expected to find practical applications in proton spectroscopy for two reasons. First, the proton homonuclear spin-spin coupling constants J, which range from 2 to 20 Hz, are very small and thus require the use of relatively long τ periods (of the order of 50 ms). Relaxation during the three delay periods in the compensated sequence will render it ineffective in enhancing signals. This will be compounded further by short proton relaxation times when the molecule is large. Second, proton spin systems are generally complex networks (not simple AX spin systems) so that signal modulation due to passive spin-spin coupling is expected. Indeed, proton double quantum experiments on crotonaldehyde showed that responses obtained using the J-compensated sequence were less intense than those obtained with the conventional sequence.

J-compensated INADEQUATE in Carbon-13 Spectroscopy

The usefulness of the J-compensated INADEQUATE sequence can be better realized in carbon spectroscopy where coupling constants can range from 10 to 170 Hz,

relaxation times are longer, and most spin systems are ideal AX systems. Off-resonance effects significantly degrade the performance of rf pulses in carbon spectroscopy due to the large spectral widths required. Since double-quantum experiments are very sensitive to rf imperfections, the *J*-compensated INADEQUATE sequence, which has more pulses than the regular sequence, is expected to be extremely prone to sensitivity degradation due to resonance offset effects. There is, therefore, a need to further compensate this sequence by the use of composite pulses.

In this study, we have investigated the feasibility of using the symmetric phase-alternating composite pulses devised by Shaka and Pines (14) to compensate for resonance offset effects in both regular and J-compensated INADEQUATE experiments. Composite pulses of this kind should be ideal for INADEQUATE since they are expected to behave like ideal single pulses in the presence of resonance offset effects. The results of this investigation are presented in the following sections.

The Efficiency of the Symmetric Phase-alternating Composite 180° Pulses in the INADEQUATE sequence

In the presence of rf pulse imperfections, the observed reduction in sensitivity in a multiple-pulse experiment can be attributed to the combined errors of the rf pulses in the sequence. Proper replacement of one or more rf pulses with appropriate composite pulses should therefore give an improvement in sensitivity . It is, however, very important to take special care in selecting the type of composite pulse to be used. The 180° pulse in the INADEQUATE sequence, for example, should be able to invert z-magnetization efficiently over a wide bandwidth and, at the same time, refocus transverse magnetizations accurately without large phase distortions. Many existing composite pulse sequences do not meet these strict cri-

teria. The $90^\circ_0 180^\circ_{90} 90^\circ_0$ composite sequence, for example, is very good at inverting z-magnetization in the presence of rf field inhomogeneity and resonance offset effects (6), but is not overly effective in refocusing transverse magnetization, due to the unwanted phase shifts caused by rf imperfections (7,23,24). This undesirable feature may be removed by performing an even number of refocusing pulses as in the revised Meiboom-Gill spin-echo experiment (25), but the increase in the number of pulses makes it less attractive for use in INADEQUATE experiments. Nonetheless, an INADEQUATE sequence incorporating only a single $90^\circ_0 180^\circ_{90} 90^\circ_0$ sequence has been reported (26), but Schenker and Philippsborn (21) found that no improvement was achieved with this sequence.

A composite sequence which is expected to provide better off-resonance compensation for the INADEQUATE experiment is the $90^\circ_0 240^\circ_{90} 90^\circ_0$ sequence. This pulse cluster is a modified version of the $90^\circ_0 270^\circ_0 90^\circ_0$ sequence, originally developed by Levitt and Freeman (25) and later derived by Tycko et al. (10) using the Magnus expansion approach. It has the desirable feature of producing very small offset-dependent phase errors when used as a refocusing pulse, yet it provides efficient population inversion over a large bandwidth. Schenker and Philippsborn (21), however, found this composite pulse to be even less effective than the simple 180° when incorporated into the INADEQUATE sequence.

The failure of these two popular composite 180° pulses in compensating the INADEQUATE experiment led us to investigate the use of symmetric phase-alternating composite 180° pulses (14) as alternatives to the simple 180° pulse. To assess the usefulness of this type of composite pulse, its performance in a regular INADEQUATE experiment was compared with that of the simple 180° pulse and those of the two common composite pulses mentioned above. The replacement of a 180° refocusing pulse with the composite pulse must include proper phase-shifting

of the composite pulse with respect to the orientation of the effective rotation axis, as shown in Fig. 4.3. The composite sequence $90^\circ_0 240^\circ_{90} 90^\circ_0$, for example, should be implemented as $90^\circ_{135} 240^\circ_{225} 90^\circ_{135}$ in order to replace a 180°_{90} pulse. Of the symmetric phase-alternating composite 180° pulses presented (14), only the three-pulse, $59^\circ_{180} 298^\circ_0 59^\circ_{180}$, and the five pulse, $58^\circ_0 140^\circ_{180} 344^\circ_0 140^\circ_{180} 58^\circ_0$, sequences were tested since longer sequences may lead to significant loss of magnetization through spin-spin interactions during the duration of the composite sequence.

The INADEQUATE experiments were carried out on a Bruker AM-400 using a modest rf field of 30.5 kHz (90° pulse length of 8.2 μs). A ^{13}C-dilabeled acetaldehyde sample, whose two carbon resonances are separated by 170 ppm, was used as a model compound and the basic 16 step phase cycle (11,21) for INADEQUATE was adopted. The τ period was set to 12.6 ms to match the $^1J_{1,2}$ of 39.6 Hz. For fair comparison, two sets of experiments were performed. In set I, the carrier was positioned at 110 ppm so that the resonances are offset by $\Delta B/B_2 = \pm 0.28$. In set II, the carrier was placed at 150 ppm corresponding to an offset of 0.14 for the carbonyl resonance and -0.42 for the methyl resonance.

The intensities of the carbonyl antiphase doublet of acetaldehyde, obtained using the regular INADEQUATE (N) and the various modified sequences (A-D) given in Fig. 4.3, are shown in Fig 4.4. The peak intensities in set I are generally larger than those in II. This is somewhat surprising since the carbonyl resonance offset is smaller in II than in I. However, magnetization is also transferred from the methyl carbon (whose offset is larger in the second set than in the first set) to the carbonyl carbon and accounts for approximately half of the intensity of the observed carbonyl antiphase doublet. The differences in intensities in the two sets of experiments should be attributed therefore to the combined efficiency of the 90° pulses in transforming the methyl and carbonyl coherences. Assuming that the

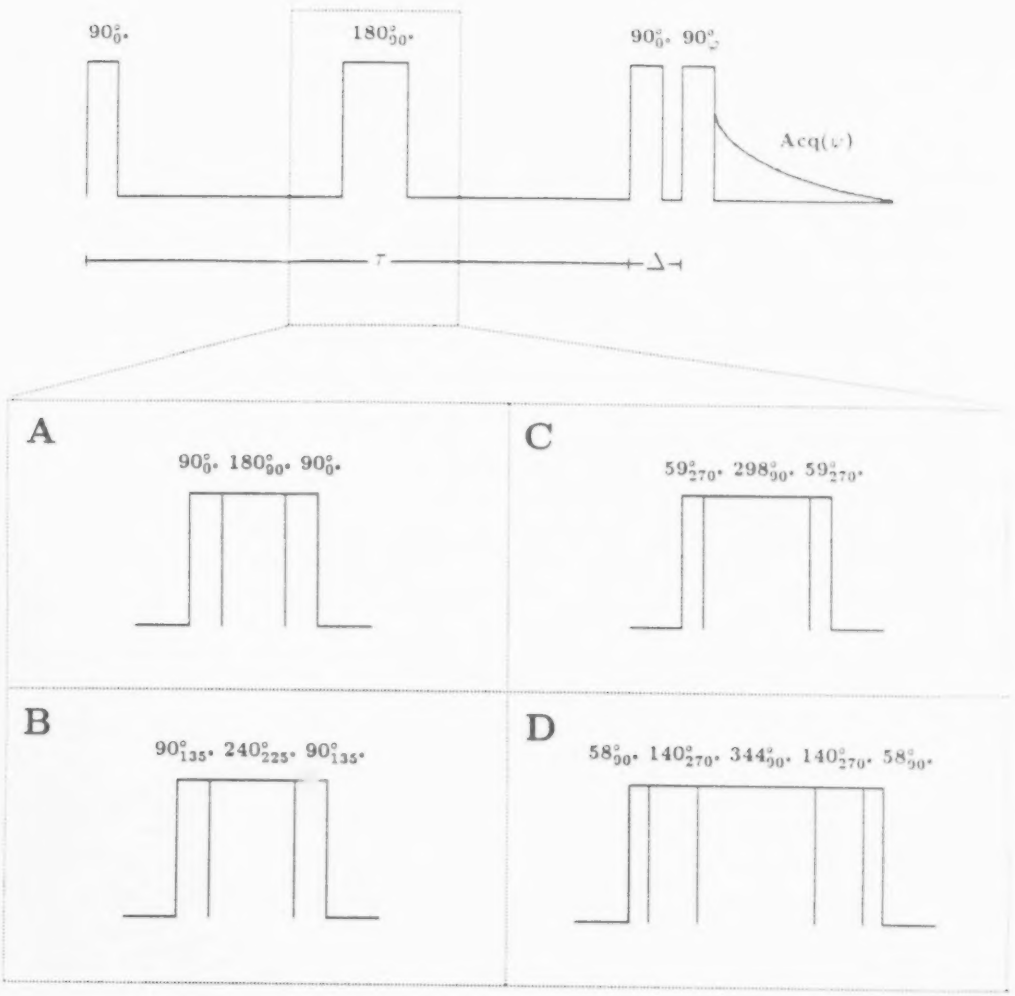

Figure 4.3: Pulse sequences for regular (top) and the modified INADEQUATE experiments (A – D) in which the 180° is replaced by various composite 180° pulses: (A) 90-180-90, (B) 90-240-90, (C) 59-298-59, and (D) 58-140-344-140-58. The composite pulse in each modified sequence has been phase-shifted in order to make the orientation of the effective rotation axis equivalent to that of 180°_{90} pulse.

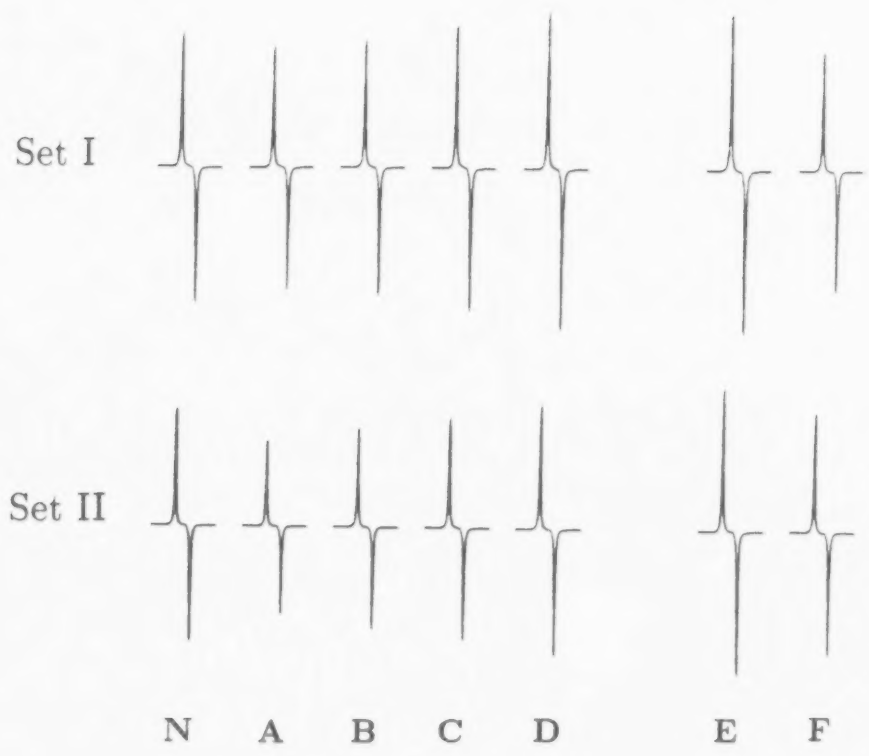

Figure 4.4: The carbonyl antiphase doublet of ^{13}C-dilabeled acetaldehyde obtained with the regular (N), modified (A-D), C-INADEQUATE (E) , and Levitt and Ernst compensated INADEQUATE (F) sequences. In set I, the carrier was positioned in the middle of the two resonances so that the resonance offsets ($\Delta B/B_2$) are 0.28 for the carbonyl spins and -0.28 for the methyl spins. In set II, the resonance offsets are, 0.14 for the carbonyl spins and -0.42 for the methyl spins. The intensities of the carbonyl antiphase peaks reflect the efficiencies of the various pulse sequences.

180° pulse is perfect, product operator calculations (27) show that the intensity of the carbonyl doublet in II should be about 80% of that in I.

In both sets of experiments, sequence A, which employs a $90^\circ_0 180^\circ_{90} 90^\circ_0$ composite pulse, generated the smallest peaks — in fact smaller peaks than those produced by the conventional sequence N. Sequence B, which incorporates the $90^\circ_0 240^\circ_{90} 90^\circ_0$ sequence produced larger peaks than A, but these responses are still smaller than those obtained using N. Sequences C and D, which incorporate the three step $59^\circ_{180} 298^\circ_0 59^\circ_{180}$ and the five step $58^\circ_0 140^\circ_{180} 344^\circ_0 140^\circ_{180} 58^\circ_0$ composite pulses respectively, performed better than A and B. Sequence C gave intensities comparable to those obtained using N, while sequence D produced consistently higher intensities. These results definitely show the superiority of the symmetric phase-alternating composite pulses over the two popular composite pulses in compensating the 180° pulse of the INADEQUATE experiment.

Product operator calculations of the efficiencies to be expected of the regular and the various composite pulse sequences under the two sets of experimental conditions were performed in order to verify the observed trends. In simplifying the calculations, it was convenient to focus our attention on the $\tau - 180^\circ - \tau$ refocusing part of the INADEQUATE sequence. Under ideal conditions where $\tau = 1/2J$ and the 180° pulse is perfect, the refocusing sequence transforms $-I_{1y}$ perfectly to $2I_{1x}I_{2z}$. In the experiment where τ is matched perfectly to the coupling constant J, the efficiency of a particular 180° pulse can be estimated by determining the magnitude of the $2I_{1x}I_{2z}$ coherence created by the refocusing sequence incorporating this pulse. In order to make the calculation manageable, it is assumed that the resonance offset is the only source of rf imperfection. Since half of the observed antiphase signal for one spin is due to the magnetization transferred from the other spin, and the phases of the refocusing pulses are cycled through 0°, 90°, 180°, and

Table 4.1: Calculated efficiencies of simple and composite 180° pulses in INADEQUATE experiments on $^{13}CH_3{}^{13}CHO$.

Pulse	Set I[a]	Set II[b]
(N) 180°_{90}	0.80	0.77
(A) $90^\circ_0 180^\circ_{90} 90^\circ_0$	0.81	0.78
(B) $90^\circ_0 240^\circ_{90} 90^\circ_0$	0.96	0.94
(C) $59^\circ_{180} 298^\circ_0 59^\circ_{180}$	0.98	0.93
(D) $58^\circ_0 140^\circ_{180} 344^\circ_0 140^\circ_{180} 58^\circ_0$	1.00	0.99

[a] $\Delta B_{\text{methyl}}/B_1 = -0.28$, $\Delta B_{\text{carbonyl}}/B_1 = +0.28$.

[b] $\Delta B_{\text{methyl}}/B_1 = -0.42$, $\Delta B_{\text{carbonyl}}/B_1 = +0.14$.

270°, it is more appropriate to present the average efficiencies obtained for the transformation of the two spins. The calculated efficiencies of the regular and the various composite sequences for the two sets of INADEQUATE experiments are given in Table 1. These efficiencies are directly related to the observed intensities of the carbonyl doublets and indicate the combined efficiencies of the different types of rf pulses in refocusing and inverting magnetizations, as required in the INADEQUATE experiment. The efficiency of the simple 180° pulse is only 80% for set I and 77% for set II. The computational results also confirm that the five pulse symmetric phase-alternating composite sequence, $58^\circ_0 140^\circ_{180} 344^\circ_0 140^\circ_{180} 58^\circ_0$, is the most efficient of the composite pulses investigated in compensating the INADEQUATE experiment. Contrary to the experimental results, the calculated data show that A should be as efficient as the simple 180° pulse, and B should be more efficient than a simple 180° pulse in the two sets of experiments.

The exceptionally poor performance of composite pulses $90^\circ_0 180^\circ_{90} 90^\circ_0$ and $90^\circ_0 240^\circ_{90} 90^\circ_0$ in sequences A and B may be attributed to their sensitivity to the effects of rf field inhomogeneity when used as refocusing pulses (28). This sensitivity arises because, in contrast to the simple 180° pulse, the $59^\circ_{180} 298^\circ_0 59^\circ_{180}$ and

the $58^\circ_0 140^\circ_{180} 344^\circ_0 140^\circ_{180} 58^\circ_0$ composite pulses, the effective rotation axis in these two common composite pulse sequences varies significantly with rf field strength. As a consequence, these composite pulses do not properly refocus the transverse magnetizations when rf inhomogeneity is present, and this leads to a significantly reduced signal.

C-INADEQUATE: a Resonance Offset Compensated INADEQUATE based on Symmetric Phase-Alternating Composite Pulses

Since the five-step symmetric phase-alternating composite 180° pulse is eminently suitable for INADEQUATE experiments, we have created a fully resonance offset-compensated INADEQUATE sequence by replacing the 90° pulses with five-step symmetric phase-alternating composite 90° pulses, $24^\circ_0 152^\circ_{180} 346^\circ_0 152^\circ_{180} 24^\circ_0$, and the 180° pulse with the $58^\circ_0 140^\circ_{180} 344^\circ_0 140^\circ_{180} 58^\circ_0$ composite pulse (14). This compensated sequence (E), which we refer to as C-INADEQUATE, is expected to give further sensitivity enhancements by eliminating the offset-dependent phase shifts introduced by the 90° pulses, and to provide more efficient coherence transformations during the pulse sequence. As shown in Fig. 4.4, sequence E indeed produced larger carbonyl antiphase peaks than those obtained using sequence D which incorporates only the five-step composite 180° pulse.

The performance of the widely-used compensated INADEQUATE sequence (F) devised by Levitt and Ernst (11) was investigated under the same experimental conditions, and the results were compared with those obtained with sequence N and with the C-INADEQUATE sequence E. As shown in Fig. 4.4, no intensity enhancement is observed using sequence F as compared to sequence N. In addition, peaks produced by F are substantially smaller than those generated by E. The

poor performance of the compensated sequence F can be attributed to the known inefficiency of the $90^\circ_0 180^\circ_{180} 270^\circ_0$ in inverting spin populations near $\Delta B/B_2 = \pm 0.28$ and $\Delta B/B_2 = \pm 0.42$ (12,13). At resonance offsets greater than ± 0.50, sequence F is expected to enhance double quantum peaks more effectively than sequence E. This was confirmed in an experiment where the 90° pulse length was deliberately doubled to 16μs. The above results nevertheless show the superiority of C-INADEQUATE at reasonable offsets.

JC-INADEQUATE: a Doubly Compensated INADEQUATE Sequence

The results presented above show that resonance offset compensation of INADEQUATE can be readily accomplished by substituting the appropriate five-step symmetric phase-alternating composite pulse for each pulse in the sequence. One can therefore make similar replacements in the J-compensated INADEQUATE sequence [4-21] to make it fully compensated to resonance offsets. The 60°_{90} pulse in this case is replaced by the $12^\circ_{90} 158^\circ_{270} 352^\circ_{90} 158^\circ_{270} 12^\circ_{90}$ composite pulse, which was derived by numerical optimization of the overall propagator U of the five-pulse sequence (29), as suggested by Shaka and Pines (14). The new sequence, which we term JC-INADEQUATE, is doubly compensated – to dispersion in J couplings and to resonance offset.

To test the effectiveness of JC-INADEQUATE, we performed natural abundance ^{13}C double-quantum experiments on a Bruker AM-300 spectrometer using 5-hexene-2-one as a model molecule. This compound was chosen since it has a wide chemical shift range: $\delta_{C\text{-}1} = 29.2$ ppm, $\delta_{C\text{-}2} = 206.4$ ppm, $\delta_{C\text{-}3} = 42.2$ ppm, $\delta_{C\text{-}4} = 27.6$ ppm, $\delta_{C\text{-}5} = 137.3$ ppm, $\delta_{C\text{-}6} = 114.5$ ppm, and a wide range of homonuclear spin-spin coupling constants: $^1J_{1,2} = 40.4$ Hz, $^1J_{2,3} = 38.6$ Hz, $^1J_{3,4} = 35.6$ Hz,

$^1J_{4,5} = 42.2\,\text{Hz}$, $^1J_{5,6} = 69.5\,\text{Hz}$, $^2J_{1,3} = 14.6\,\text{Hz}$. The 90° pulse length was set to 13.8 μs corresponding to an rf field of 18.1 kHz and τ was 12.5 ms which is appropriate for $J_{\text{Avg}} = 40\,\text{Hz}$.

Regions of the ^{13}C natural abundance 1D spectra of 5-hexene-2-one using regular (A), C-INADEQUATE (B), and JC-INADEQUATE (C) sequences are shown in Fig. 4.5. There is a clear sensitivity enhancement in the compensated spectra B and C. For the C-4 region, the improvement in intensities for the C-4/C-5 antiphase doublet is about 50% for spectra B and 40% for spectra C. These enhancements are undoubtedly due to resonance offset compensation by the symmetric phase-alternating pulses, since the C-4 region is about 90ppm away from the carrier. Note also that the C-4/C-5 antiphase doublet in the C-5 region is enhanced by about 50% despite its nearness to the carrier. This enhancement is due to the fact that some of the C-4/C-5 double-quantum coherence originating from z-magnetization of the C-4 spins is detected in the C-5 region.

One significant difference between the regular spectra A and the compensated spectra B and C is the presence of additional antiphase peaks, namely, the C-3/C-4 and C-1/C-3 doublets, in B and C. In the normal experiment, rf transformations leading to the C-3/C-4 and C-1/C-3 signals are not efficient because the resonance offsets of the two coupled spins are both large. The incorporation of symmetric phase-alternating composite pulses in C-INADEQUATE and JC-INADEQUATE makes the transformations of each coherence more efficient, leading to significantly more intense antiphase signals.

The antiphase peaks in spectra C are generally smaller than those in B. Small rf errors and relaxation effects can account for this difference since the JC-INADEQUATE sequence has more pulses and delays than the C-INADEQUATE sequence. It is not surprising then that, as an exception to the observed general peak enhance-

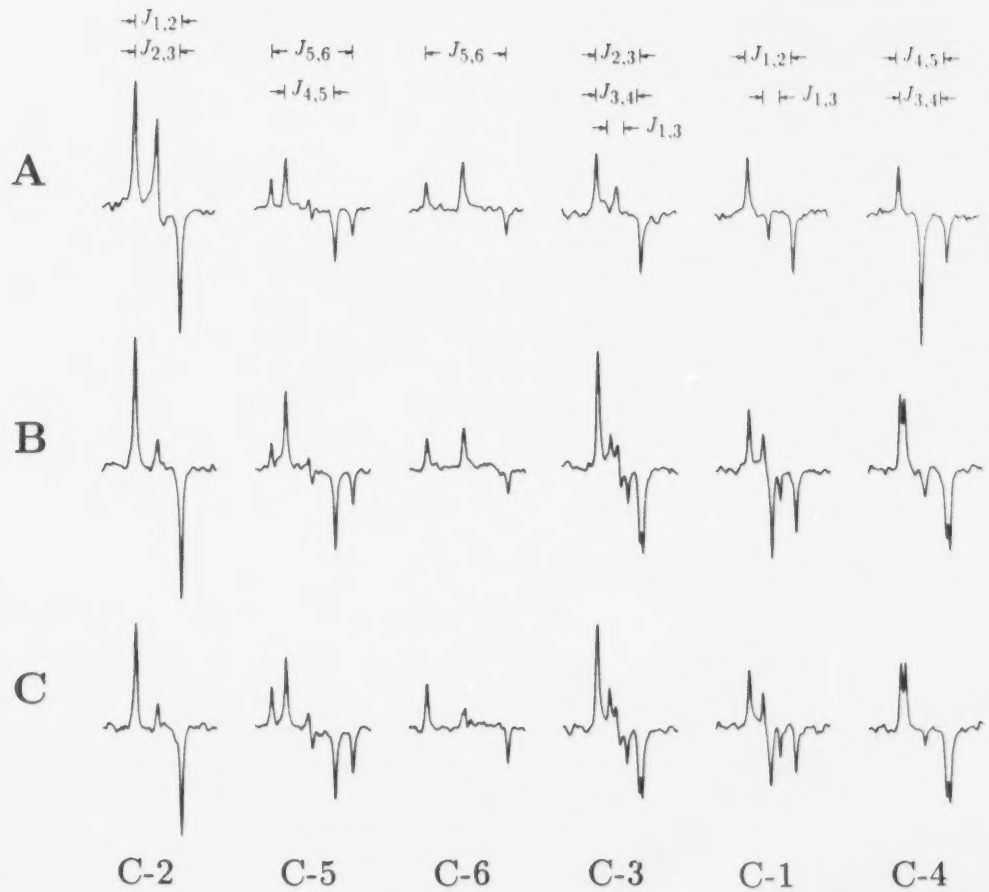

Figure 4.5: Selected regions from the ^{13}C natural abundance 1D spectra of 5-hexene-2-one obtained with (A) INADEQUATE, (B) C-INADEQUATE, and (C) JC-INADEQUATE sequences. All spectra are plotted with the same absolute intensity.

ment, the C-1/C-2 peak in the C-1 and C-2 regions of spectra C are slightly smaller than the corresponding peaks in the spectra A.

The superiority of the JC-INADEQUATE sequence over C-INADEQUATE and the regular sequence is apparent, however, when the C-5/C-6 antiphase doublet is considered. Since $J_{5,6} = 69.5\,\text{Hz}$ is large compared to the $J_{\text{avg}} = 40.0\,\text{Hz}$ for which τ was set, the C-5/C-6 doublet in the C-5 and C-6 regions of the regular spectra A are found to be relatively small compared to other doublets. These doublets are not significantly enhanced in the C-INADEQUATE spectra B since the offsets of the C-5 and C-6 spins are small so that no significant improvement is obtained when the pulses are replaced with composite pulses. J-compensation proves successful in enhancing the C-5/C-6 peak as shown by the notable increase in the intensities of these peaks in C. Measurements reveal that the increase in intensity of this doublet is about 60% for the C-5 region and 50% for the C-6 region. Enhancement of the C-1/C-3 antiphase peaks is also expected since $J_{1,3} = 14.6\,\text{Hz}$ is small compared to $J_{\text{avg}} = 40.0\,\text{Hz}$, but for some reason this is not observed in the C-1 and C-3 regions of spectra C relative to B.

To further evaluate the effectiveness of incorporating the J-compensated spin-echo and the symmetric phase-alternating composite sequences into the INADEQUATE sequence, we performed 2D INADEQUATE experiments on a Bruker AMX-500 spectrometer using a crotonaldehyde sample. The chemical shifts: $\delta_{\text{C-1}} = 193.4\,\text{ppm}$, $\delta_{\text{C-2}} = 134.8\,\text{ppm}$, $\delta_{\text{C-3}} = 153.9\,\text{ppm}$, $\delta_{\text{C-4}} = 18.5\,\text{ppm}$, and spin-spin coupling constants: ${}^1J_{1,2} = 53.2\,\text{Hz}$, ${}^1J_{2,3} = 67.0\,\text{Hz}$, ${}^1J_{3,4} = 41.2\,\text{Hz}$, ${}^3J_{1,4} = 7.4\,\text{Hz}$, vary over wide ranges. The 90° pulse length used was $8.5\,\mu\text{s}$ (rf field equal to $29.4\,\text{kHz}$), and τ was set to $13.2\,\text{ms}$ corresponding to $J = 38\,\text{Hz}$. In contrast to the 1D experiments, only the regular INADEQUATE and the JC-INADEQUATE 2D experiments were carried out due to the large amounts of time required to perform

consecutive 2D experiments. The JC-INADEQUATE results are expected to exemplify the broadband resonance offset characteristics of the C-INADEQUATE experiment, as illustrated in the 1D experiments on 5-hexene-2-one described above. In addition, the read pulse was set to 135° instead of 90° in order to increase the intensities of the echo signals and to effectively suppress the antiecho signals (30). The five-step symmetric phase-alternating composite pulse $39_0144_{180}345_0144_{180}39_0$ (14), which approximates an ideal 135° pulse, was employed as the read pulse in the 2D JC-INADEQUATE sequence.

Selected f_2 sections of the INADEQUATE and JC-INADEQUATE spectra of crotonaldehyde are shown in Fig. 4.6. For clarity, only expanded plots of the regions containing the double quantum peaks are presented. The peaks observed at the centers of some of the doublets are unsuppressed singlets which are not of concern here. In all cases, one observes that the double quantum peaks in the f_2 sections of JC-INADEQUATE spectra are more intense than those in the regular spectra. These observed enhancements in the JC-INADEQUATE spectra can be attributed to the combined beneficial effects of incorporating the J-compensated spin-echo sequence and the symmetric phase-alternating composite pulses into the regular INADEQUATE sequence. By comparing the enhancements of each of the doublets, one finds the C-2/C-3 and C-1/C-4 doublets are enhanced more significantly than the other doublets. Since ${}^1J_{2,3} = 67.0\,\text{Hz}$ differs considerably from $J = 38\,\text{Hz}$ for which τ was set, and the C-2 and C-3 spins are relatively close to the carrier, the noted improvement in intensities of the C-2/C-3 doublets is undoubtedly due to J-compensation rather than resonance offset compensation. For the C-1/C-4 doublets of JC-INADEQUATE spectra, both J-compensation and resonance offset compensation play significant roles in increasing the intensities of the two pairs of doublets, since both the C-1 and C-4 spins have larger offsets from the carrier and

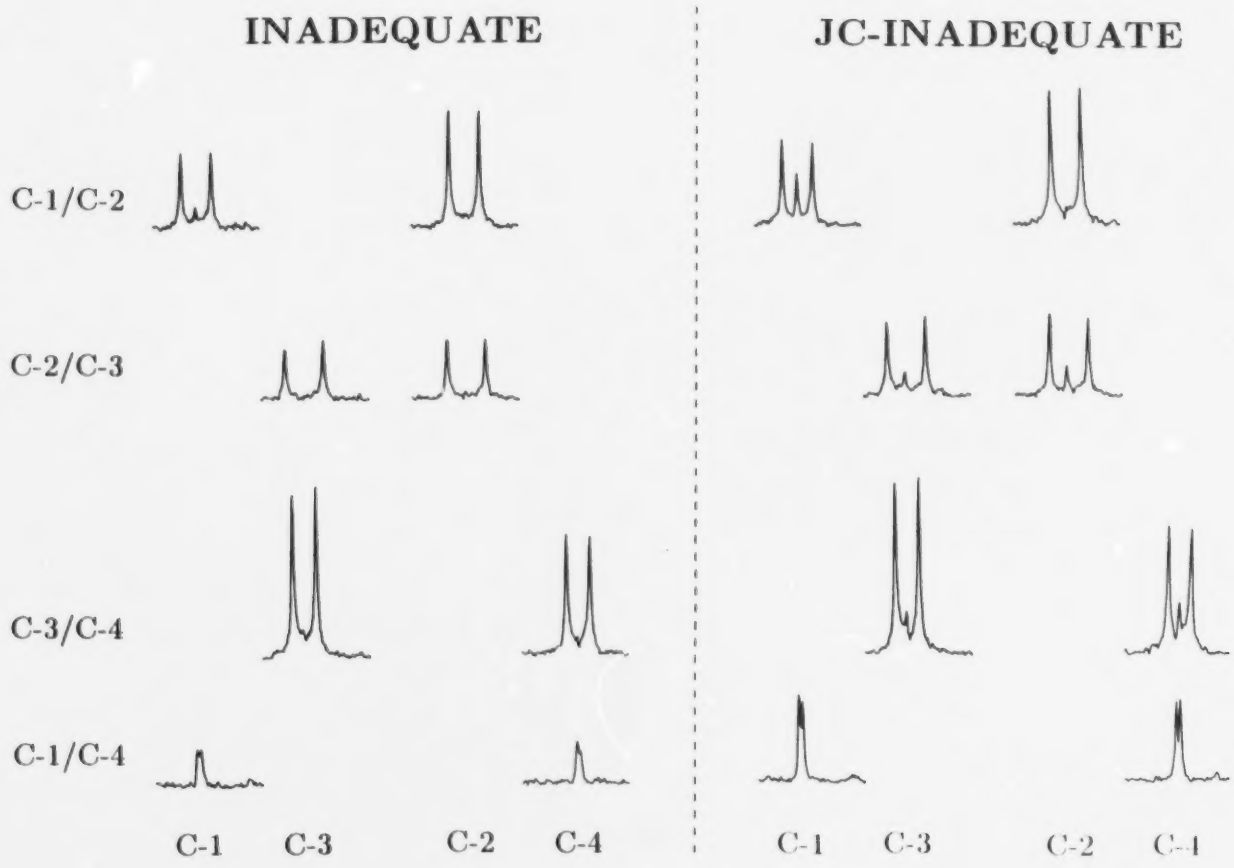

Figure 4.6: Selected f_2 sections of the INADEQUATE and JC-INADEQUATE 2D spectra of crotonaldehyde. All spectra are plotted with the same absolute intensity.

the 7.4 Hz coupling is much smaller than the value of 38 Hz used to select τ.

The above results certainly illustrate how much signal intensity may be lost in the conventional INADEQUATE experiment and how it may be recovered through the use of compensated pulses and delays. The C-INADEQUATE and the JC-INADEQUATE experiments presented in this chapter have both demonstrated advantages over the regular INADEQUATE experiment. For routine applications, we expect the C-INADEQUATE method to be adequate in providing spectra with enhanced sensitivity. If, however, a wide range of coupling constants is anticipated and/or there is a problem in choosing a suitable value for the delay τ, it may be more appropriate to employ the JC-INADEQUATE sequence.

4.2 Conclusions

In this chapter, we have developed a formal operator analogy between the homonuclear spin-spin coupling of the AX spin system and the rf pulse, and have used this analogy as the basis for the creation of a J-compensated homonuclear spin-echo sequence from a ΔB_1-compensated composite pulse sequence. This compensated spin-echo sequence was shown to improve the performance of the INADEQUATE experiment. In the course of applying J-compensated INADEQUATE in carbon spectroscopy, we established experimentally that symmetric phase-alternating composite pulses are very efficient in minimizing resonance offset effects in both the regular and J-compensated INADEQUATE experiments. We therefore recommend the use of such composite pulses in compensating resonance offset effects in other multiple-pulse NMR experiments.

References

1. A. Bax, R. Freeman, and S. P. Kempsell, *J. Am. Chem. Soc.* **102**, 4849 (1980).

2. A. Bax, R. Freeman, and T. A. Frenkiel, *J. Am. Chem. Soc.* **103**, 2102 (1981).

3. A. Bax, R. Freeman, T. A. Frenkiel, and M. H. Levitt, *J. Magn. Reson.* **43**, 478 (1981)

4. T. H. Mareci and R. Freeman, *J. Magn. Reson.* **51**, 531 (1983)

5. S. L. Patt and J. N. Shoolery, *J. Magn. Reson.* **46**, 535 (1982); D. T. Pegg, D. M. Doddrell, and M. R. Bendall, *J. Chem. Phys.* **77**, 2745 (1982); G. A. Morris and R. Freeman, *J. Am. Chem. Soc.* **101**, 760 (1979); D. P. Burum and R.R Ernst, *J. Magn. Reson.* **39**, 163 (1980).

6. M. H. Levitt and R. Freeman, *J. Magn. Reson.* **33**, 473 (1979).

7. M. H. Levitt and R. Freeman, *J. Magn. Reson.* **38**, 453 (1980).

8. M. H. Levitt, *Prog. NMR Spectrosc.* **18**, 61 (1986).

9. S. Wimperis and G. Bodenhausen, *J. Magn. Reson.* **71**, 355 (1987).

10. R. Tycko, H. M. Cho, E. Schneider, and A. Pines, *J. Magn. Reson.* **61**, 90 (1985).

11. M. H. Levitt, and R. R. Ernst, *Mol. Phys.* **73**, 2084 (1983).

12. A. J. Shaka, J. Keeler, T. F. Frenkiel, and R. Freeman, *J. Magn. Reson.* **52**, 335 (1983).

13. A. J. Shaka, J. Keeler, and R. Freeman, *J. Magn. Reson.* **53**, 313 (1983).

14. A. J. Shaka and A. Pines, *J. Magn. Reson.* **71**, 495 (1987).

15. T. M. Barbara, R. Tycko and D. P. Weitekamp, *J. Magn. Reson.* **62**, 54 (1985).

16. S. Wimperis and G. Bodenhausen, *J. Magn. Reson.* **69**, 264 (1986).

17. A. M. Torres and R. E. D. McClung, *J. Magn. Reson.* **92**, 45 (1991).

18. A. M. Torres, R. E. D. McClung, and T. T. Nakashima, *J. Magn. Reson.* **87**, 189 (1990).

19. O. W. Sørensen, G. W. Eich, M. H. Levitt, G. Bodenhausen, and R. R. Ernst, *Prog. NMR Spectrosc.* **16**, 163 (1983).

20. M. H. Levitt, *J. Magn. Reson.* **48**, 234 (1982).

21. K. V. Schenker and W. von Philippsborn, *J. Magn. Reson.* **66**, 219 (1986).

22. L. Müller, *J. Magn. Reson.* **59**, 326 (1984).

23. S. Wimperis, *J. Magn. Reson.* **93**, 199 (1991).

24. A. E. Derome, *J. Magn. Reson.* **78**, 113 (1988).

25. M. H. Levitt and R. Freeman, *J. Magn. Reson.* **43**, 65 (1981).

26. G. E. Martin and A. S. Zektzer, "Two-Dimensional NMR Methods for Establishing Molecular Connectivity, " VCH Publisher, Inc., New York, 1988.

27. T. T. Nakashima and R. E. D. McClung, *J. Magn. Reson.* **70**, 187 (1986).

28. R. R. Ernst, G. Bodenhausen, and A. Wokaun, "Principles of Nuclear Magnetic Resonance in One and Two Dimensions, " Clarendon Press, Oxford, 1987.

29. A. J. SHAKA, *Chem. Phys. Letters* **120**, 201 (1985).

30. T. H. MARECI AND R. FREEMAN, *J. Magn. Reson.* **48**, 158 (1982).

CHAPTER 5

EFFICIENCY OF PURGING SEQUENCES IN THE LONG-RANGE HETERONUCLEAR SHIFT CORRELATION EXPERIMENT*

5.1 Introduction

One of the most popular 2D NMR methods used in structure elucidation of complex organic molecules is the C–H shift correlation experiment which is optimized for long-range magnetization transfer (1). The 2D maps obtained using this technique are very useful in establishing C–C connectivities in a molecule since they show correlations between ^{13}C and protons which are separated by two or three bonds. Unfortunately, many unwanted responses from protons directly attached to ^{13}C are often visible. These direct correlations are undesirable since they needlessly complicate spectral interpretation; thus it is not surprising that many studies have been done in attempting to remove these unwanted responses (2-9).

It has been shown that incorporating a BIRD pulse sequence (10) midway through Δ_2 significantly improves the efficiency of the basic long-range C–H shift correlation experiment (2-6). Besides decreasing the intensities of directly bonded correlation peaks, this appended BIRD pulse sequence suppresses one-bond modulation effects which can otherwise attenuate long-range responses (2). However, the suppression of one-bond correlations using this innovation is far from complete (7) especially if the sample compound has a wide range of proton-carbon coupling constants. Improvements to this sequence are therefore needed to more effectively suppress the directly bonded correlations.

*A version of this chapter has been accepted for publication. A.M. Torres, T.T Nakashima, and R.E.D. McClung, 1992. *Journal of Magnetic Resonance*. Copyright © 1992 by Academic Press, Inc.

Several kinds of pulse sequences may be utilized in the preparation part of the long-range heteronuclear shift correlation experiments to remove transverse magnetizations associated with protons directly attached to ^{13}C so that they do not give observable signals. Kogler and co-workers (11) have successfully eliminated directly bonded correlations in the heteronuclear relay experiment using low-pass J filters. Similar applications of low-pass J filters in the long-range C–H shift correlation experiment with a BIRD sequence in the middle of Δ_2 have been reported (7) but the maps obtained were found to contain artifacts in addition to some direct connectivities. Wimperis and Freeman (12) have introduced the TANGO pulse sequence which discriminates between long-range and direct CH couplings. This excitation sequence has been shown to be efficient in removing one-bond correlations in long-range heteronuclear shift correlation experiments employing a constant t_1 evolution period (2). Recently, a broadband purge sequence derived from the J-compensated INEPT preparation sequence developed by Wimperis and Bodenhausen (13) has been found to be effective in suppressing directly bonded correlations in the HOHAHA relay experiment (14).

In this chapter, we evaluate the efficiencies of various purging sequences (see Fig. 5.1) in order to select the best sequence to be incorporated into the long-range C–H shift correlation sequence with a BIRD midway through Δ_2. In addition, we evaluate the efficiency of the resulting sequence by comparing its performance with those of the purgeless sequence which includes only a BIRD in the center of Δ_2 and of the FLOCK sequence, developed by Reynolds *et al.* (8), which has been shown to give very effective suppression of directly bonded responses.

5.2 Experimental

The experiments were performed on Bruker AM-400 and AM-300 spectrometers. The samples used were a 90%(v/v) solution of 2,3-dihydrofuran (**1**) in $CDCl_3$ and 100mg of norharmane (*β*-carboline, **2**) in 0.4ml of DMSO-d_6. The two solutions were slightly doped with chromium (III) acetylacetonate so that repetition times

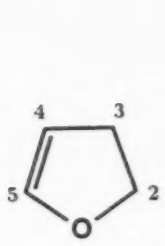

1

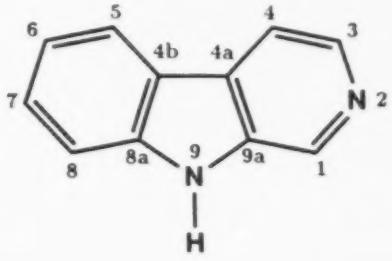

2

of about 2 seconds could be used. Two dummy scans were performed prior to acquisition in all experiments. For the comparison of various purging sequences in the long-range experiment using **1** (Fig. 5.2), the AM-400 was used, and 32 scans per t_1 increment were collected for sequences N, A, and B while the minimum of sixty-four scans, as required in the phase cycle, were gathered for sequences C, D, and E (see Fig. 5.1). The spectral widths were 2024 Hz for f_1 and 16129 Hz for f_2. The 2D data sets consisted of 64 1K FIDs, were zero-filled twice and were apodized with a shifted sine-squared function in the f_1 domain. The weighting function in f_2 was an exponential broadening corresponding to the digital (Hz/pt) resolution. The spectra are displayed in magnitude mode.

For the 1D comparison of the residual directly correlated signals shown in Fig. 5.3, the same phase cycle as in the 2D experiment was used with 32 scans

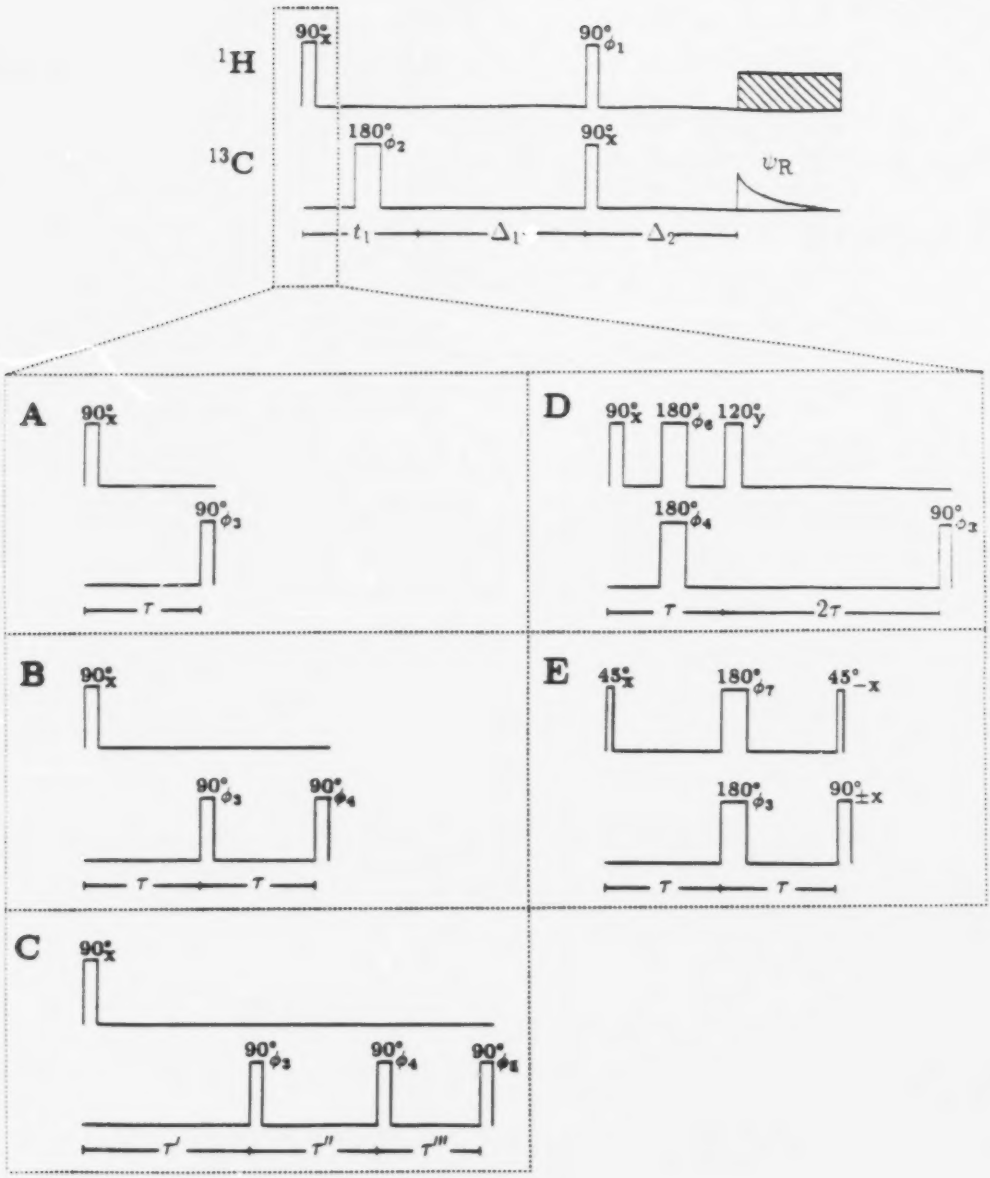

Figure 5.1: Pulse sequence for the long-range heteronuclear shift correlation experiment (top) and purge sequences (A – E) which replace the initial 90° ^{1}H pulse. (A) one-step J filter sequence, (B) two-step J filter sequence, (C) three-step J filter sequence, (D) J-compensated purge, (E) TANGO. Delays Δ_1 and Δ_2 are optimized for long-range couplings, $\tau = 1/2\ ^1J_{CH}^{nom}$, $\tau' = 4.12$ms, $\tau'' = 3.12$ms, and $\tau''' = 2.50$ms, and the phase cycles are $\phi_1 = \psi_R = 0\ 1\ 2\ 3$ ($\equiv 0, \pi/2, \pi, 3\pi/2$), $\phi_2 = (0)_4\ (2)_4$, $\phi_3 = (0)_8\ (2)_8$, $\phi_4 = (0)_{16}\ (2)_{16}$, $\phi_5 = (0)_{32}\ (2)_{32}$, $\phi_6 = (1)_{32}\ (3)_{32}$, $\phi_7 = (1)_{16}\ (3)_{16}$.

per experiment. All 1D spectra are displayed in magnitude mode. For the experimental verification of the calculated profiles with respect to the delay period τ (Fig. 5.5), the AM-300 spectrometer was used.

The 2D experiments on **2** were carried out on the AM-300 spectrometer. Sixty-four scans were accumulated for each value of t_1 to complete the phase cycles. In both FLOCK and BIRDTRAP experiments, the 2D data sets were acquired as 128 1K FIDs and covered frequency ranges of 1562 Hz (^{1}H) and 11364 Hz (^{13}C). Processing of the 2D data sets of **2** was done in a manner similar to that for **1**.

5.3 Results and Discussion

Efficiency of Various Purging Sequences in Suppressing Directly Bonded Correlations

The pulse sequence for the long-range heteronuclear chemical shift correlation experiment (1) is shown in Fig. 5.1. The mechanism of this coherence transfer sequence is very similar to that of the regular 1D INEPT experiment (15,16). In contrast to regular heteronuclear shift correlation experiments in which only directly bonded C–H correlations are observed, the delays Δ_1 and Δ_2 are optimized for long-range couplings so that both direct and long-range correlations are displayed in the spectra.

The directly bonded C–H correlations may overlap and obscure the long-range correlations, and it is desirable to suppress the directly bonded responses (2). In this chapter, we investigate the efficiencies of the five different modifications (A through E) to the preparation part of the long-range C–H correlation sequence shown in Fig. 5.1. Each of these modifications is expected to "purge" the directly bonded correlations from the 2D map by transferring the magnetizations of protons directly bonded to ^{13}C nuclei into multiple quantum coherences or longitu-

dinal proton-carbon two-spin order. Hence, we may view these purging sequences as coherence traps since the coherences generated by directly bonded C–H pairs are not observable during acquisition. Suppression of direct correlations in all of these purge sequences makes use of the large difference in the magnitudes of direct and long-range coupling constants. In purge sequence A, a one-step J filter, the transverse magnetization associated with a proton directly attached to carbon-13 is essentially transformed into proton magnetization which is antiphase with respect to carbon during the τ period, which is nominally equal to $1/2(^1J_{CH})$. Meanwhile, the transverse magnetization of remote protons is basically unchanged because $^2J_{CH}$, $^3J_{CH}$, and $^4J_{CH}$ are small. Application of a carbon $(\pi/2)$ pulse then converts the antiphase proton magnetization into multiple-quantum coherence so that no antiphase magnetization corresponding to the directly attached proton is present during Δ_1. Since multiple-quantum coherence may be converted into observable carbon magnetization in later parts of the sequence, the phase of the purging carbon $(\pi/2)$ pulse is cycled to cancel such signals. If the delay τ is exactly equal to $1/(2\ ^1J_{CH})$, the direct transverse proton magnetization is completely eliminated, leading to spectra that show only long-range responses.

The deficiencies of purge sequence A are readily apparent if the sample has a wide range of coupling constants, $^1J_{CH}$. For some protons in the sample, the delay τ chosen will not be perfect so that considerable transverse magnetization may remain after the purging carbon $(\pi/2)$ pulse. Incorporation of a second purging pulse sequence, as in sequence B, is therefore needed to remove the directly bonded transverse magnetizations that remain after the first purge. Hence, we expect that the two-step purge sequence B, which contains two identical τ periods nominally equal to $1/(2\ ^1J_{CH})$, will be more effective in suppressing one-bond responses over a wider range of coupling constants than the one-step purge sequence A. It is

important to note that the two-step J filter recommended by Kogler *et al.* (11) which involves two different fixed delay periods ($\tau' = 3.58$ms and $\tau'' = 2.39$ms) was not used in this investigation since this sequence, although effective over a wide range of coupling constants, leaves significant residual transverse magnetization for typical values of $^1J_{CH}$.

The efficiency of purge sequence B can be improved further by appending a third purge pulse (sequence C). For this particular sequence, we employed a tailored three-step J filter based on the scheme devised by Kogler *et al.* (11). The original three-step J filter used to remove direct responses in the heteronuclear relay experiment (11) involved three different fixed delays $\tau' = 3.79$ms,$\tau'' = 2.87$ms , and $\tau''' = 2.30$ms and suppressed one-bond correlations very efficiently to below 2.2% for the $^1J_{CH}$ range of 175±50Hz. In order to make the comparison with other purging sequences easier, the delays in this purging sequence were altered to match the average coupling constant of the sample. For **1**, the delays are $\tau' = 4.12$ms, $\tau'' = 3.12$ms, and $\tau''' = 2.50$ms. It is expected that this modified three-pulse purge sequence C will effectively suppress directly bonded C–H responses to below 2.2% for coupling constants in the range 161±46 Hz. We have also investigated the effectiveness of the three-step J filter with $\tau' = \tau'' = \tau'''$, which we refer to as sequence C′.

The J-compensated INEPT preparation sequence developed by Wimperis and Bodenhausen (13) can also be used as a broadband purging sequence since it converts directly bonded proton transverse magnetization into longitudinal proton-carbon two spin order, $2I_zS_z$, so that it does not give detectable magnetizations during signal acquisition (14). Product operator analyses (17) show that this purging sequence can be simplified (since long-range 2D maps need not be phase-sensitive) by removing the second pair of refocusing pulses and replacing the final proton

$(\pi/2)_{30}$ pulse with a carbon $(\pi/2)$ pulse to obtain purge sequence D. This modified sequence transforms transverse magnetization from directly bonded protons into multiple quantum coherence, $2I_xS_y$, and proton magnetization that is antiphase with respect to carbon, $2I_xS_z$. These coherences do not lead to observable signals provided that the phase of the carbon $(\pi/2)$ pulse is cycled.

The last purging sequence which we have considered is the TANGO pulse cluster introduced by Wimperis and Freeman (12). This sequence has been used in long-range heteronuclear shift correlation experiments to excite remote protons and invert directly attached protons so that they do not give observable signals (2,12). Detailed analysis of the mechanics of the TANGO purge sequence, which Bauer *et al.* (2) employed as an excitation sequence, reveals that if the delay τ is not perfectly "matched", some transverse magnetization of the proton directly attached to carbon-13 is converted to antiphase proton magnetization which gives additional observable carbon magnetization during the later part of the long-range sequence (12). Elimination of these unwanted signals can be accomplished by adding a phase-alternated $(\pi/2)$ carbon pulse coincident to the second $(\pi/4)$ proton pulse, as in purge sequence E, so that the antiphase proton magnetization is transformed into multiple quantum coherence.

In testing the performance of the purge schemes shown in Fig. 5.1, the BIRD sequence was not incorporated at the center of the Δ_2 period in order to make the comparison easier since the BIRD sequence itself partially suppresses direct responses. We used **1** as a model compound for the investigation since it has a wide range of direct coupling constants: ^1J(C-2,H-2) = 148.2Hz, ^1J(C-3,H-3) = 133.5Hz, ^1J(C-4,H-4) = 174.8Hz,^1J(C-5,H-5) = 187.6Hz (7), and its carbon and proton resonances are well separated. In all cases, Δ_1 = 50.0ms and Δ_2 = 33.3ms based on the assumption of 10Hz long-range couplings (7).

The f_1 cross-sections of the long-range C–H correlation maps for **1** obtained with the purge sequences shown in Fig. 5.1 are presented in Fig. 5.2. For convenience, all spectra for a given carbon are scaled so that the biggest peak in each has the same intensity. The absolute intensities of the largest long-range peaks in the maps obtained with sequences A and B were essentially equal and the corresponding intensities in maps obtained using sequences C, D, and E were twice as large because these three sequences required twice as many scans as the others.

Examination of Fig. 5.2 shows that there is a significant variation of the intensities of the directly bonded peaks when comparing the conventional correlation spectra (N) to any of the purged spectra (A – E). The intensities of the direct correlations in N are significant and sometimes larger than those of the long-range peaks, however they are much weaker in A – E, and are completely suppressed in some cases.

In the spectra obtained with the one-step J filter sequence A, the directly bonded peaks in the C-5 and C-3 cross-sections are much larger than those in C-4 and C-2 cross-sections. This inefficiency of Method A in suppressing one-bond correlations can be attributed to the wide range of coupling constants present in **1**. The chosen delay ($\tau = 3.1$ms) is based on the average coupling constant of 161 Hz, and thus leaves considerable direct proton transverse magnetization for H-5 and H-3 since their coupling constants deviate from the average and this ultimately leads to sizable directly bonded C–H responses.

Good elimination of the directly bonded responses at C-5 and C-3 is illustrated in the cross-sections of the 2D map obtained with purge sequence B, confirming that the two-step purge sequence is more effective than the one-step sequence over a wider range of coupling constants. Moreover, unlike the A cross-sections, the B cross-sections at C-4 and C-2 show no trace of direct responses.

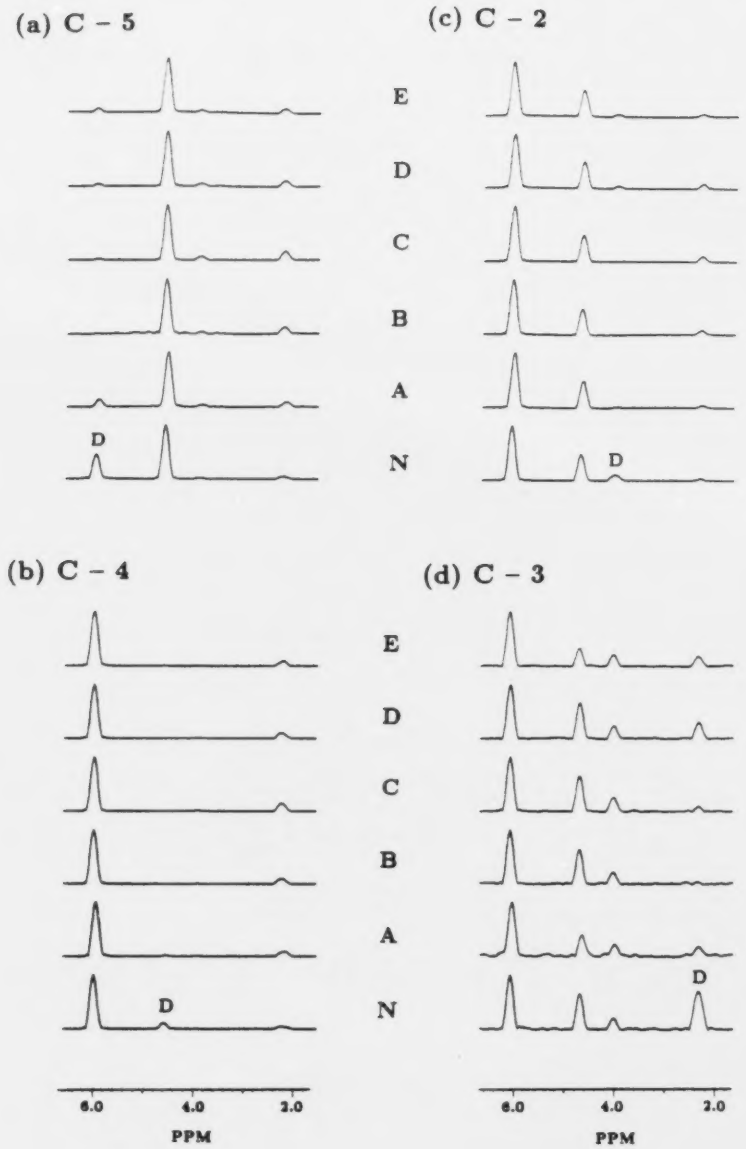

Figure 5.2: f_1 slices from the long-range C–H correlation maps of **1** obtained with the conventional sequence (N) and with purge sequences A – E. The spectra for a given carbon are scaled so that the biggest peak in each has the same intensity. Peaks labelled D are direct connectivity responses which are significantly intense in the regular spectra (N).

The three-step J filter sequence C gives results essentially equivalent to those obtained with sequence B. Suppression of one-bond connectivity peaks is complete in the C-4 and C-2 slices and nearly complete in the C-5 and C-3 cross-sections. In contrast to the results of Salazar *et al.* (7) , where long-range experiments on **1** using a three-step J filter sequence and a BIRD pulse sequence at the center of Δ_2 produced artifacts and sizable attenuation of long-range signals, the cross-sections of the 2D map obtained with sequence C did not show any artifacts nor any significant attenuation of long-range responses. Increasing the number of purging steps from two (sequence B) to three (sequence C) does not, however, give better suppression of directly bonded correlations.

Sequence D incorporates a broadband purging sequence based on the J-compensated sequence devised by Wimperis and Bodenhausen (13) and shows total elimination of the C-4–H-4 direct response. Although D suppresses the C-5–H-5 directly bonded peak better than A does, its performance is less impressive than either B or C. Surprisingly, for the C-3 and C-2 slices, sequence D appears to be less efficient than A in eliminating directly bonded responses.

The TANGO purge sequence E is more efficient than A in suppressing one-bond correlations. This is especially apparent in the C-5 and and C-3 slices where E shows much smaller direct peaks than A. In comparison to other purge sequences, however, E exhibits larger directly bonded peak intensities and demonstrates the overall inferiority of the TANGO purging sequence.

Efficiency of Various Purging Sequences in Eliminating Transverse Magnetizations of Directly Bonded Protons

In order to evaluate the efficiency of one-bond cross-peak suppression of each of the purging sequences in Fig. 5.1 more directly, we have performed experiments on **1**

using 1D analogs of the sequences shown in Fig. 5.1. For these 1D experiments, the t_1 evolution period was removed and the delays Δ_1 and Δ_2 were set to 3.1 ms and 2.1 ms, respectively, to optimize the conversion of the magnetizations of protons directly bonded to ^{13}C into carbon magnetizations. In this way, the observed carbon signal intensities should reflect the amount of transverse magnetization from protons directly attached to ^{13}C nuclei which remains after the purging or trapping sequence. The phase cycles employed were identical to the 2D phase cycles, and the spectra are displayed in magnitude mode in Fig. 5.3. It is clear that A is the least efficient while C′ is the most efficient at purging magnetization of protons directly bonded to ^{13}C. Sequence E, which employs TANGO, is slightly more efficient than A, but considerably less effective than B – D. The two-step (B), three-step (C and C′), and the J-compensated (D) purge sequences show very small residual ^{13}C intensities, demonstrating their superiority over TANGO (E) and the one-step purge (A) sequences.

The behavior expected for the transverse magnetizations of the directly attached proton subjected to each of the various purging sequences was analyzed using product operators (17). The one-bond responses are expected to be proportional to: $|\cos(\pi\,{}^1J_{CH}\ \tau)|$ for the one-step purge sequence (A), $\cos^2(\pi\,{}^1J_{CH}\ \tau)$ for the two-step purge sequence (B) and the TANGO purge sequence (E), $|\cos^3(\pi\,{}^1J_{CH}\ \tau)|$ for the J-compensated sequence (D) and three-step purge sequence (C′), and $|\cos(\pi\,{}^1J_{CH}\ \tau')\cos(\pi\,{}^1J_{CH}\ \tau'')\cos(\pi\,{}^1J_{CH}\ \tau''')|$ for the tailored three-step purge sequence (C). The theoretical variation of the residual transverse proton magnetizations with ${}^1J_{CH}$ for τ = 3.1ms (A, B, C′, D, E) and τ' = 4.12ms,τ'' = 3.12ms, and τ''' = 2.50ms (C) are shown in Fig. 5.4. The single step purge sequence (A) gives the narrowest profile and is the least efficient in removing direct responses in a sample having a wide range of coupling constants. The tailored 3-step purge

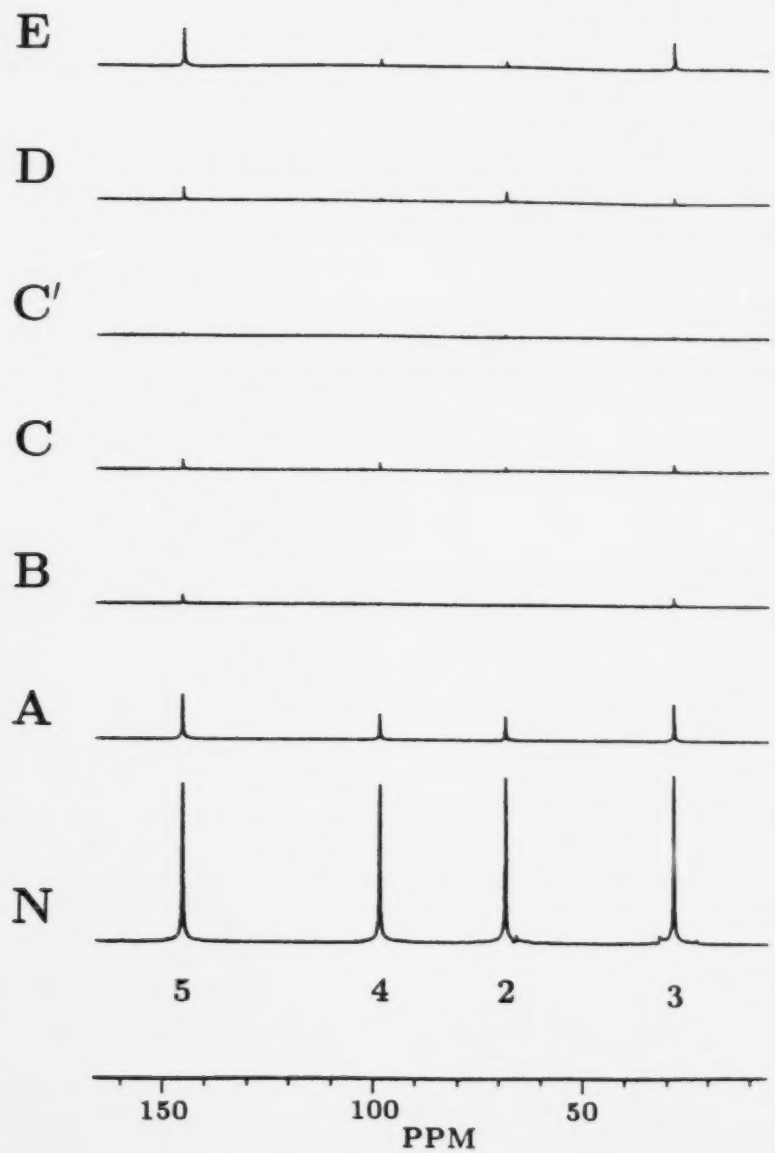

Figure 5.3: Effectiveness of purge sequences A – E in eliminating transverse magnetizations of directly bonded protons. Spectra were obtained using the 1D analogs of the purge sequences in Fig. 5.1 with delays Δ_1 and Δ_2 optimized for direct coupling, and are displayed in magnitude mode. The intensities of the carbon peaks reflect the magnitudes of the transverse magnetizations of directly attached protons that remain after purging.

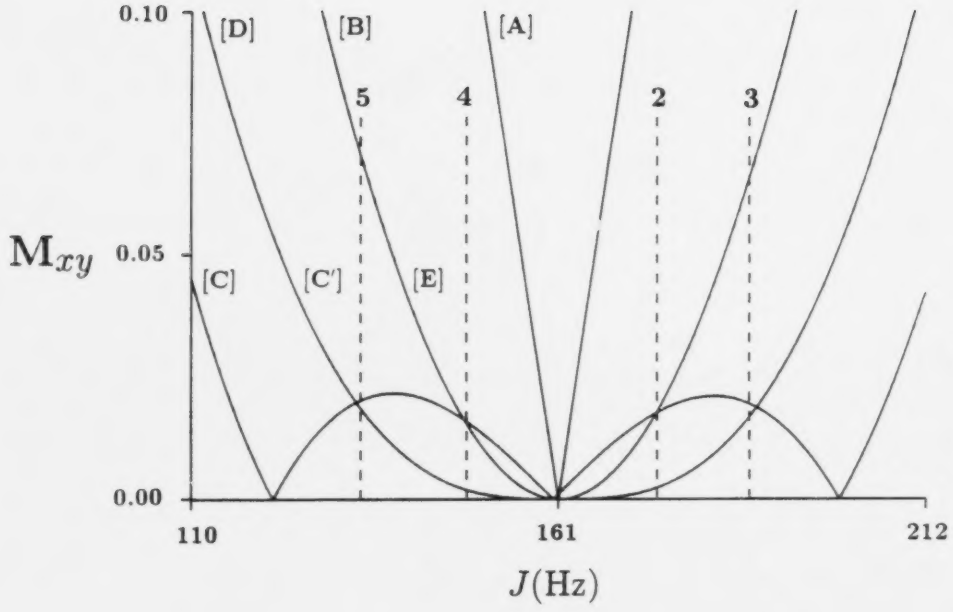

Figure 5.4: Calculated variation of the residual transverse magnetizations with $^1J_{CH}$ for purge sequences in Fig. 5.1. τ = 3.1ms for A, B, C′, D, and E, and τ' = 4.12ms, τ'' = 3.12ms, and τ''' = 2.50ms for sequence C. The residual transverse magnetizations are expected to be proportional to: $|\cos(\pi\,{}^1J_{CH}\,\tau)|$ for A ; $\cos^2(\pi\,{}^1J_{CH}\,\tau)$ for B and E; $|\cos^3(\pi\,{}^1J_{CH}\,\tau)|$ for D and C′; and $|\cos(\pi\,{}^1J_{CH}\,\tau')\cos(\pi\,{}^1J_{CH}\,\tau'')\cos(\pi\,{}^1J_{CH}\,\tau''')|$ for C. Dashed lines with labels indicate the $^1J_{CH}$ contants found in compound **1**.

(C) (11) is the most broadband, but this is not obvious from the results for compound **1** shown in Fig. 5.3 since for the particular values of $^1J_{CH}$ for this molecule, the intensities for the tailored 3-step purge (C) are very similar to those for the J-compensated sequence (D) and for the three-step sequence with equal τ delays (C′). The theoretical plots also show that the TANGO sequence (E) should be as efficient as the two-step purge sequence (B), contrary to the experimental results in Fig. 5.3 which show significant differences in the efficiencies of these sequences.

Experiments to verify the calculated variations in the "unpurged" signal intensity with the length of the delay period τ were also performed using the 1D

versions of sequences A, B, C′, D, and E with Δ_1 and Δ_2 optimized for $^1J_{CH}$ as above. In these experiments, the delay τ was incremented from 0 to 6.2 ms in 20 equal steps, the spectral data were processed in magnitude mode, the intensities of the peaks were measured and plotted against $J\tau$ as shown in Fig. 5.5. In order to accurately compare the observed and theoretical profiles, we have included an exponential decay factor in the calculated profiles to account for relaxation effects and have normalized each curve. The calculated curves are included in Fig. 5.5 and the agreement between the calculated and observed intensity variations with $J\tau$ is very good.

It is apparent from the fitted curves in Fig. 5.5 that A has the narrowest profile of all the trapping sequences and that its performance is therefore most sensitive to the choice of τ. The fitted curves obtained using sequences B and E are very similar, but less broadband than the profiles obtained using sequences C′ and D. Despite the similarities of the fitted curves, significant profile differences can still be observed when the experimental points are considered. The absolute observed intensities near $\tau = 0$ and $\tau = 1/(^1J_{CH})$ (not apparent in Fig. 5.5 since curves have been normalized) are larger for sequences B and C′ than those observed for sequences D and E. The differences in signal intensity may be attributed to pulse imperfections since sequences B and C′ have fewer pulses than D and E. It is therefore more effective to use the low-pass J filter sequences B and C′ in the long-range heteronuclear shift experiment since they will give stronger long-range responses. In addition, sequences B and C′ yielded smaller signals than D and E near $\tau = 1/(2\,^1J_{CH})$, demonstrating their superiority in eliminating one-bond correlation signals.

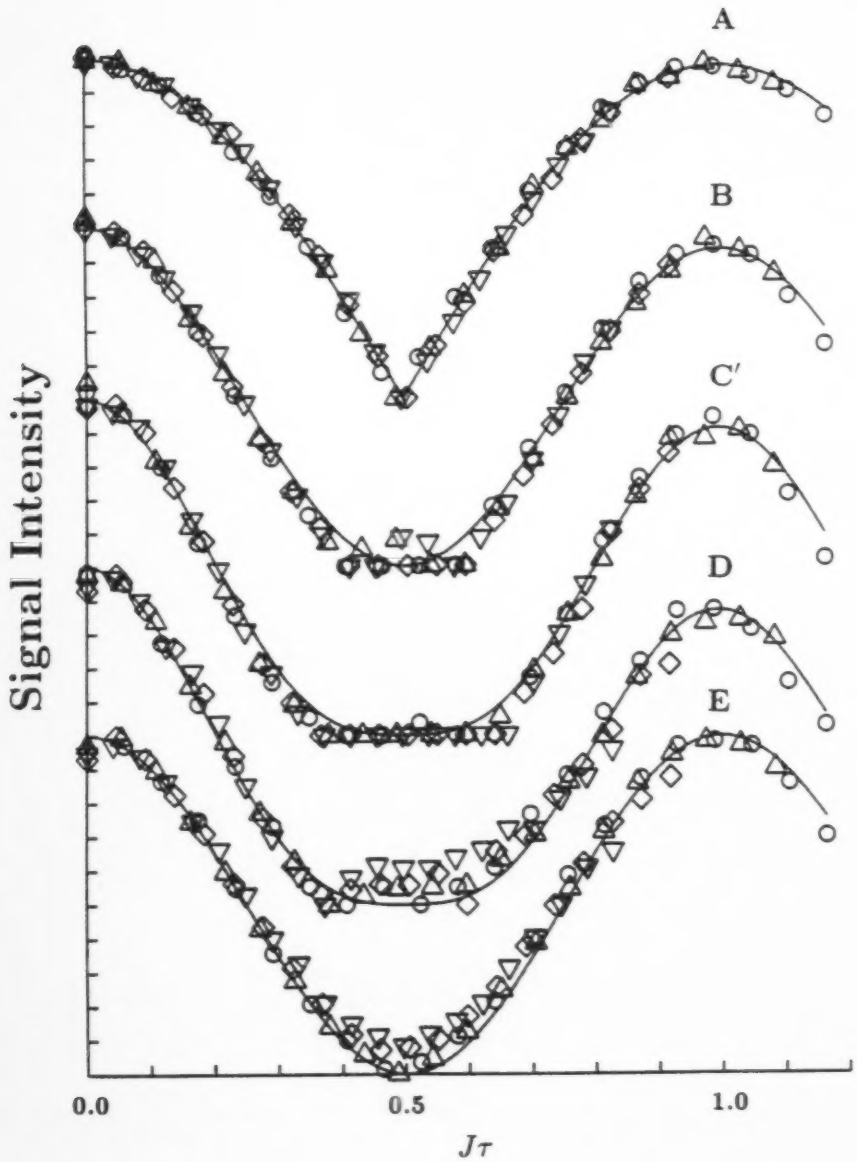

Figure 5.5: Comparison of calculated and observed signals in 1D analogs of the purge sequences in Fig. 5.1. ◇ - C–2, ▽ - C–3, △ - C–4, ◯ - C–5, and — - best fit calculated curve. An exponential decay factor is included in the calculated curve to account for relaxation effects. All experimental curves are normalized.

Incorporation of BIRD and Two-Step *J* Filter Sequences to the Conventional Method: The BIRDTRAP Sequence

As pointed out above, the inclusion of a BIRD sequence in the middle of the refocusing period Δ_2 in long-range heteronuclear correlation shift experiments removes one-bond modulation effects (2) and suppresses one-bond correlations to a limited extent (7). In order to increase the suppression efficiency of this sequence (Fig. 5.6a), one may incorporate a purging sequence at the front end of the sequence. Of the purge sequences investigated here, we chose to incorporate the two-step J filter (B) since: (1) it is definitely better than the sequences A and E; (2) long-range peaks are more intense than with sequences C, C′ and D; (3) it has a shorter phase cycle than sequences C, C′ and D; and (4) the elimination of one-bond responses is expected to be more than adequate. This long-range correlation sequence with a BIRD and two-step purge (TRAP) sequences, which we will refer to as the BIRDTRAP sequence, is shown in Fig. 5.6b.

In order to assess the efficiency of the BIRDTRAP sequence, long-range correlation experiments were performed on **1** using the conventional pulse sequence (Fig. 5.1), the sequence which incorporates a BIRD sequence in Δ_2 (Fig. 5.6a), and the BIRDTRAP sequence (Fig. 5.6b). Shown in Fig. 5.7 are the f_1 slices at the carbon peaks of **1** obtained using the three sequences. The cross-sections for a given carbon are plotted at the same absolute intensity in order to allow comparison of the sensitivities of each method. It can be seen in Fig. 5.7 that there are significant differences between the intensities of some peaks in the conventional spectrum (Fig. 5.7a) and the corresponding peaks in the spectra obtained with sequences including BIRD (Fig. 5.7b and 5.7c). Long-range peaks are generally more intense in the latter spectra, while the directly bonded correlations are smaller. The increase in sensitivity for some long-range peaks, which is particularly evident

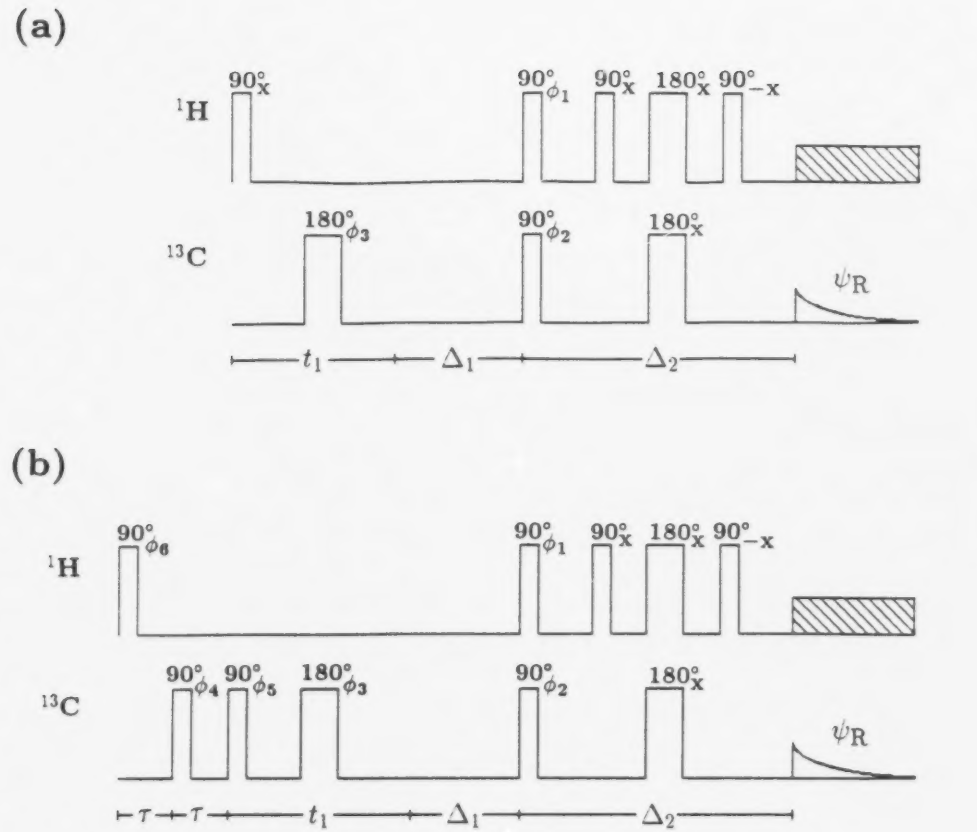

Figure 5.6: Pulse sequences for (a) the long-range heteronuclear shift experiment with a BIRD sequence in the middle Δ_2 and (b) the BIRDTRAP sequence. $\tau = 1/2\ {}^1J_{CH}^{nom}$. Phase cycles for ϕ_1, ϕ_2, ϕ_3, ϕ_4, ϕ_5 are given in Fig. 5.1, $\phi_6 = 0$, $\psi_R = 0\ 1\ 2\ 3\ 2\ 3\ 0\ 1$ in experiments on **1** and $\phi_6 = (0)_8\ (1)_8$, $\psi_R = 0\ 1\ 2\ 3\ 2\ 3\ 0\ 1\ 3\ 0\ 1\ 2\ 1\ 2\ 3\ 0$ in experiments on **2**.

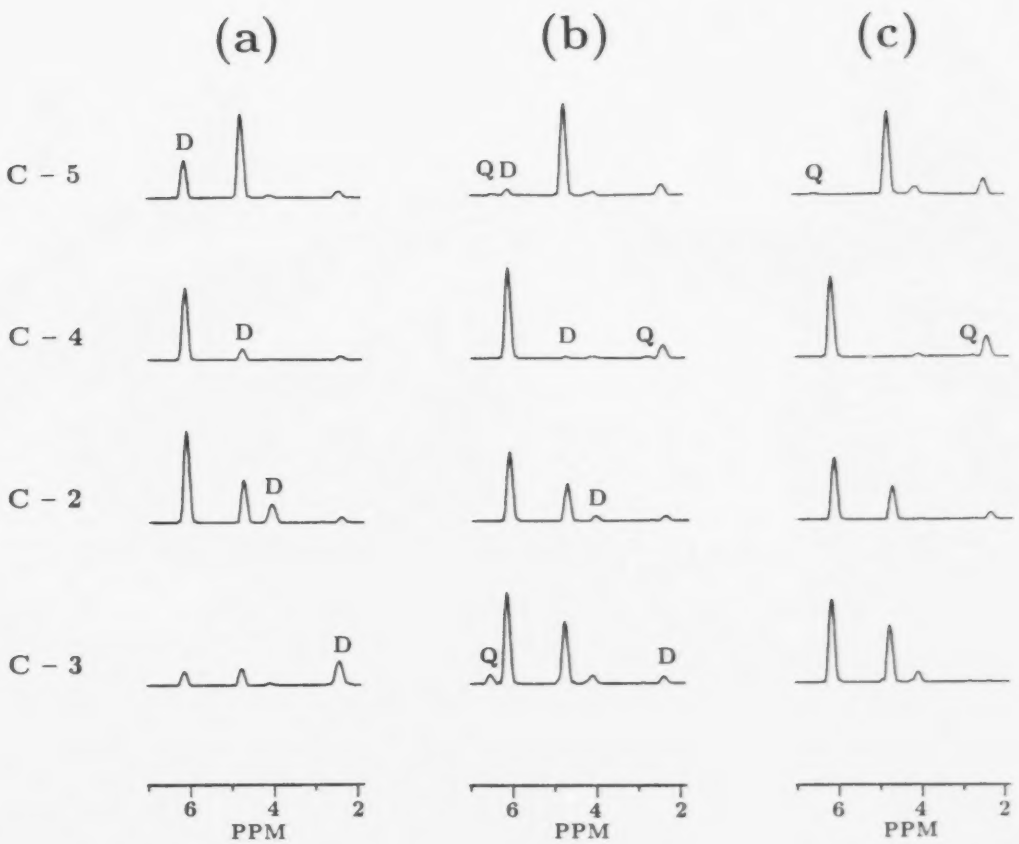

Figure 5.7: f_1 slices from the 2D map of **1** obtained with (a) the regular long-range sequence in Fig. 5.1, (b) the long-range sequence with a BIRD sequence midway through Δ_2 (Fig. 5.6a) and (c) the BIRDTRAP sequence (Fig. 5.6b). Cross-sections for a given carbon are plotted at the same absolute intensity. Peaks marked D are directly correlated responses and those marked Q are quad images.

in the long-range C-3/H-5 and C-3/H-4 correlations, can be attributed to suppression of one-bond modulation effects by the incorporation of the BIRD sequence at the center of Δ_2 (2). Furthermore, the substantial decrease in the directly bonded correlations observed when Fig. 5.7b is compared to Fig. 5.7a, is due to the BIRD sequence acting as a purge. In Figs. 5.7b and 5.7c, one can observe the presence of small quad images which are undoubtedly due to imperfections in the pulses in the BIRD sequence. These artifacts in the BIRDTRAP spectra can be minimized by a more elaborate phase cycling which was employed in later experiments.

The benefit of incorporating the two-step J filter sequence into the long-range heteronuclear shift experiment with a BIRD midway through Δ_2 can be appreciated by comparing the intensities of the direct responses in Fig. 5.7b and 5.7c. In contrast to Fig. 5.7b, where direct responses in all cross sections were still visible, Fig. 5.7c shows no directly bonded responses. In addition, the sensitivities of these experiments are not significantly different in spite of the fact that the BIRDTRAP sequence (Fig. 5.6b) involves more rf pulses and has a longer time period between excitation and detection than the unpurged sequence (Fig. 5.6a).

Comparison of BIRDTRAP and FLOCK

To provide a more stringent test of the effectiveness of the BIRDTRAP sequence, we have compared its performance with that of the FLOCK sequence devised by Reynolds *et al.* (8). The FLOCK sequence includes three BIRD sequences which serve to eliminate direct responses and simultaneously increase the sensitivity of long-range signals by removing proton-proton couplings in f_1. This sequence has been shown to give better suppression of one-bond responses and other artifacts than COLOC (18) and XCORFE (3). In the comparison, the 64 step phase cycle recommended by Reynolds *et al.* (8) was used for FLOCK, while the phase cycle employed for BIRDTRAP was designed to remove quad images (see Fig. 5.6).

Norharmane (β-carboline, **2**) was employed in the comparison of the two methods. Since only methine carbons were to be observed, Δ_1 and Δ_2 were set equal to $1/2(^3J_{CH})$ based on a 10.4Hz coupling (6). The τ delays in the trapping and BIRD sequences were optimized for $^1J_{CH}$ = 170Hz. The 2D maps for **2** obtained in the two experiments are shown in Fig. 5.8. Note that due to the limited width of the f_1 window, the H-9 correlations are folded between the H-1 and H-3 peak positions. In the BIRDTRAP 2D map, only one directly bonded correlation, C-6/H-6, is present, but its true intensity is difficult to determine since it is overlapped by the intense neighboring C-4b/H-6 correlation. On the other hand, the FLOCK map does not show any one-bond connectivity peaks, but does contain a large number of f_1 zero frequency peaks and other artifacts. Several f_1 slices obtained from the 2D maps in Fig. 5.8 are displayed in Fig. 5.9. These carbon slices for all of the protonated carbons of **2** are plotted at the same absolute intensity for a given carbon. Very weak C-6/H-6 and C-7/H-7 correlations are present in the slices of the BIRDTRAP map, but the FLOCK slices show no direct correlations. The weak direct responses in BIRDTRAP could be eliminated if trapping sequence C′ were employed, but this would lead to reduced sensitivity. It is apparent that in most carbon slices, BIRDTRAP gives peaks of higher intensity than FLOCK does. One important difference between the BIRDTRAP and FLOCK 2D maps is displayed in the cross-sections through C-4 where the C-4/H-3 peak in FLOCK is much more intense. This is attributed to the BIRD sequence in the middle of t_1 which removes ^{1}H-^{1}H coupling in f_1. This advantage of FLOCK over BIRDTRAP is not however observed in other peaks because of the limited f_1 resolution.

The higher sensitivity of the BIRDTRAP experiments on norharmane is unexpected since FLOCK has been shown (8) to have significantly higher sensitivity than other long-range correlation experiments similar to BIRDTRAP. It has been shown (4) that the use of composite 180° carbon pulses improves the sensitivity

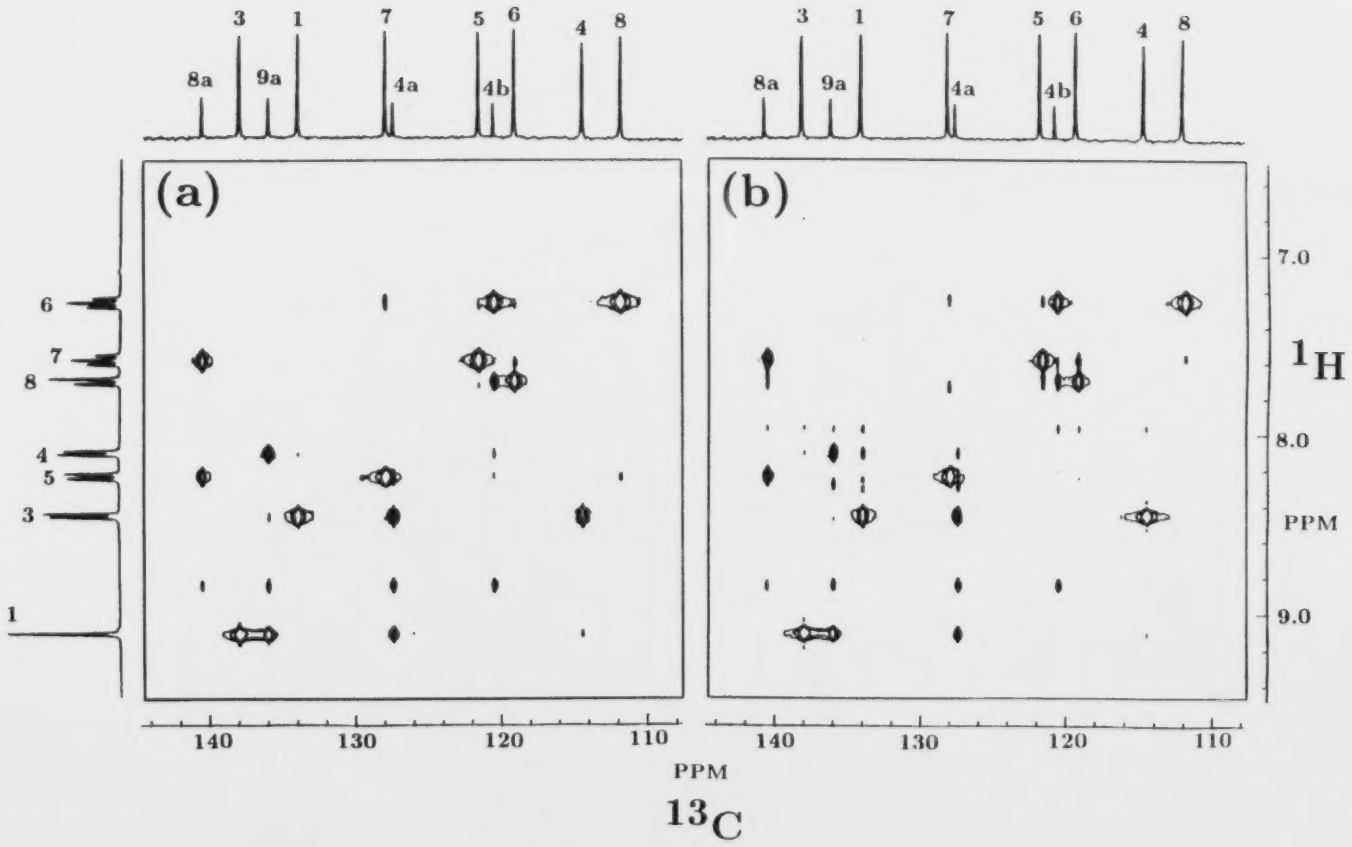

Figure 5.8: Long-range correlation spectra of **2** obtained with (a) BIRDTRAP and (b) FLOCK.

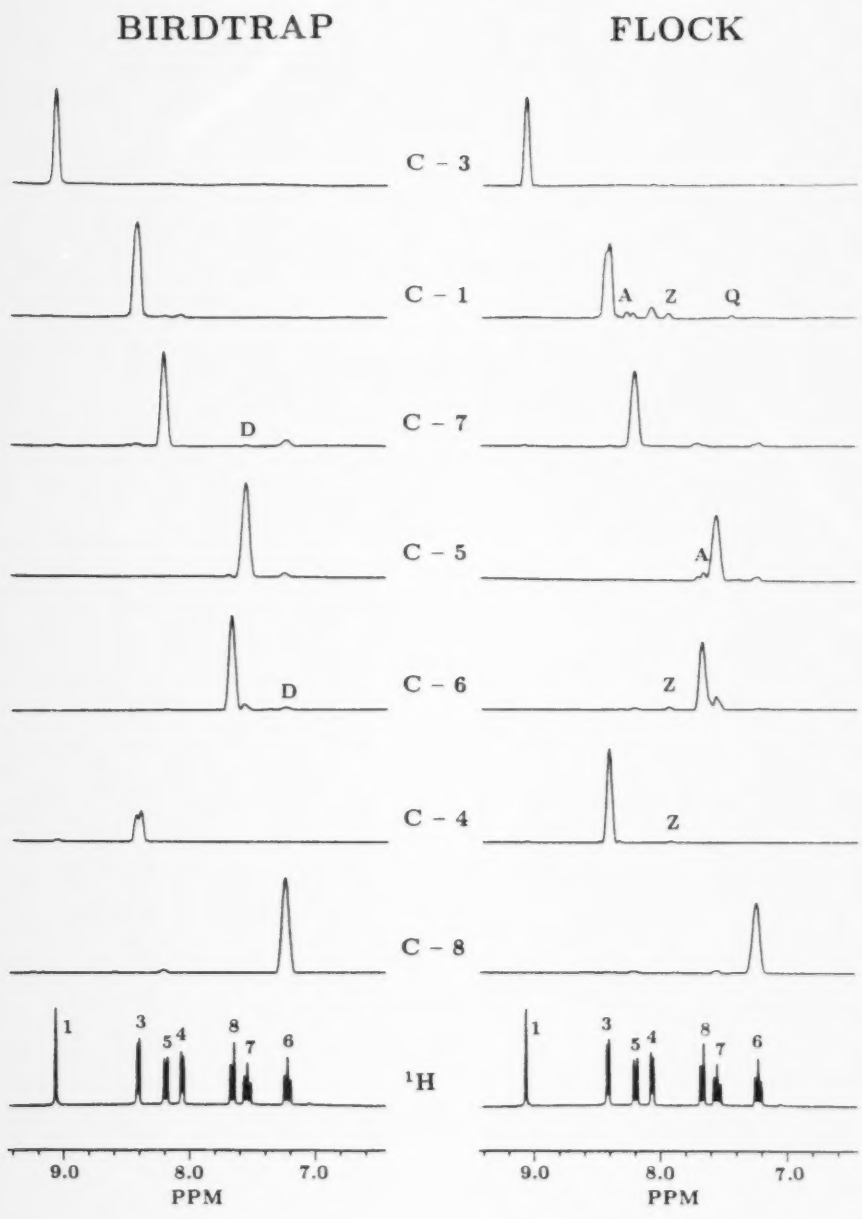

Figure 5.9: f_1 slices of the 2D maps in Fig. 5.8 corresponding to the protonated carbons of **2**. Peaks marked D are directly correlated responses. Artifacts are marked as: Z for f_1 zero frequency; Q for quad images; and A for unaccounted.

of long range heteronuclear correlation experiments and suppresses zero frequency and quad image artifacts. We have not observed significant improvement in the quality of FLOCK correlation maps obtained using composite carbon refocusing pulses on the Bruker AM-400 spectrometer, nor on the Varian Unity-500 spectrometer. Comparisons of 400 MHz BIRDTRAP, "simple" FLOCK (no composite carbon refocusing pulses) and "composite" FLOCK (using composite carbon refocusing pulses) maps for 2-pentanone showed that the sensitivities of "composite" FLOCK and "simple" FLOCK were the same, and ≈15% higher than the BIRDTRAP sensitivity. In the corresponding experiments at 500 MHz, the BIRDTRAP and "simple" FLOCK experiments had comparable sensitivity, while the "composite" FLOCK experiment had ≈20% higher sensitivity. However, in all cases, the FLOCK maps contained a number of artifacts which were not present in the BIRDTRAP maps. Clearly, the effectiveness of composite refocusing carbon pulses in FLOCK, and the relative sensitivities of FLOCK and BIRDTRAP depend on the spectrometer used and the molecule studied.

Figures 5.8 and 5.9 show that the FLOCK map is contaminated by a number of artifacts which are not present in the BIRDTRAP map. In addition to the zero frequency peaks in most of the FLOCK cross-sections, a quad image of the C-1/H-3 correlation is observed in the C-1 cross-section. Since the intensities of these artifacts are comparable to those of the long-range correlation peaks, their presence detracts significantly from the effectiveness of FLOCK experiments in the determination of molecular structure. It may be possible to suppress these artifacts by modifying the FLOCK phase cycle (19). At present, the BIRDTRAP sequence provides cleaner long-range C–H shift correlation maps on the specrometers which we have used, and BIRDTRAP appears to be a more effective tool for structure determination. The presence of very weak direct correlations does not impair BIRDTRAP's utility.

References

1. W. F. Reynolds, R. G. Enriquez, L. I. Escobar, and X. Lozoya, *Can. J. Chem.* **62**, 2421 (1984); C. Wynants, K. Hallenga, G. van Binst, A. Michel, and J. Zanen, *J. Magn. Reson.* **57**, 93 (1984); M. J. Quast, E. L. Ezell, G. E. Martin, M. L. Lee, M. L. Tedjamulia, J. G. Stuart, and R. N. Castle, *J. Heterocyc. Chem.* **21**, 1453 (1985).

2. C. Bauer, R. Freeman, and S. Wimperis, *J. Magn. Reson.* **58**, 526 (1984).

3. W. F. Reynolds, D. W. Hughes, M. Perpick-Dumont and R. G. Enriquez, *J. Magn. Reson.* **63**, 413 (1985).

4. M. Perpick-Dumont, R. G. Enriquez, S. McLean, F. V. Puzzuoli and W. F. Reynolds, *J. Magn. Reson.* **75**, 414 (1987).

5. A. S. Zektzer, B. K. John, R. N. Castle, and G. E. Martin, *J. Magn. Reson.* **72**, 556 (1987).

6. A. S. Zektzer, B. K. John, G. E. Martin, *Magn. Reson. Chem.* **25**, 752 (1987).

7. M. Salazar, A. S. Zektzer, and G. E. Martin, *Magn. Reson. Chem.* **26**, 28 (1988).

8. W. F. Reynolds, S. McLean, M. Perpick-Dumont, and R. G. Enriquez, *Magn. Reson. Chem.* **27**, 162 (1989).

9. D. J. Meyerhoff, *J. Magn. Reson.* **78**, 333 (1988).

10. J. R. Garbow, D. P. Weitekamp, and A. Pines, *Chem. Phys. Lett.* **93**, 504 (1982).

11. H. Kogler, O. W. Sørensen, G. Bodenhausen and R. R. Ernst, *J. Magn. Reson.* **55**, 157 (1983).

12. S. Wimperis and R. Freeman, *J. Magn. Reson.* **58**, 348 (1984).

13. S. Wimperis and G. Bodenhausen, *J. Magn. Reson.* **69**, 264 (1986).

14. D. R. Muhandiram, T. T. Nakashima, and R. E. D. McClung, *J. Magn. Reson.* **87**, 56 (1990).

15. G. A. Morris and R. Freeman, *J. Am. Chem. Soc.* **101**, 760 (1979).

16. D. P. Burum and R. R. Ernst, *J. Magn. Reson.* **39**, 163 (1980).

17. T. T. Nakashima and R. E. D. McClung, *J. Magn. Reson.* **70**, 187 (1986).

18. H. Kessler, C. Griesinger, J. Zarbock, and H. R. Loosli, *J. Magn. Reson.* **57**, 331 (1984)

19. W. F. Reynolds, private communication.

CHAPTER 6

GENERAL DISCUSSION AND CONCLUSIONS

The derivation of several J-compensated magnetization transfer sequences from B_1 inhomogeneity-compensated rf pulses, using the product operator analogies between rf pulses and spin-spin coupling, has been presented in this thesis. The J-compensated sequences developed are useful since they can be incorporated into the pulse sequences of various experiments, making the sequences more effective over a wide range of spin-spin coupling constants J and less sensitive to the choice of τ period. Their role in multiple-pulse experiments is not limited only to enhancing signals, but to suppressing unwanted signals as well.

The key to the development of J-compensated magnetization transfer sequences was the establishment of the product operator analogies between rf pulses and spin-spin coupling. The analogies provide the crucial link to the creation of J-compensated magnetization transfer sequences from B_1 inhomogeneity-compensated pulses. For heteronuclear spin systems, pictorial representations were found useful in recognizing the analogous transformation properties of operators involved in rf pulses and those involved in heteronuclear spin-spin coupling. This was not, however, true for the homonuclear spin case, where it was difficult to pictorially depict the coherences and transformations involved in spin-spin coupling in a consistent manner. The direct comparison of the transformations using product operator notations was used instead.

The operator analogies presented in this thesis directly relate spin-spin coupling and rf pulses. This is in contrast to other analogies (1-5) used in creating J-compensated experiments where the whole sequence or a part of the sequence

which contains the J-dependent precession period was connected to the rf pulse. The advantage of the direct operator analogy has been illustrated clearly. It was shown, for example, that the compensated sequence $\tau - 120^{\circ}_{270} - 2\tau - 60^{\circ}_{270}$ (Eq. [2-18]), which transforms I_y into $-2I_xS_z$, can be used to derive the broadband-INEPT perparation sequence $90^{\circ}_{0} - \tau - 120^{\circ}_{90} - 2\tau - 30^{\circ}_{90}$ proposed by Wimperis and Bodenhausen (2). It is also important to point out that the $60^{\circ}_{180} - 2\tau - 120^{\circ}_{0} - \tau$ (Eq.[2-25]) sequence, which also transforms I_y into $-2I_xS_z$ and which was included in a practical version of DEPT (6) in which the first part was J-compensated (DEPTC1), could be incorporated into the INEPT sequence (7,8) to construct a J-compensated INEPT preparation sequence which is rather different from Wimperis-Bodenhausen sequence (2).

Since J-compensated magnetization transfer sequences are based on composite pulses, they have more pulses and delays than simple uncompensated sequences. This is probably the biggest drawback of J-compensated sequences since, as a result of such long sequences, they are more sensitive to rf pulse imperfection and relaxation effects than simple sequences. In addition, passive spin-spin couplings with other nuclei (which are neglected in the theoretical development) can be significant in a long J-compensated sequence so that its performance may be reduced markedly. For these reasons, the practical J-compensated magnetization transfer sequences presented in this thesis are derived from short but effective B_1 inhomogeneity-compensated pulses (9,10).

J-compensated magnetization transfer sequences which convert I_y to $-I_y$ were patterned after composite inversion pulses and were used in constructing compensated APT (11) or spin-flip (12) experiments. The Compensated Attached Proton Test (CAPT) and the Rectangular Attached Proton Test (RAPT) incorporated J-compensated magnetization transfer sequences based on Levitt's $90^{\circ}_{0}180^{\circ}_{90}90^{\circ}_{0}$ (9)

and Wimperis' rectangular $180^{\circ}_{0}360^{\circ}_{90}360^{\circ}_{225}$ (13) composite inversion sequences respectively. For the CH and CH_3 spin systems, CAPT showed broader inversion profiles than the uncompensated spin-flip and RAPT experiments. Unfortunately, the CAPT signal profile for the CH_2 spin system was narrower than the others. This undesirable property does not significantly impair CAPT's utility since the largest variations in $^1J_{CH}$ are expected for the CH fragment. CAPT may be used for spectral editing, just as APT is, so that the carbon peaks may be easily assigned to a particular spin-system. RAPT displayed the expected rectangular shaped signal profiles for CH and CH_2 spin-systems. As a consequence of this rectangular shape, RAPT has the broadest maximum around $\beta' = 180^{\circ}$ for these spin systems. The RAPT inversion profile for the CH_3 spin system did not, however, show significant advantages over the regular spin-flip experiment. In contrast to CAPT, RAPT is not expected to find practical applications since it involves much longer precession periods.

Heteronuclear J-compensated magnetization transfer sequences which convert I_y to $-I_xS_z$ and $2I_xS_z$ to I_y were all patterned after Levitt's $90^{\circ}_{0}180^{\circ}_{120}$ composite 90° pulse (10). Sequences of this type were useful in improving experiments like INEPT and DEPT since these sequences require interconversion of heteronuclear in-phase and antiphase magnetizations in transferring proton magnetization to carbon. The operation of the compensated transformation $2I_xS_z \xrightarrow{(\beta')\,2I_zS_z} \xrightarrow{(-2\pi/3)\,2I_xS_z} \xrightarrow{(2\beta')\,2I_zS_z} \xrightarrow{(\pi/3)\,2I_xS_z} I_y$ (Eq. [2-22]), which was devised by exploiting the analogous transformation properties of the sets of operator $\{I_x, I_y, I_z\}$ and $\{I_y, 2I_zS_z, 2I_xS_z\}$, was investigated in detail and provided useful insight for the derivation of different compensated sequences. The $\xrightarrow{(-2\pi/3)\,2I_xS_z}$ element of this conversion represents a phase shifted spin-spin coupling between nuclei I and S. Its role in the J-compensated transformation is to store part of the $I_y \sin\beta'$

magnetization as longitudinal spin-order, $2I_zS_z$, so that it will be invariant to the $\xrightarrow{(2\beta')\ 2I_zS_z}$ spin-spin coupling propagator. The stored magnetization is later revived by the $\xrightarrow{(\pi/3)\ 2I_xS_z}$ element. The discovery of this coherence storing mechanism was the key which led to the construction of different compensated sequences that store magnetizations as coherences other than longitudinal spin-order $2I_zS_z$. The compensated sequence $60^{\circ}_{180} - 2\tau - 120^{\circ}_{0} - \tau$ (Eq.[2-25]), for example, stores magnetization as longitudinal coherence I_z. DEPTC2 includes a $(-2\pi/3)_x$ proton pulse which stores part of $4H_{2z}H_{1x}C_y$ as $4H_{2y}H_{1x}C_y$ so that it will not be transformed by spin-spin coupling during the second precession period.

A detailed investigation of the DEPT signal pathways for CH, CH_2, and CH_3 spin systems was conducted prior to the incorporation of J-compensation in the DEPT sequence. For convenience, the DEPT sequence was divided into three parts with each part incorporating a τ period. During the first τ period, it was found that the transformation of H_{1y} to $-2H_{1x}C_z$ was common for all three spin-systems. J-compensated magnetization transfer sequences [2-18] and [2-25], which both transform I_y to $-I_xS_z$, were thus incorporated into the first part of DEPT, resulting in two DEPTC1 sequences. The DEPTC1 sequence which incorporates sequence [2-25] was preferable over the other sequence which includes sequence [2-18] since it has far fewer pulses.

For all spin systems, it was shown through theoretical calculations and experimental studies that DEPTC1 was less sensitive to variations in $^1J_{CH}$ and/or τ delay misset than DEPT. The DEPTC1 overall signal profile was, however, only slightly broader than that of the regular DEPT sequence due to the fact that only one of the three parts of DEPT was compensated in this sequence.

Compensating the second and third parts of DEPT proved to be more complicated than first anticipated. For CH_2 and CH_3 spin systems, it was found that

more than one product operator term contributes to the detected carbon signals. It was therefore difficult to devise sequences for the second and third parts of DEPT which simultaneously compensated the transformation of all terms. J-compensated sequences which were finally developed for the second part of DEPT (DEPTC2) gave a broadband profile for carbon signals originating from the principal terms. The benefit gained was, however, overshadowed by the unfavorable effects on the transformation of the ancillary terms. In short, DEPTC2 gave overall signal profiles for CH_2 and CH_3 which were narrower than the profiles obtained using the regular DEPT sequence. The DEPT sequence in which the third part was compensated (DEPTC3) produced a broadband profile for the CH spin system, but failed to give broader overall profiles for CH_2 and CH_3 spin systems.

The construction of the J-compensated homonuclear magnetization transfer sequences which transform $(I_{1y} + I_{2y})$ into $-(2I_{1x}I_{2z} + 2I_{1z}I_{2x})$ was presented in Chapter 4. In order to avoid significant loss of coherence during the sequence, the short but effective Levitt's $90^\circ_0 180^\circ_{120}$ composite 90° pulse (10) was again used as the basis for deriving the J-compensated sequence. In a manner similar to that used in the compensation of the DEPT experiment, a product operator analysis of the transformations of the magnetization as it progresses through the INADEQUATE experiment (14) was conducted prior to the incorporation of a J-compensated magnetization transfer sequence. It was shown that half of the total double quantum signal assigned to a particular spin is due to magnetization transferred from the other spin. This means that, in the presence of resonance offset effects, the antiphase doublet assigned to a spin located near the carrier could be significantly reduced if this spin were coupled to a spin located far from the carrier. Since the role of the precession period in the INADEQUATE sequence is to convert homonuclear in-phase into antiphase magnetization, this part of the sequence was

replaced by a J-compensated homonuclear magnetization transfer sequence, resulting in the J-compensated INADEQUATE sequence. A more practical form of this compensated sequence was obtained through product operator manipulations. Calculations and proton experiments on the 2,3-dibromothiophene sample (AX spin system) confirmed that the signal profile of the new INADEQUATE sequence was broader than the signal profile of the regular INADEQUATE sequence. The compensated sequence is not, however, expected to be of practical use in proton spectroscopy where spin systems are generally complex networks and the spin-spin coupling constants are small. The utility of J-compensated INADEQUATE in carbon spectroscopy showed more promise since the spins systems involved are generally simple AX systems and the spin-spin coupling constants are relatively large. However, the extreme vulnerability of double-quantum experiments to sensitivity degradation due to resonance offset effects presented a big challenge in the practical application of the J-compensated INADEQUATE sequence, since this sequence has more pulses than the regular INADEQUATE sequence.

Various composite refocusing pulses were tested in an effort to make the regular and the J-compensated INADEQUATE experiments less sensitive to resonance offset effects. It was found that the five-step symmetric phase-alternating composite 180° pulse $58^\circ_0 140^\circ_{180} 344^\circ_0 140^\circ_{180} 58^\circ_0$ (15) was the most effective in minimizing resonance offset effects when $\Delta B/B_1$ for the coupled spins ranged from -0.42 to 0.28. As a consequence, all rf pulses in the regular and in the J-compensated sequences were replaced by the appropriate five-step symmetric phase-alternating composite pulses, resulting in sequences referred to as C-INADEQUATE and JC-INADEQUATE respectively. C-INADEQUATE produced double-quantum peaks which were larger than the peaks obtained using an INADEQUATE sequence where only the 180° was replaced by a five-step symmetric composite pulse. For com-

parison, the performance of the compensated INADEQUATE sequence devised by Levitt and Ernst (16) was also investigated. For the above range of offsets, it was found that this sequence did not produce enhanced double-quantum responses and this was attributed to inefficiency of the $90^\circ_0 180^\circ_{180} 270^\circ_0$ composite pulse (17,18) element of the sequence in inverting z-magnetizations at these moderate resonance offset conditions. At greater resonance offsets ($\Delta B/B_1 \geq \pm 0.50$), however, the Levitt-Ernst compensated sequence gave significantly enhanced double-quantum peaks which were even larger than those obtained using the C-INADEQUATE sequence. Besides enhancing double quantum peaks, the C-INADEQUATE experiment excites peaks which are not excited by the regular INADEQUATE sequence. This was shown in INADEQUATE experiments on 5-hexene-2-one where double quantum correlations associated with the two spins that are far from the carrier were not perceptable in the regular spectra, but were clearly visible in C-INADEQUATE spectra.

The JC-INADEQUATE sequence exhibited the insensitivity to resonance offset of C-INADEQUATE plus an added beneficial feature. Like the C-INADEQUATE method, JC-INADEQUATE produced significantly enhanced double-quantum peaks, although these peaks were less intense than those produced by C-INADEQUATE, due to the additional pulses and delays in the JC-INADEQUATE sequence. In addition, one-bond correlations with large carbon-carbon couplings and long-range correlations where couplings are small were larger in the JC-INADEQUATE spectra than in the regular INADEQUATE and C-INADEQUATE spectra. These results illustrated the superiority of the JC-INADEQUATE method in producing double-quantum peaks in the presence of moderate resonance offsets and a wide range of spin-spin coupling constants.

The utility of different J-compensated magnetization transfer sequences in en-

hancing signal intensities were clearly illustrated in Chapters 2 to 4, where J-compensation of the DEPT, spin-flip, and INADEQUATE experiments were considered. With the exceptions of the J-compensated sequences developed for the second and third delays in DEPT, all of the J-compensated experiments derived in this thesis demonstrated the expected broadband properties in the presence of a wide range of coupling constants J, by producing signals which were generally more intense than those obtained using uncompensated sequences.

Besides enhancing signals in the experiments described above, J-compensated sequences may be used to suppress unwanted peaks in other experiments. This was illustrated in Chapter 5 where the efficiencies of a modified version of the broadband-INEPT preparation sequence developed by Wimperis and Bodenhausen (2), the one-step J filter, the two-step J filter, the three-step J filter with equal delays, a tailored three-step J filter (19), and the TANGO sequence (20) were evaluated for use in removing directly-bonded responses from long-range C–H shift correlation maps (21). The results of these experiments showed that the modified J-compensated INEPT-preparation sequence was not as effective as the two step J filter in removing directly bonded peaks in the presence of a wide range of $^1J_{CH}$ constants. This was contrary to expectations based on theoretical calculations which showed that the directly bonded intensity in a long-range C–H shift sequence which includes the modified J-compensated sequence was proportional to$|\cos^3(\pi\,{}^1J_{CH}\,\tau)|$ while that for a long-range sequence with a two-step J filter was proportional $|\cos^2(\pi\,{}^1J_{CH}\,\tau)|$. The observed efficiency of the two step J filter in removing direct responses was significantly better than the efficiencies of the one step J filter and the TANGO sequence, and was comparable to those of the three step J filter with equal delays and the tailored three-step J filter. Incorporation of this two step J filter at the front end of a long-range C–H shift correlation sequence

that included a BIRD sequence in the middle of the refocusing period (22), gave a sequence (BIRDTRAP) which was expected to produce 2D maps with minimum one-bond correlations.

In 2D experiments with 2,3-dihydorfuran, BIRDTRAP was shown to give much better suppression of one-bond responses than the long-range heteronuclear shift correlation experiment which only incorporates a BIRD at the middle of the refocusing period. Despite the added pulses and delays, BIRDTRAP did not show significant reduction in the intensities of the long-range peaks. As a final test, the performance of BIRDTRAP was compared to that of the FLOCK sequence (23) using norharmane (β-carboline) as a model compound. It was observed that very weak direct responses were still present in some of the f_1 slices of the BIRDTRAP maps, while none of these peaks was present in the FLOCK slices. These direct responses in the BIRDTRAP map were, however, too weak to obscure the presence of other long-range peaks. The long-range peak intensities in the BIRDTRAP map appeared to be slightly greater than those in the FLOCK map. In later experiments, it was shown that the relative sensitivities of the these two methods depend on the molecule studied and the spectrometer used. Perhaps the most significant difference between the maps obtained with the two experiments was the presence of a number of artifacts in the FLOCK map which were clearly absent in the BIRDTRAP map. The FLOCK map contained quad images and zero frequency peaks which may be reduced in intensity with more effective phase cycling (24) as described in the Appendix. Nonetheless, it appears that the artifact suppression in the standard FLOCK sequence is inferior to that of BIRDTRAP.

The work reported in this thesis has shown the usefulness of different J-compensated magnetization transfer sequences in enhancing and in suppressing signals for various spin systems in many multiple-pulse experiments. In establishing the

formal analogies which were used as the basis for the construction of J-compensated sequences from composite pulses, the spin-system was assumed to be a simple two spin-$\frac{1}{2}$ IS spin system. For multispin systems, the performance of the J-compensated sequences was sometimes not very impressive . Sørensen and co-workers (3,4) have recently presented a J-compensation study on simultaneous refocusing of antiphase magnetizations for different spin systems. Developmental work is still needed before one can create J-compensated sequences which would efficiently and simultaneously interconvert in-phase and antiphase magnetizations for various spin systems. In addition, the development of J-compensated sequences need not be based only on common composite pulses where the magnitude of the flip angles and phases are limited to multiples of 90°. In describing their work in compensated refocusing, Sørensen and co-workers (4) presented a number of unconventional composite pulse sequences, for example a $24.1^{\circ}_{90}45.9^{\circ}_{337.7}$ composite pulse, which were obtained by numerical optimization procedures. Such composite pulses may be used as the basis for the construction of J-compensated sequences which may be shorter and more effective than those presented in this thesis.

References

1. J. R. Garbow, D. P. Weitekamp, and A. Pines, *Chem. Phys. Lett.* **93**, 504 (1982).

2. S. Wimperis and G. Bodenhausen, *J. Magn. Reson.* **69**, 264 (1986).

3. O. W. Sørensen, J. C. Madsen, N. C. Nielsen, H. Bildsoe, and H. J. Jakobsen, *J. Magn. Reson.* **77**, 170 (1988).

4. N. C. Nielsen, H. Bildsoe, H. J. Jakobsen, and O. W. Sørensen, *J. Magn. Reson.* **85**, 359 (1989).

5. T. M. Barbara, R. Tycko and D. P. Weitekamp, *J. Magn. Reson.* **62**, 54 (1985).

6. D. T. Pegg, D. M. Doddrell, and M. R. Bendall, *J. Chem. Phys.* **77**, 2745 (1982).

7. G. A. Morris and R. Freeman, *J. Am. Chem. Soc.* **101**, 760 (1979).

8. D. P. Burum and R. R. Ernst, *J. Magn. Reson.* **39**, 163 (1980).

9. M. H. Levitt and R. Freeman, *J. Magn. Reson.* **33**, 473 (1979).

10. M. H. Levitt, *J. Magn. Reson.* **48**, 234 (1982).

11. S. L. Patt and J. N. Shoolery, *J. Magn. Reson.* **46**, 535 (1982).

12. G. Bodenhausen, R. Freeman, R. Niedermeyer, and D. L. Turner, *J. Magn. Reson.* **24**, 291 (1976)

13. S. Wimperis, *J. Magn. Reson.* **83**, 509 (1989).

14. A. Bax, R. Freeman, and S. P. Kempsell, *J. Am. Chem. Soc.* **102**, 4849 (1980).

15. A. J. Shaka and A. Pines, *J. Magn. Reson.* **71**, 495 (1987).

16. M. H. Levitt, and R. R. Ernst, *Mol. Phys.* **73**, 2084 (1983).

17. A. J. Shaka, J. Keeler, T. F. Frenkiel, and R. Freeman, *J. Magn. Reson.* **52**, 335 (1983).

18. A. J. Shaka, J. Keeler, and R. Freeman, *J. Magn. Reson.* **53**, 313 (1983).

19. H. Kogler, O. W. Sørensen, G. Bodenhausen and R. R. Ernst, *J. Magn. Reson.* **55**, 157 (1983).

20. S. Wimperis and R. Freeman, *J. Magn. Reson.* **58**, 348 (1984).

21. W. F. Reynolds, R. G. Enriquez, L. I. Escobar, and X. Lozoya, *Can. J. Chem.* **62**, 2421 (1984); C. Wynants, K. Hallenga, G. van Binst, A. Michel, and J. Zanen, *J. Magn. Reson.* **57**, 93 (1984); M. J. Quast, E. L. Ezell, G. E. Martin, M. L. Lee, M. L. Tedjamulia, J. G. Stuart, and R. N. Castle, *J. Heterocyc. Chem.* **21**, 1453 (1985).

22. C. Bauer, R. Freeman, and S. Wimperis, *J. Magn. Reson.* **58**, 526 (1984).

23. W. F. Reynolds, S. McLean, M. Perpick-Dumont, and R. G. Enriquez, *Magn. Reson. Chem.* **27**, 162 (1989).

24. W. F. Reynolds, private communication.

APPENDIX

A.1 Implementation of FLOCK on Bruker AM-300 and AM-400 Spectrometers

The FLOCK experiment which Reynolds and co-workers (1) devised has an unusually long pulse sequence. It incorporates three BIRD clusters (2) into the long-range C−H shift correlation sequence, with each BIRD sequence utilizing a $90^\circ_0 180^\circ_{90} 90^\circ_0$ composite carbon inversion pulse (3). The sequence, which includes 21 rf pulses, is easily implemented on a Varian XL400 spectrometer (1), but its implementation on Bruker's AM-300 and AM-400 spectrometers presented a big problem. A Bruker DISNMR pulse program for the standard FLOCK experiment with a typical set of acquisition parameters is given in Fig. A.1. Attempts to execute this pulse program on the AM-400 spectrometer consistently resulted in the machine stopping with error message

PULSER ERROR INTERRUPT. LEVEL 2.

This error, which is commonly associated with the failure of the pulser to execute short rf pulses and delays, is always obtained. On the AM-300 spectrometer, the pulse program is executed for a few minutes, after which the execution halts and the computer either gives the above error message or an undecipherarable unknown message like

77777777 6 6 13033 13033 30126 26147

43703 2273 AUCLKN 8601101.1, JOB 1.

Efforts to make the pulse program work by changing the acquisition parameters and by using different versions of Bruker's DISNMR programs were not successful. Specialists at Bruker Canada were unable to figure out why this FLOCK pulse

```
1 ZE
2 D1 DO S1
  P1:D PH1
  DO
  (P1 PH6 D5):D
  (P2 PH7 D5):D (P3 PH11 P4 PH3 P3 PH11)
  P1:D PH8
  DO
3 D4
  (P1 PH9 D5):D
  (P2 PH9 D5):D (P3 PH11 P4 PH3 P3 PH11)
  (P1 PH10 D4):D
4 (P1 PH2 D2):D  P3 PH1
  (P1 PH11 D5):D
  (P2 PH11 D5):D (P3 PH1 P4 PH4 P3 PH1)
  P1:D PH12
5 D2 S2
6 GO=2 PH5 CPD
7 D2 DO
8 WR #1
9 IF #1
10 IN=1
11 EXIT
PH1=0 0 0 0 2 2 2 2
PH3=1
PH4=1 1 1 1 3 3 3 3
PH6=0 0 0 0 0 0 0 0 0 0 0 0 0 0 0 0
    1 1 1 1 1 1 1 1 1 1 1 1 1 1 1 1
    2 2 2 2 2 2 2 2 2 2 2 2 2 2 2 2
    3 3 3 3 3 3 3 3 3 3 3 3 3 3 3 3
PH7=1 1 1 1 1 1 1 1 1 1 1 1 1 1 1 1
    2 2 2 2 2 2 2 2 2 2 2 2 2 2 2 2
    3 3 3 3 3 3 3 3 3 3 3 3 3 3 3 3
    0 0 0 0 0 0 0 0 0 0 0 0 0 0 0 0
PH8=2 2 2 2 2 2 2 2 2 2 2 2 2 2 2 2
    3 3 3 3 3 3 3 3 3 3 3 3 3 3 3 3
    0 0 0 0 0 0 0 0 0 0 0 0 0 0 0 0
    1 1 1 1 1 1 1 1 1 1 1 1 1 1 1 1
PH9=0 0 0 0 1 1 1 1 2 2 2 2 3 3 3 3
PH10=2 2 2 2 3 3 3 3 0 0 0 0 1 1 1 1
PH11=0
PH12=2
PH2=0 3 2 1 2 1 0 3
PH5=R0 R1 R2 R3

;D1 = (1-5*T1 FOR 1H)
;S1,S2 = 0H, NORMAL POWER FOR CPD
;P1,P2 = 90, 180 1H PULSE
;P3,P4 = 90, 180 X PULSE
;D5 = 0.5/J(XH) FOR DIRECT COUPLING
;D4 + D5 = 0.25/J(XH) FOR LONG-RANGE COUPLING
;D2 + D5 = 0.125/J(XH) FOR LONG-RANGE COUPLING
;           TO OBSERVE ALL MULTIPLICITIES
;RD=PW=0
;IN = 0.25/SW1, SW1=0.5*(1H SHIFT RANGE)

;TYPICAL PARAMETERS FOR AM-300
;D1 = 1.100000      S1 = 0H          P1 = 12.80
;D0 = 0.000003      D5 = 0.0034483   P2 = 25.60
;P3 =    7.00       P4 =   14.00     D4 = 0.0605517
;D2 = 0.0125517     S2 = 15H         RD = 0
;PW = 0.0           DE = 31.30       NS = 64
;DS = 2             P9 =  95.00      NE = 128
;IN = 0.0002500
;
```

Figure A.1: Bruker DISNMR pulse program for standard FLOCK sequence ("composite" FLOCK) with typical set of acquisition parameters. This program does not work on both AM-300 and AM-400 spectrometers.

```
1 ZE
2 D1 DO S1
  P1:D PH1
  DO
  (P1 PH6 D5):D
  (P2 PH7 D5):D P4 PH11
  P1:D PH8
  DO
3 D4
  (P1 PH9 D5):D
  (P2 PH9 D5):D P4 PH11
  (P1 PH10 D4):D
4 (P1 PH2 D2):D  P3 PH1
  (P1 PH11 D5):D
  (P2 PH11 D5):D P4 PH1
  P1:D PH12
5 D2 S2
6 GO=2 PH5 CPD
7 D2 DO
8 WR #1
9 IF #1
10 IN=1
11 EXIT
PH1=0 0 0 0 2 2 2 2
PH6=0 0 0 0 0 0 0 0 0 0 0 0 0 0 0 0
    1 1 1 1 1 1 1 1 1 1 1 1 1 1 1 1
    2 2 2 2 2 2 2 2 2 2 2 2 2 2 2 2
    3 3 3 3 3 3 3 3 3 3 3 3 3 3 3 3
PH7=1 1 1 1 1 1 1 1 1 1 1 1 1 1 1 1
    2 2 2 2 2 2 2 2 2 2 2 2 2 2 2 2
    3 3 3 3 3 3 3 3 3 3 3 3 3 3 3 3
    0 0 0 0 0 0 0 0 0 0 0 0 0 0 0 0
PH8=2 2 2 2 2 2 2 2 2 2 2 2 2 2 2 2
    3 3 3 3 3 3 3 3 3 3 3 3 3 3 3 3
    0 0 0 0 0 0 0 0 0 0 0 0 0 0 0 0
    1 1 1 1 1 1 1 1 1 1 1 1 1 1 1 1
PH9=0 0 0 0 1 1 1 1 2 2 2 2 3 3 3 3
PH10=2 2 2 2 3 3 3 3 0 0 0 0 1 1 1 1
PH11=0
PH12=2
PH2=0 3 2 1 2 1 0 3
PH5=R0 R1 R2 R3
```

Figure A.2: Bruker DISNMR pulse program for modified FLOCK sequence using simple 180° carbon pulses instead of $90^\circ_0 180^\circ_{90} 90^\circ_0$ composite pulses ("simple" FLOCK).

program would not run on the two spectrometers.

It was suspected at this point that the numerous pulses and delays in FLOCK were causing the problem. A pulse program for the FLOCK sequence which uses simple carbon 180° pulses ("simple" FLOCK) instead of the recommended $90^\circ_0 180^\circ_{90} 90^\circ_0$ composite inversion pulse ("composite" FLOCK) was then tested and was found to work well in both Bruker spectrometers. The pulse program for the "simple" FLOCK sequence is shown in Fig. A.2. It was concluded that the $90^\circ_0 180^\circ_{90} 90^\circ_0$ composite pulses were responsible for the difficulty in implementing the "composite" FLOCK sequence. In investigating long-range sequences incorpo-

rating BIRD clusters, Reynolds *et. al* (4) found that sequences which utilize simple carbon 180° inversion pulses produce maps with worse sensitivities and more artifacts than maps from sequences which use composite 180° pulses. This study was performed on 2-pentanone using a Varian XL-400 spectrometer with a 90° pulse length of 14 μs. For experiments performed on the AM-300 and AM-400 spectrometers, siginificant differences in the quality of the spectra obtained with the "simple" and "composite" FLOCK were not expected, since the 90° pulse lengths are relatively short on these spectrometers: 4.3 μs for the AM-300 and 7 μs for the AM-400. The "simple" FLOCK sequence was therefore used in the experiments with norharmane presented in Chapter 5.

After further experimentation with the "composite" FLOCK pulse program, it was discovered that one can make this program run by altering the way the phase cycle is executed. Fig. A.3 presents an example of the modified pulse program for "composite" FLOCK which works on the AM-400, but not on the AM-300. Compared to the phase program in Fig. A.1, where PH6, PH7 and PH8 have 64 phase settings, the new phase program includes only one phase setting for each of three phases. The added IP6, IP7, IP8 commands increment the PHn phase by 90°, after completing 16 scans.

In order to test the earlier assumption that the sensitivities of "simple" and "composite" FLOCK on the Bruker spectrometers would be essentially equivalent, these two FLOCK experiments were carried out on the Bruker AM-400 using 2-pentanone as a test molecule. The BIRDTRAP experiment was also performed in order to check the validity of the results presented in Chapter 5. The delays used were, 128 ms for Δ_1, 32 ms for Δ_2, and 3.4 ms for τ. The carbon spectral width was set to 21,700 Hz while the proton spectral width was deliberately doubled to 2000 Hz, in order to separate quad images from the real peaks. The 2D data

```
1 ZE
2 D1 DO S1
  P1:D PH1
  DO
  (P1 PH6 D5):D
  (P2 PH7 D5):D (P3 PH11 P4 PH3 P3 PH11)
  P1:D PH8
  DO
3 D4
  (P1 PH9 D5):D
  (P2 PH9 D5):D (P3 PH11 P4 PH3 P3 PH11)
  (P1 PH10 D4):D
4 (P1 PH2 D2):D  P3 PH1
  (P1 PH11 D5):D
  (P2 PH11 D5):D (P3 PH1 P4 PH4 P3 PH1)
  P1:D PH12
5 D2 S2
6 GO=2 PH5 CPD
  IP6
  IP7
  IP8
7 D2 DO
8 WR #1
9 IF #1
10 IN=1
11 EXIT
PH1=0 0 0 0 2 2 2 2
PH3=1
PH4=1 1 1 1 3 3 3 3
PH6=0
PH7=1
PH8=2
PH9=0 0 0 0 1 1 1 1 2 2 2 2 3 3 3 3
PH10=2 2 2 2 3 3 3 3 0 0 0 0 1 1 1 1
PH11=0
PH12=2
PH2=0 3 2 1 2 1 0 3
PH5=R0 R1 R2 R3
```

Figure A.3: Bruker DISNMR pulse program for "composite" FLOCK employing IPn commands to increment phases. This program runs on Bruker AM-400 spectrometer but not on AM-300.

sets were processed in a manner similar to the processing of the data sets for 2,3-dihydrofuran in Chapter 5.

Selected f_1 slices from the 2D maps of 2-pentanone are shown in Fig. A.4. As anticipated, the sensitivities in the "simple" and "composite " FLOCK spectra are not significantly different. Although the intensities of the artifacts in the C-2 slice of the "composite" FLOCK map are markedly reduced, the intensities of the quad images and zero frequency peaks in the other f_1 slices are still reasonably large. These results demonstrate that it is not really advantageous to use the composite $90^\circ_0 180^\circ_{90} 90^\circ_0$ carbon inversion pulse for FLOCK experiments performed on the AM-400. In contrast to the results on norharmane, where FLOCK spectra had

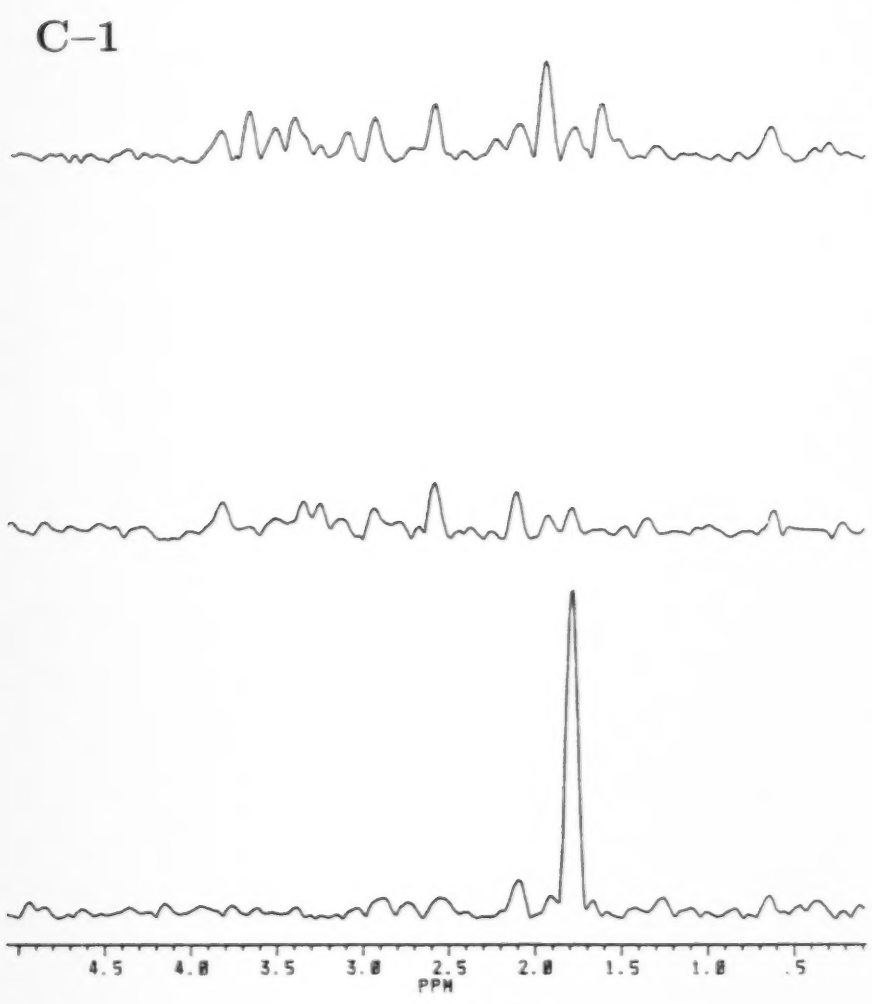

Figure A.4: f_1 slices from the 2D map of 2-pentanone obtained with (top)"composite" FLOCK (Fig. A.3), (center) "simple" FLOCK (Fig. A.2) , and (bottom) BIRDTRAP.

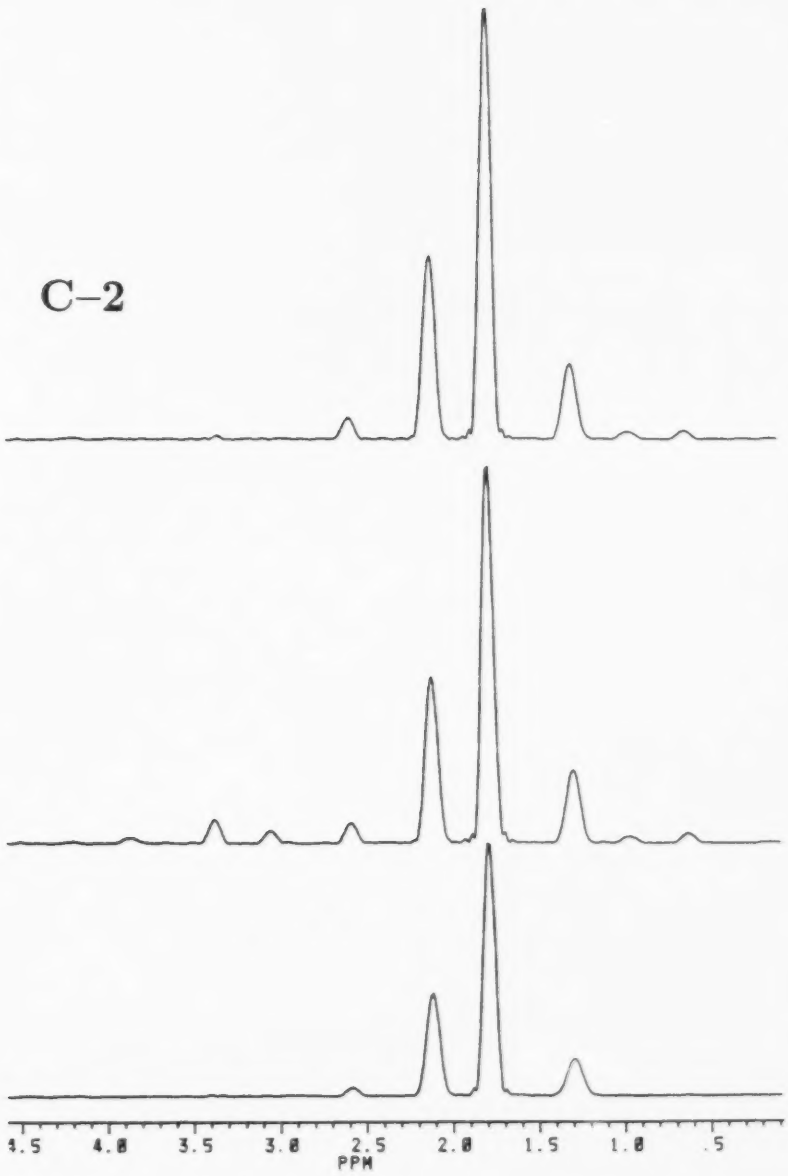

Fig. A.4: continued.

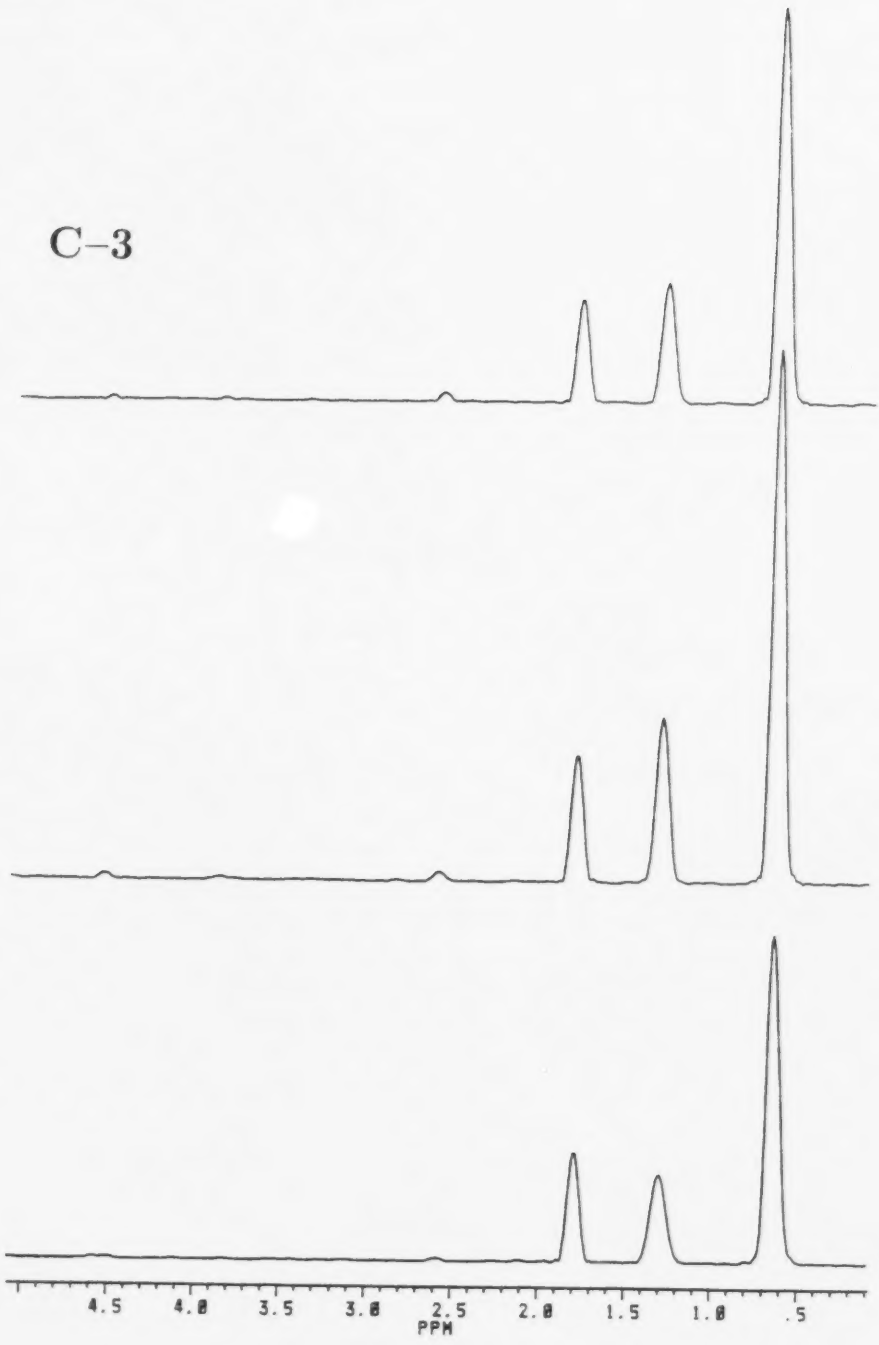

Fig. A.4 continued.

Fig. A.4 continued.

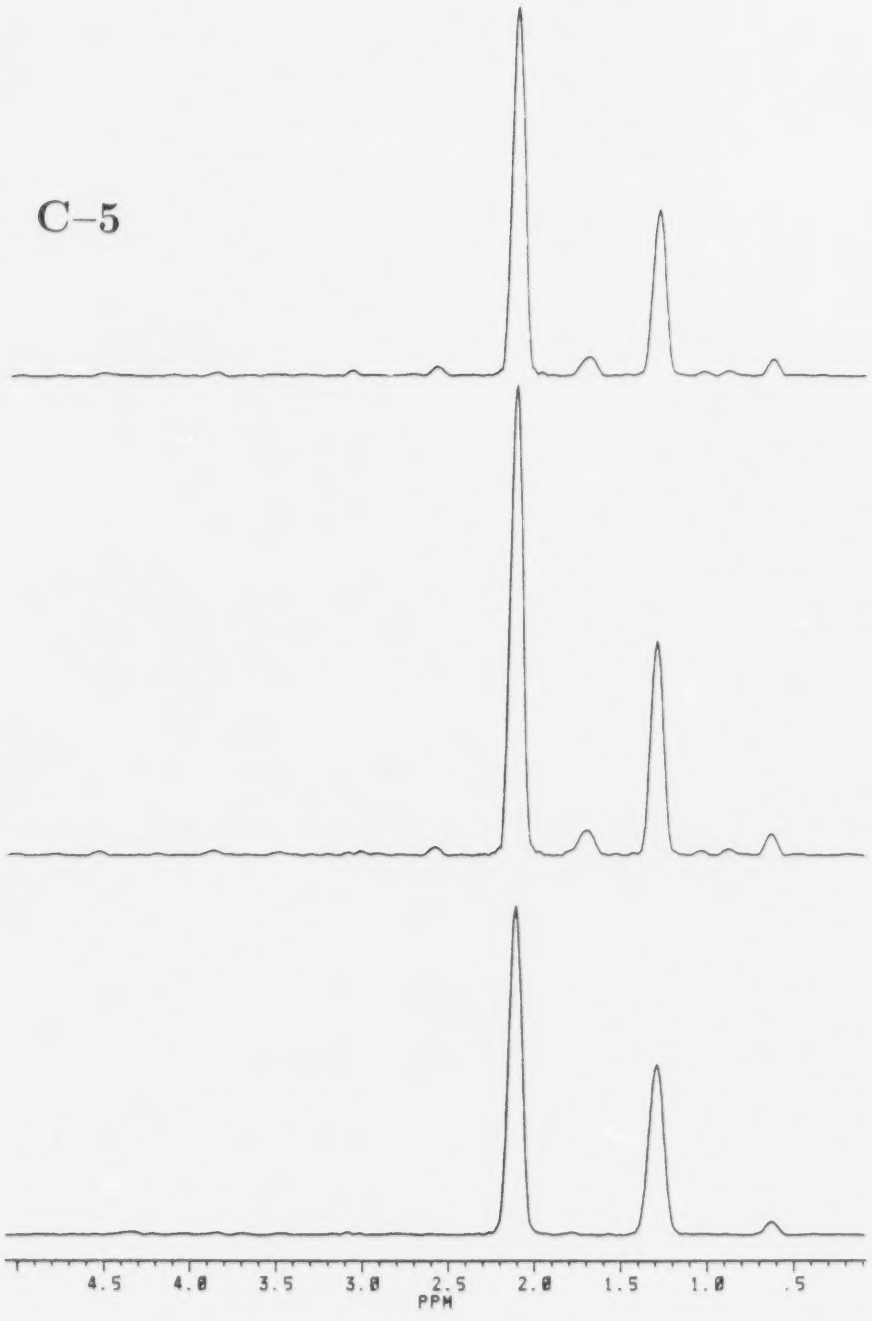

Fig. A.4 continued.

lower sensitivities than BIRDTRAP, the sensitivities in the two FLOCK spectra of 2-pentanone were about 15% higher than those in the BIRDTRAP spectra. It appears that the relative sensitivities of the FLOCK and BIRDTRAP depend on the spectrometer used and the compound investigated. Further experiments on menthol using the AM-300 spectrometer confirmed this since BIRDTRAP displayed higher sensitivity than FLOCK for most peaks.

A.2 The FLOCK Sequence with the Modified Phase Cycle

The main drawback of FLOCK applications on Bruker AM-300 and AM-400 spectrometers, which may not be true on Varian XL-400 spectrometers, is the presence of perceptible f_1 zero frequency peaks in the spectra. In this thesis, where the spectra from Bruker AM-300 and AM-400 spectrometers were used, f_1 zero frequency peaks with fairly significant intensities contaminated the FLOCK spectra of norharmane and 2-pentanone. Such artifacts did not seem to pose a real problem in the FLOCK experiments using the Varian XL-400 spectrometer since f_1 zero frequency peaks were observed to be very small in the spectra of 2-pentanone (5) and none were apparently observed in the spectra of other compounds where FLOCK was first tested (1).

A new phase cycle for FLOCK has been recently devised (5) and was found to provide improved sensitivities and artifact suppression on a Varian XL400 spectrometer, using 2-pentanone as a model compound. In order to see if this new phase cycle would bring similar beneficial results on Bruker spectrometers, FLOCK experiments using the original and the modified phase cycles were performed on the Bruker AM-400 spectrometer. The pulse program for the "simple" FLOCK sequence with the modified phase cycle is given Fig. A.5. Simple carbon 180° pulses

```
1 ZE
2 D1 DO S1
  P1:D PH1
  DO
  (P1 PH6 D5):D
  (P2 PH7 D5):D  P4 PH6
  P1:D PH8
  DO
3 D4
  (P1 PH9 D5):D
  (P2 PH9 D5):D  P4 PH6
  (P1 PH10 D4):D
4 (P1 PH2 D2):D  P3 PH1
  (P1 PH6 D5):D
  (P2 PH6 D5):D P4 PH1
  P1:D PH8
5 D2 S2
6 GO=2 PH5 CPD
7 D2 DO
8 WR #1
9 IF #1
10 IN=1
11 EXIT
PH1=0 0 0 0 2 2 2 2 0 0 0 0 2 2 2 2
    1 1 1 1 3 3 3 3 1 1 1 1 3 3 3 3
    2 2 2 2 0 0 0 0 2 2 2 2 0 0 0 0
    3 3 3 3 1 1 1 1 3 3 3 3 1 1 1 1
PH6=0
PH7=1
PH8=2
PH9=0 0 0 0 1 1 1 1 2 2 2 2 3 3 3 3
    1 1 1 1 2 2 2 2 3 3 3 3 0 0 0 0
    2 2 2 2 3 3 3 3 0 0 0 0 1 1 1 1
    3 3 3 3 0 0 0 0 1 1 1 1 2 2 2 2
PH10=2 2 2 2 3 3 3 3 0 0 0 0 1 1 1 1
     3 3 3 3 0 0 0 0 1 1 1 1 2 2 2 2
     0 0 0 0 1 1 1 1 2 2 2 2 3 3 3 3
     1 1 1 1 2 2 2 2 3 3 3 3 0 0 0 0
PH2=0 3 2 1 2 1 0 3 0 3 2 1 2 1 0 3
    1 0 3 2 3 2 1 0 1 0 3 2 3 2 1 0
    2 1 0 3 0 3 2 1 2 1 0 3 0 3 2 1
    3 2 1 0 1 0 3 2 3 2 1 0 1 0 3 2
PH5=R0 R1 R2 R3 R0 R1 R2 R3 R0 R1 R2 R3 R0 R1 R2 R3
    R1 R2 R3 R0 R1 R2 R3 R0 R1 R2 R3 R0 R1 R2 R3 R0
    R2 R3 R0 R1 R2 R3 R0 R1 R2 R3 R0 R1 R2 R3 R0 R1
    R3 R0 R1 R2 R3 R0 R1 R2 R3 R0 R1 R2 R3 R0 R1 R2
```

Figure A.5: Bruker DISNMR pulse program for "simple" FLOCK employing revised phase cycle.

were used in both experiments since, through experience, no significant advantage is obtained when composite carbon pulses are employed in FLOCK experiments performed on Bruker spectrometers. It is however important to note that it came as a big surprise that the "composite" FLOCK employing this new phase cycle (Fig. A.6) ran smoothly on both AM-300 and AM-400 spectrometers. Selected f_1 slices from the 2D maps of 2-pentanone obtained using "simple" FLOCK with the original and modified phase cycles are presented in Fig. A.7. By comparing the original and the modified FLOCK spectra, one immediately sees that f_1 zero fre-

```
1 ZE
2 D1 DO S1
  P1:D PH1
  DO
  (P1 PH6 D5):D
  (P2 PH7 D5):D (P3 PH6 P4 PH7 P3 PH6)
  P1:D PH8
  DO
3 D4
  (P1 PH9 D5):D
  (P2 PH9 D5):D (P3 PH6 P4 PH7 P3 PH6)
  (P1 PH10 D4):D
4 (P1 PH2 D2):D  P3 PH1
  (P1 PH6 D5):D
  (P2 PH6 D5):D (P3 PH1 P4 PH3 P3 PH1)
  P1:D PH8
5 D2 S2
6 GO=2 PH5 CPD
7 D2 DO
8 WR #1
9 IF #1
10 IN=1
11 EXIT
PH1=0 0 0 0 2 2 2 2 0 0 0 0 2 2 2 2
    1 1 1 1 3 3 3 3 1 1 1 1 3 3 3 3
    2 2 2 2 0 0 0 0 2 2 2 2 0 0 0 0
    3 3 3 3 1 1 1 1 3 3 3 3 1 1 1 1
PH3=1 1 1 1 3 3 3 3 1 1 1 1 3 3 3 3
    2 2 2 2 0 0 0 0 2 2 2 2 1 1 1 1
    3 3 3 3 1 1 1 1 3 3 3 3 1 1 1 1
    0 0 0 0 2 2 2 2 0 0 0 0 2 2 2 2
PH6=0
PH7=1
PH8=2
PH9=0 0 0 0 1 1 1 1 2 2 2 2 3 3 3 3
    1 1 1 1 2 2 2 2 3 3 3 3 0 0 0 0
    2 2 2 2 3 3 3 3 0 0 0 0 1 1 1 1
    3 3 3 3 0 0 0 0 1 1 1 1 2 2 2 2
PH10=2 2 2 2 3 3 3 3 0 0 0 0 1 1 1 1
     3 3 3 3 0 0 0 0 1 1 1 1 2 2 2 2
     0 0 0 0 1 1 1 1 2 2 2 2 3 3 3 3
     1 1 1 1 2 2 2 2 3 3 3 3 0 0 0 0
PH2=0 3 2 1 2 1 0 3 0 3 2 1 2 1 0 3
    1 0 3 2 3 2 1 0 1 0 3 2 3 2 1 0
    2 1 0 3 0 3 2 1 2 1 0 3 0 3 2 1
    3 2 1 0 1 0 3 2 3 2 1 0 1 0 3 2
PH5=R0 R1 R2 R3 R0 R1 R2 R3 R0 R1 R2 R3 R0 R1 R2 R3
    R1 R2 R3 R0 R1 R2 R3 R0 R1 R2 R3 R0 R1 R2 R3 R0
    R2 R3 R0 R1 R2 R3 R0 R1 R2 R3 R0 R1 R2 R3 R0 R1
    R3 R0 R1 R2 R3 R0 R1 R2 R3 R0 R1 R2 R3 R0 R1 R2
```

Figure A.6: Bruker DISNMR pulse program for "composite" FLOCK employing revised phase cycle.

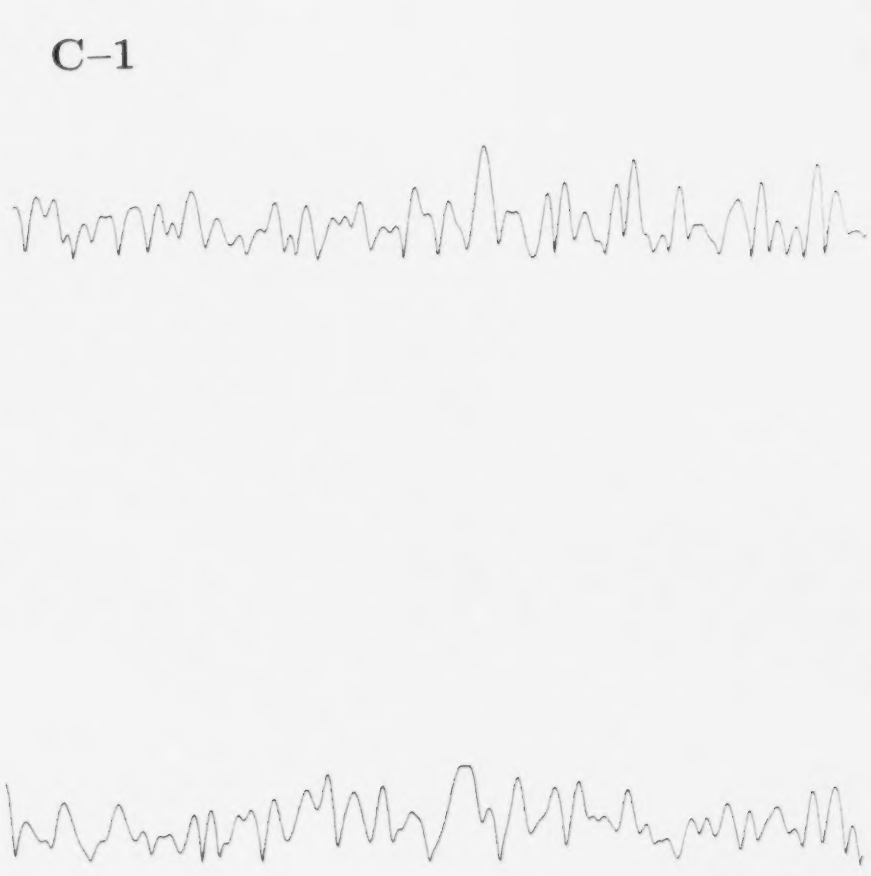

Figure A.7: f_1 slices from the 2D map of 2-pentanone obtained using "simple" FLOCK with (top) revised phase cycle (Fig. A.5) and (bottom) original phase cycle (Fig. A.6).

Fig. A.7: continued.

Fig. A.7: continued.

Fig. A.7: continued.

Fig. A.7: continued.

quency peaks are quite visible in the original FLOCK spectra while none of these artifacts are present in the modified FLOCK spectra. This difference between the two FLOCK spectra was also observed in similar experiments performed on Bruker AM-300 and Varian Unity 500 spectrometers. In addition, one notices in Fig. A.7 that the sensitivities in the modified spectra are slightly higher than the sensitivities in the original spectra. This trend was not, however, observed on FLOCK experiments performed on the AM-300, where sensitivities of the two FLOCK were essentially equivalent.

Considering the above results, one can definitely say that the modified phase cycle for FLOCK is much better than the original phase cycle. Since the "composite" FLOCK employing this new phase cycle can be implemented smoothly on Bruker AM-300 and AM-400 spectrometers, FLOCK should become a popular method for elucidating structures based on long-range correlations. The kind of spectrometer used and the sample studied appear to affect the sensitivities of FLOCK relative to BIRTDTRAP.

References

1. W. F. Reynolds, S. McLean, M. Perpick-Dumont, and R. G. Enriquez, *Magn. Reson. Chem.* **27**, 162 (1989).

2. J. R. Garbow, D. P. Weitekamp, and A. Pines, *Chem. Phys. Lett.* **93**, 504 (1982).

3. M. H. Levitt and R. Freeman, *J. Magn. Reson.* **33**, 473 (1979).

4. M. Perpick-Dumont, R. G. Enriquez, S. McLean, F. V. Puzzuoli and W. F. Reynolds, *J. Magn. Reson.* **75**, 414 (1987).

5. W. F. Reynolds, private communication.